MATSCIENCE REPORT 65

REPORT ON
RECENT EXPERIMENTAL DATA
1967

K. VENKATESAN

THE INSTITUTE OF MATHEMATICAL SCIENCES, MADRAS-20. (INDIA)

MATSCIENCE REPORT 65

REPORT ON
RECENT EXPERIMENTAL DATA
1967

K.Venkatesan

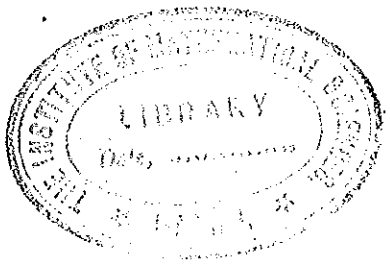

THE INSTITUTE OF MATHEMATICAL SCIENCES, MADRAS-20
(INDIA)

Preface

The present report consists of a collection of the reports on Recent Experimental Data issued monthly during the year 1967. Nothing spectacular happened during the year. In the field of strong interactions the main activity continues to be the discovery of new resonances or confirmation of existing ones.

JANUARY 1967

Introduction

The present report begins with the determination of the polariza tion of the recoil neutron in the $\pi^- p$ charge exchange scattering at 5.9 and 11.2 Bev/c.

The cross-sections for K^{*-} and $\overline{K}^{*0}$ production in $K^- p$ collisions at 2 and 2.24 Bev/c are given.

Evidence for a $\pi^+\pi^-$-resonance in the 1.5-1.6 Bev region is forthcoming from a study of $\pi^- p$ interaction at 4.7 Bev/c.

The differential cross-sections for η photoproduction from threshold to 940 Mev are given.

A backward peaking is observed in the associated production of Λ^0 or Σ^0 in $\pi^- p$ collisions at 6 Bev/c.

Differential cross-sections for various boson and nucleon resonances in pp collisions at 12.3 Bev/c are given.

A study of the decay properties of the A_2 meson confirms the assignment $J^P = 2^+$. Production cross-sections are given.

Finally a determination of the phase of the CP nonconservation parameter η_{+-} in neutral K decay gives a value 0.44 ± 0.44.

ELEMENTARY PARTICLES

$\pi^- p \to \pi^0 n$ polarization at 5.9 and 11.2 Bev/c[1]:-

The polarization, $P_0(t)$ for the $\pi^- p$ charge exchange scattering at 5.9 and 11.2 Bev/c was studied using a target containing polarized protons. The values of $P_0(t)$ for various momentum transfer intervals are given in the following table. Averaging over the squared momentum transfer range $0.04 \leq -t \leq 0.24$ $(\text{Bev/c})^2$, the values found were

$$\langle P_0(t) \rangle = + 16\% \pm 3.5\% \quad \text{at 5.9 Bev/c}$$

and

$$\langle P_0(t) \rangle = + 14\% \pm 4.5\% \quad \text{at 11.2 Bev/c}$$

which shows that there is no fast decrease of $P_0(t)$ with increasing energy.

The Regge-pole model (assuming the dominance of exchange of a single ρ -Regge trajectory) predicts zero polarization of the recoil proton. Thus the observed polarization would indicate the presence of an additional background term. Also the energy dependence of the polarization might be accounted for by taking into account absorption effects or a Regge cut

[$P_0(t)$ is given by

$$P_0(t) = \frac{2\,\mathrm{Im}\{f(t)\,g^*(t)\}}{|f(t)|^2 + |g(t)|^2}$$

where $f(t)$ and $g(t)$ the non-spin-flip and spin flip amplitudes, respectively].

-t internal $(Bev/c)^2$	$P_0(t) \times 100$ at 5.9 Bev/c			$P_0(t) \times 100$ at 11.2 Bev/c
	Right	Left	Average	(Average R,L)
0.01 - 0.04	-14 ± 10	+15 ± 11	+0 ± 8	2 ± 8
0.04 - 0.07	+11 ± 9	+15 ± 9	+13 ± 6	14 ± 6
0.07 - 0.10	+21 ± 9	+3 ± 9	+13 ± 6	
0.10 - 0.13	+24 ± 10	+21 ± 10	+22 ± 7	15 ± 8
0.13 - 0.16	+21 ± 11	+15 ± 10	+19 ± 7	
0.16 - 0.19	+3 ± 14	+17 ± 12	+12 ± 10	13 ± 9
0.19 - 0.24	+10 ± 22	+27 ± 21	+19 ± 16	
0.24 - 0.34				7 ± 14

Cross-sections for K^{*-} and $\overline{K^{*0}}$ production in collisions[2]:-

The two prong reactions

$$K^- p \rightarrow K^- \pi^0 p \qquad (1)$$

$$\rightarrow \overline{K}^0 \pi^- p \qquad (2)$$

$$\rightarrow K^- \pi^+ n \qquad (3)$$

were studied using K^- mesons of 2.0 Bev/c and 2.24 Bev/c incident momenta on the Brookhaven 20H hydrogen bubble chamber.

At 2.0 Bev/c, 1383 inelastic events were analyzed and at 2.4 Bev/c, 2319 events, both elastic and inelastic, were studied.

Events with $M(K\pi) = 890 \pm 50$ Mev were treated as production events. The total cross-sections are given in the following table.

Channel	2.0 Bev/c	2.24 Bev/c
$K^- p \pi^0$	1.29 ± 0.10	1.24 ± 0.20
$K^- \pi^+ n$	2.94 ± 0.15	1.84 ± 0.20
$\overline{K^0} \pi^- p$	1.78 ± 0.13	1.26 ± 0.20
$K^{*-} p$	1.30 ± 0.18	0.80 ± 0.40
$\overline{K^{*0}} n$	1.07 ± 0.10	0.55 ± 0.30
All inelastic two prongs	12.49 ± 0.36	12.00 ± 1.2
Elastic $K^- p$	7.18 ± 0.21	6.16 ± 0.70

Evidence for $\pi^+\pi^-$ resonance at 1.5 - 1.6 Bev in 4.7 Bev/c $\pi^- p$ interaction[3)]

Two prong stars were sought for in 60,000 pictures of the interaction of a 4.7 Bev/c π^- beam in a hydrogen bubble chamber. Events satisfying the hypothesis, $\pi^- p \rightarrow \pi^+ \pi^- n$ were selected.

For plotting the effective mass distribution 349 events with $-t \leq 15\mu^2$ were selected. In the $\pi^+\pi^-$ system, two peaks at 780 and 1250 Mev could be attributed to the ρ^0 and f^0 mesons. In addition there was an enhancement at $M_{\pi\pi} = 1500$ - 1600 Mev. If it is attributed to a resonance in the $\pi^+\pi^-$ - system its parameters are M = 1549 ± 30 Mev and Γ = 100 ± 25 Mev.

Eta photoproduction in the region from threshold to 940 Mev[4]:-

Photoproduction of η^0 meson was studied in the region from threshold to about 940 Mev. The differential cross-section near 90° c.m.s. shows a rapid rise near threshold reaching a maximum value of $1\ \mu b/_{sr}$ at approximately 40 Mev above threshold. Beyond this, the cross-section decreases to a value of $0.3\ \mu b/_{sr}$ at a laboratory photon energy of about 900 Mev. Several different angles were chosen at a laboratory photon energy of 790 Mev for studying the angular distribution which was found to be consistent with isotropy. This implies either an S or P wave with $T = \frac{1}{2}$, $J = \frac{1}{2}$ near threshold. The ratio of the differential corss-sections for π^0 and η^0 in the photon energy range 760-800 Mev around 90° c.m.s. was found to be

$$\frac{d\sigma/d\Omega^*|_{\pi^0}}{d\sigma/d\Omega^*|_{\eta^0}} \simeq 4$$

At 760 Mev this result is inconsistent with the hypothesis that all the η_0 yield near threshold comes from the $D_{3/2}$ N^{**} (1512 Mev) on the basis of the relative size of the D-wave angular-momentum barrier for π^0 against η^0 production and on the assumption that the η^0 nucleon and π^0 nucleon couplings are approximately equal. The angular distribution near threshold also tends to rule out pure D-wave production of η_0 since this requires a $2+3\sin^2\theta^*$ angular distribution.

The S- and P-wave $J=\frac{1}{2}$ production for the η_0 near threshold suggests that it should be identified with the N_1^* (1550 Mev) S_{11} state. The differential cross-sections for η^0 production are given in Figs. 1a and 1b.

Observation of a backward peak in the reaction $\pi^- + p \rightarrow Y^0 + K^0$ at 6 Bev/c [5]

142 events of the reaction

$$\pi^- + p \rightarrow Y^0 + K^0$$

were analysed to study the angular distribution at 6 Bev/c. The motivation was to find whether there is a backward peaking as is the case for large angle $\pi^{\pm} p$ elastic scattering in the region of 4 to 8 Bev/c. The $Y^0 K^0$ state (where Y^0 is the either a Λ or a Σ^0) does show such a backward peak. The slope of this peak is fitted by $\exp[-n_b(u-u_0)]$ where u is the square of the fourth-momentum transfer in the

relevant crossed channels, u_0 is the kinematic maximum value of u and η_b has a value, $\eta_b = 5.7 \pm 2$ Bev^{-2}. There is also a forward peak fitted by exp $[-\eta_f(t-t_0)]$ where t is the square of the four-momentum transfer for the direct channel and $\eta_f = 7.8 \pm 0.5$ Bev^{-2}. Almost none of the events are found outside the forward or backward peaks. η_f does not have a strong energy dependence having practically a constent value from $p_\pi \sim$ 2 to 6 Bev/c.

Boson production in p-p collisions at 12.3 Bev/c[6]:-

The observation of three-body final states

$$p + p \longrightarrow p + p + MM \text{ (missing mass)}$$

in p-p collisions at 12.3 Bev/c, indicates that the MM (corresponding to a neutral boson) spectra have considerable structure and can be associated with defined boson resonances. The most striking of these reactions was the production of ω^0 which accounts for about 6% of the reactions of this type. Reactions of the type

$$p + p \longrightarrow p + \pi^+ + MM$$

were also studied. Here MM is associated with nucleon isobars. The first of the following tables gives the differential cross-sections at 12.7 Bev/c for the N^* resonance production. The second table gives the differential cross-section $\partial^3\sigma / dm_2 \partial t \partial\Omega_2^b$ in $\mu b / sr$ Bev

for boson-nucleon final states is given as a function of m_{23}, where the subscript 2 indicates the particle detected in the low-momentum arms and m_3 the mass of the remainder.

Table I

Process	$-t$ (Bev^2)	$\partial\sigma/\partial t$ (μb/Bev^2)
$p+p \rightarrow p+p$	1.31	7.3 ± 1.5
$p+p \rightarrow p+N^*(1518)$	1.17	1.4 ± 0.4
$p+p \rightarrow p+N^*(1688)$	1.13	3.7 ± 0.9

Table II

m_{23} (Bev)	$-t$ (Bev^2)	Boson-nucleon final state			
		$p\pi^0$	$p\pi^+$	$p\eta^0$	$p\omega^0$
1.5	1.18	7.2 ± 0.7			
1.6	1.15	2.2 ± 0.3			
1.7	1.12	1.4 ± 0.2	1.3 ± 0.2	1.1 ± 0.4	
1.8	1.09	1.1 ± 0.2	1.7 ± 0.1	0.75 ± 0.28	
1.9	1.06	1.1 ± 0.2	1.3 ± 0.1	0.33 ± 0.19	1.8 ± 0.4
2.0	1.02	0.75 ± 0.14	0.69 ± 0.09	0.39 ± 0.19	0.91 ± 0.29
2.1	0.98	0.58 ± 0.13	0.51 ± 0.08	0.32 ± 0.15	0.65 ± 0.23
2.2	0.94	0.28 ± 0.08	0.25 ± 0.06	0.02 ± 0.11	1.0 ± 0.2
2.3	0.96	0.17 ± 0.07	0.05 ± 0.03		0.53 ± 0.16
2.4	0.86	0.13 ± 0.07			0.30 ± 0.12
2.5	0.84				0.02 ± 0.09

The decay properties of the $A_2(1310)$ Meson[7]:-

The present experiment was carried out to resolve the J^P assignement (2^+ , 1^+ or 2^-) for the A_2- meson from its decay properties. In the case of the 1^+ or 2^- assignment the $K\bar{K}$ peak at 1310 Mev would and represent the decay of a new particle (and not the A_2 meson). By studying the quantum numbers independently for the $K\bar{K}$ and $\pi\rho$ peaks it was found that both these are possible decay modes of the A_2 meson and the quantum number assignment is

$$I^G J^P = 1^- 2^+$$

The following two tables give the cross-sections for the final states analyzed and for A_2 meson production respectively.

Table I

Final state	Cross section (μb)	
	3.2 Bev/c	4.2 Bev/c
$p\pi^+\pi^-\pi^-$	1910 ± 80	1920 ± 100
pK^0K^-	65.1 ± 5.3	65.7 ± 7.9
$nK_1^0K_1^0$	45.3 ± 4.1	36.6 ± 5.1

Table II

Reaction	Cross section (μb)	
	3.2 Bev/c	4.2 Bev/c
$\pi^- + p \to A_2^- + p$; $A_2^- \to K^0 + K^-$	18 ± 4	17 ± 5
$\pi^- + p \to A_2^0 + n$; $A_2^0 \to K + \pi$	36 ± 10	18 ± 9
$\pi^- + p \to A_2^- + p$; $A_2^- \to \rho^0 + \pi^-$	150 ± 50	175 ± 45

Determination of the phase of the CP-nonconservation parameter η_{+-} in neutral K decay[8]:-

The phase of the parameter η_{+-} given by

$$\eta_{+-} = \frac{\langle \pi^+ \pi^- | K_L^0 \rangle}{\langle \pi^+ \pi^- | K_S^0 \rangle}$$

was determined by measuring the phase between $K_L^0 \rightarrow \pi^+ + \pi^-$ and the regenerated $K_S^0 \rightarrow \pi^+ + \pi^-$ and evaluating the regeneration phase by means of an optical model calculations. The value obtained for the phase was

$$\arg \eta_{+-} = 0.44 \pm 0.44.$$

References

1) P.Bonamy et al, Physics Letters 23, 501 (1966)

2) M.Dickenson et al, Physics Letters 23, 505 (1966)

3) V.M.Guzhavin et al, Physics Letters 23, 719 (1966)

4) R.Prepost et al, Phys. Rev. Letters 18, 82 (1967)

5) D.J.Crennell et al, Phys. Rev. Letters 18, 86 (1967)

6) H.L.Anderson et al, Phys. Rev. Letters 18, 89 (1967)

7) S.U.Cheng et al, Phys. Rev. Letters 18, 100 (1967)

8) R.E.Mischke et al, Phys. Rev. Letters 18, 138 (1967)

....

FIG. 1b

FIG. 1a

FEBRUARY 1967

Introduction

The present report commences with an experiment on η-meson production near threshold which shows a linear increase of the cross-section with momentum.

Elastic scattering of 3.55 Bev/c positive and negative pions at angles in the range 165° to 177° c.m. shows a well-defined peak in the backward direction.

A study of the polarization of $\bar{p}$ in $\bar{p}p$ scattering at 1.18 Bev/c gives an upper limit of 20%.

The polarization parameters in high energy $\pi^{\pm}p$ and pp scattering for various incident momenta in the squared momentum transfer-range 0.1 - 0.75 $(\text{Bev/c})^2$ are given. The polarization in $\pi^{+}p$ scattering decreases more rapidly with the incident beam energy than in the corresponding $\pi^{-}p$ scattering.

Evidence for a hyperon resonance $Y_1^{*}(1680)$ of width $\Gamma = 120 \pm 30$ Mev is forthcoming from an experiment on $K^{-}p$ interactions at 5.5 Bev/c.

Finally a brief account is given of the new method of Morpurgo to detect fractionally charged particles. Preliminary results give no evidence for the existence of quarks.

ELEMENTARY PARTICLES

η production near threshold[1)]

The reactions

$$\pi^- + p \longrightarrow n + \eta$$

was studied at the Rutherford Laboratory accelerator using a neutron time-of-flight technique. For the η C.M. range 15 Mev/c. $< p <$ 113 Mev/c, the following results were obtained.

(a) There was no evidence for a non-isotropic angular distribution.

(b) The cross-section is nearly linear in momentum with $A = 11.8 \pm 1.6\ \mu b\ (\text{Mev/c})^{-1}$ where $\sigma = A p$.

(c) The branching ratio $R = \dfrac{\eta \longrightarrow 2\gamma}{\eta \longrightarrow \text{neutrals}} = 0.39 \pm 0.06$

(d) The width of the η is $< 0.9\ \text{Mev/c}^2$.

The angular distribution of backward elastically scattered pions at 3.55 Bev/c[2)]

The scanty events for elastic scattering of high energy pions by nucleons in the backward direction studied in earlier experiments indicate peaks in the angular distribution at 180°. As part of a programme to study large angle pion-nucleon scattering, 864 elastic scatterings of 3.55 Bev/c positive and negative pions were measured in the present experiment at angles in the range 165° to 177° in the centre of mass. The differential cross-sections are given in the following table. The $\pi^+ p$ differential cross-section agrees well with the fit

$$\frac{d\sigma}{du} = A e^{Bu}$$

where u is the four-momentum transfer squared between the incident pion and the outgoing proton and

$$A_+ = (46.2 \pm 5.0)\ \mu b/(\text{Bev/c})^2$$

$$B_+ = (11.9 \pm 1.7)\ \ (\text{Bev/c})^{-2}$$

For $\pi^- p$ scattering the values are

$$A_- = (15.8 \pm 2.0)\ \mu b\ /\ (\text{Bev/c})^2$$

$$B_- = (2.4 \pm 2.0)\ \ (\text{Bev/c})^{-2}$$

The data support the earlier evidence of a well-defined peak, when the exchanged baryon (in a one-particle exchange graph in the u -channel) has isotopic spin $T = \frac{1}{2}$ and give a much smaller effect for $T = 3/2$.

$$\text{Ratio } \pi^+/\pi^- \quad (180^0) = 7.4 \pm 1.0$$

$$\text{Ratio } \pi^+/\pi^- (u=0) = 2.9 \pm 0.5$$

Particle	$\cos\theta_{c.m}$	$-t$ $(Bev/c)^2$	u $(Bev/c)^2$	No. of events	$d\sigma/d\Omega$ $(\mu b/sr)$	$\frac{d\sigma/d\Omega}{(d\sigma/d\Omega)_0}$ $(\times 10^3)$	$\frac{d\sigma}{du} = \frac{d\sigma}{d(-t)}$ $\mu b/(Bev/c)^2$
π^-	-0.996	5.853	0.086	89	10.3 ± 1.1	0.42	21.0 ± 2.4
	-0.992	5.841	0.075	61	9.4 ± 1.2	0.39	20.0 ± 2.6
	-0.988	5.830	0.063	39	6.7 ± 1.1	0.27	14.4 ± 2.3
	-0.984	5.818	0.051	27	5.7 ± 1.1	0.23	12.3 ± 2.4
	-0.980	5.806	0.039	22	6.4 ± 1.4	0.26	13.7 ± 2.9
	-0.976	5.795	0.028	21	7.7 ± 1.7	0.32	16.6 ± 3.6
	-0.972	5.783	0.016	20	11.0 ± 2.5	0.45	23.5 ± 5.3
	-0.968	5.771	0.004	10	7.7 ± 2.4	0.32	16.5 ± 5.2
	-0.964	5.759	-0.008	12	10.5 ± 3.0	0.43	22.5 ± 6.5
	-0.960	5.748	-0.019	4	4.8 ± 2.4	0.20	10.3 ± 5.1
π^+	-0.994	5.847	0.080	196	60.5 ± 4.4	3.02	129.6 ± 9.5
	-0.990	5.836	0.069	115	46.1 ± 4.4	2.30	98.8 ± 9.3

Particle	$\cos\theta_{c.m.}$	$-t$ $(Bev/c)^2$	u $(Bev/c)^2$	No. of events	$d\sigma/d\Omega$ $(\mu b/sr)$	$\frac{d\sigma/d\Omega}{(d\sigma/d\Omega)_0}$ $(\times 10^3)$	$\frac{d\sigma}{du} = \frac{d\sigma}{d(-t)}$ $(\mu b/(Bev/c)^2)$
π^+	-0.986	5.824	0.057	82	37.8 ± 4.2	1.89	81.0 ± 9.0
	-0.982	5.812	0.045	54	33.3 ± 4.6	1.66	71.3 ± 9.8
	-0.978	5.800	0.033	40	34.3 ± 5.4	1.71	73.5 ± 11.6
	-0.974	5.789	0.022	25	26.4 ± 5.3	1.32	56.5 ± 11.4
	-0.970	5.777	0.010	24	31.6 ± 6.5	1.58	67.8 ± 14.0
	-0.966	5.765	-0.002	9	14.8 ± 5.0	0.74	31.7 ± 10.7
	-0.962	5.754	-0.014	11	25.9 ± 7.9	1.29	55.6 ± 16.9
	-0.958	5.742	-0.025	4	13.1 ± 6.6	0.65	28.2 ± 14.1
π^+ $(u=0)$	-0.967	5.767	0.000		21.6 ± 2.3	1.08	46.2 ± 5.0
π^- $(u=0)$	-0.967	5.767	0.000		7.4 ± 0.9	0.30	15.8 ± 2.0
π^+ (180, extrapol.)	-1.000	5.865	0.098		69.1 ± 6.0	3.45	148.1 ± 12.9
π^- (180, extrapol.)	-1.000	5.865	0.098		9.3 ± 0.9	0.38	19.9 ± 1.9

Polarization of antiproton scattering in $\bar{p}p$ scattering at 1.18 Bev/c [3)]

2764 events out of a total of 210000 pictures of scattering of an integrated flux of 2.28×10^6 antiprotons of 1.18 ± 0.02 Bev/c momentum in the Saclay hydrogen bubble chamber corresponded to the case of double scattering of the $\bar{p}$. The angular distribution after double scattering is given by

$$I(\varphi) = I_0 (1 + e \cos\varphi)$$

where I_0 is the cross-section for scattering of an unpolarized beam at the second target. The asymmetry parameter e is the product of the polarization arising from the first and second scatterings (P_1, and P_2). If the energy difference between the two scatterings is small, $P_1 = P_2 = P$ and $e = P^2$. φ is given by $\cos\varphi = \vec{n_1} \cdot \vec{n_2}$ where $\vec{n_1}$ and $\vec{n_2}$ are unit vectors perpendicular to the first and second scattering planes respectively.

Fig.1 gives the angular distribution at the first scattering. The plot of $|\cos\varphi|$ against the centre of mass angles $\theta_{1\,c.m.}$ and $\theta_{2\,c.m.}$ between 15° and 60° gives a symmetrical distribution. The value of e found was

$$e = (-2.3 \pm 3)\ \%$$

For events with either $\theta_{1\,c.m.}$ or $\theta_{2\,c.m.}$ less than

15°,

$$e = (-13.0 \pm 6.5)\ \%$$

For the first case the polarization of $\bar{p}$ has an upper limit of 20%. The corresponding values for pp scattering at about the same energy is $52 \pm 2\%$.

<u>The polarization parameter in $\pi^{\pm} p$ and pp elastic scattering from 6 to 12 Bev/c[4]</u>

The polarization parameter P_0 in high energy $\pi^{\pm} p$ and pp elastic scattering was measured for incident momenta of 6.0, 8.0, 10.8 and 12.0 Bev/c for π^- and of 6.0, 10.0 and 12.0 Bev/c for π^+ and p, in the interval of invariant four-momentum transfer squared, $-t$ from 0.1 to 0.75 $(\text{Bev/c})^2$. The target proton was polarized. The polarization parameters for π^-, π^+ and p scattering are given below in Tables 1, 2 and 3 respectively. The results show that the polarization in $\pi^+ p$ scattering decreases more rapidly with the incident beam energy than the corresponding $\pi^- p$ data where it appears to be constant.

Table 1

Beam momentum = 6.0 Bev/c		Beam momentum =8.0 Bev/c		Beam momentum =10.0 Bev/c		Beam momentum =12.0 Bev/c	
$-t$ (Bev/c)^2	P_0	$-t$ (Bev/c)^2	P_0	$-t$ (Bev/c)^2	P_0	$-t$ (Bev/c)^2	P_0
0.109	-0.130 ± 0.034	0.104	-0.132 ± 0.026	0.102	-0.150 ± 0.038	0.116	-0.151 ± 0.040
0.136	-0.166 ± 0.018	0.131	-0.156 ± 0.014	0.129	-0.154 ± 0.019	0.163	-0.177 ± 0.030
0.166	-0.153 ± 0.014	0.162	-0.155 ± 0.012	0.159	-0.146 ± 0.014	0.198	-0.158 ± 0.023
0.198	-0.176 ± 0.014	0.195	-0.140 ± 0.012	0.192	-0.128 ± 0.013	0.237	-0.122 ± 0.022
0.233	-0.115 ± 0.015	0.231	-0.151 ± 0.013	0.228	-0.131 ± 0.014	0.279	-0.110 ± 0.023
0.269	-0.146 ± 0.017	0.270	-0.120 ± 0.014	0.267	-0.093 ± 0.014	0.324	-0.089 ± 0.025
0.311	-0.093 ± 0.020	0.311	-0.076 ± 0.017	0.308	-0.089 ± 0.016	0.372	-0.039 ± 0.031
0.354	-0.080 ± 0.022	0.356	-0.112 ± 0.019	0.353	-0.073 ± 0.017	0.424	-0.063 ± 0.035
0.400	-0.058 ± 0.027	0.403	-0.061 ± 0.020	0.401	-0.075 ± 0.020	0.478	-0.028 ± 0.036
0.447	-0.038 ± 0.037	0.454	-0.087 ± 0.024	0.451	-0.071 ± 0.021	0.536	-0.086 ± 0.041
0.497	+0.018 ± 0.042	0.506	-0.087 ± 0.028	0.504	-0.044 ± 0.026	0.597	-0.043 ± 0.048
0.549	+0.033 ± 0.076	0.562	-0.060 ± 0.037	0.560	-0.023 ± 0.030	0.661	-0.036 ± 0.056
0.604	+0.004 ± 0.074	0.620	-0.014 ± 0.038	0.619	-0.002 ± 0.037	0.762	-0.020 ± 0.062
0.661	+0.080 ± 0.082	0.680	-0.028 ± 0.052	0.680	-0.080 ± 0.042		
0.720	+0.054 ± 0.121	0.742	-0.082 ± 0.052	0.748	-0.066 ± 0.056		
0.780	+0.117 ± 0.266	0.807	-0.066 ± 0.056				

Table 2

Beam momentum =6.0 Bev/c		Beam momentum =10.0 Bev/c		Beam momentum = 12.0 Bev/c	
$-t$ $(Bev/c)^2$	P_0	$-t$ $(Bev/c)^2$	P_0	$-t$ $(Bev/c)^2$	P_0
0.122	0.011 ± 0.049	0.90 < -t < 0.143	0.105 ± 0.088	0.090 < -t <0.180	0.053 ± 0.067
0.166	0.283 ± 0.041	0.143 < -t < 0.209	0.168 ± 0.034	0.180 < -t <0.257	0.077 ± 0.037
0.198	0.205 ± 0.025	0.209 < -t <0.287	0.132 ± 0.024	0.267 < -t <0.347	0.043 ± 0.040
0.233	0.182 ± 0.022	0.287 < -t <0.377	0.087 ± 0.028	0.347 < -t <0.566	0.004 ± 0.040
0.271	0.282 ± 0.022	0.377 < -t <0.477	0.092 ± 0.034	0.566 <-t <0.833	- 0.120 ± 0.094
0.311	0.160 ± 0.022	0.477 < -t <0.589	-0.046 ± 0.048		
0.354	0.149 ± 0.027	0.589 < -t <0.776	0.060 ± 0.060		
0.399	0.126 ± 0.030				
0.447	0.131 ± 0.029				
0.497	0.092 ± 0.036				
0.550	0.007 ± 0.048				
0.604	0.055 ± 0.066				
0.690	0.307 ± 0.144				

Table 3

Beam momentum =6.0 Bev/c		Beam momentum =10.0 Bev/c		Beam momentum =12.0 Bev/c	
$-t$ $(Bev/c)^2$	P_0	$-t$ $(Bev/c)^2$	P_0	$-t$ $(Bev/c)^2$	P_0
0.109	0.124 ± 0.069	0.102	0.074 ± 0.072	0.103	0.034 ± 0.055
0.136	0.041 ± 0.034	0.129	0.059 ± 0.030	0.131	0.032 ± 0.023
0.166	0.122 ± 0.025	0.159	0.058 ± 0.023	0.163	0.036 ± 0.018
0.198	0.138 ± 0.016	0.192	0.097 ± 0.015	0.199	0.042 ± 0.013
0.233	0.101 ± 0.014	0.228	0.098 ± 0.013	0.237	0.066 ± 0.012
0.271	0.117 ± 0.014	0.267	0.071 ± 0.013	0.279	0.064 ± 0.013
0.312	0.096 ± 0.015	0.309	0.082 ± 0.014	0.324	0.081 ± 0.014
0.355	0.141 ± 0.017	0.354	0.093 ± 0.017	0.373	0.055 ± 0.017
0.400	0.117 ± 0.018	0.401	0.081 ± 0.018	0.424	0.031 ± 0.019
0.448	0.083 ± 0.019	0.452	0.067 ± 0.019	0.479	0.046 ± 0.020
0.499	0.108 ± 0.023	0.505	0.024 ± 0.023	0.537	0.073 ± 0.023
0.551	0.063 ± 0.029	0.561	0.067 ± 0.028	0.629	0.066 ± 0.026
0.606	0.135 ± 0.041	0.620	0.077 ± 0.037	0.762	0.002 ± 0.056
0.665	0.062 ± 0.080	0.681	0.117 ± 0.046		
0.723	0.092 ± 0.164	0.745	0.080 ± 0.045		

Excited hyperon of mass 1680 Mev [5]

Out of 370000 pictures of a 5.5 Bev/c K^- beam interacting in a 30-inch hydrogen bubble chamber at Argonne, 328 fits to the final state $\Lambda\pi^+\pi^-$ and 89 fits to $\Sigma^0\pi^+\pi^-$. The Dalitz plot and the mass-squared projection for the $\Lambda\pi^+\pi^-$ system showed strong production of $Y_1^*(1385)^+ + \pi^-$ and of $\Lambda + \rho^0$. Further, a significant enhancement was observed at $M^2(\Lambda\pi^+) \sim 2.8$ Bev^2 which would correspond to a resonance $Y_1^*(1680)$. The $\Sigma^0\pi^+$ mass distribution shows no enhancement and the upper limit of 0.25 for the ratio

$$\frac{Y_1^{*+}(1680) \longrightarrow \Sigma^0 + \pi^+}{Y_1^{*+}(1680) \longrightarrow \Lambda + \pi^+}$$

shows that the new resonance is distinct from the $Y_1^*(1660)$ which would give a value 3.4 ± 1.5 for this ratio. The best estimates for the mass and width of the peak are $M = 1683 \pm 15$ Mev and $\Gamma = 120 \pm 30$ Mev. The dominant decay modes is

$$Y_1^*(1680) \longrightarrow Y_1^*(1385) + \pi$$

and

$$Y_1^*(1680) \longrightarrow \Lambda + \pi$$

Search for fractionally charged particles by the magnetic levitation electrometer [6]

Preliminary results in search of terrestrial quarks using a new method are reported.

The method consists in levitating a small grain of a diamagnetic substance, the charge of which is to be determined, in

a magnetic valley. The grain has a stable equilibrium position at the bottom of the valley. When a homogeneous horizontal electric field is applied transverse to the magnetic field, the grain moves to a new equilibrium position. The displacement Δ is given by $\Delta = qER/mg$ where q is the charge, E the electric field and R the radius of curvature of the valley. Δ can also be written as $\Delta = n\delta$ where n is an integer and δ is the displacement corresponding to a change in the charge of the object by one electron charge. If the grain contains a quark, $\Delta = n\delta \pm \frac{1}{3}\delta$. By successive ionizations one can determine the value of δ and determine whether a quark is present or not.

The result of an examination of a total of 1.3×10^8 gm of pyrolitic graphite containing about 10^{16} nucleons shows no evidence for a quark.

References

1) W.G.Jones et al, Physics Letters 23, 597 (1966)

2) W.F.Baker et al, Physics Letters 23, 605 (1966)

3) L.Dobrzynski et al, Physics Letters 23, 614 (1966)

4) M.Borghini et al, Physics Letters 23B, 77 (1967)

5) M.Derrick et al, Phys. Rev. Letters 18, 266 (1967)

6) G.Galliano and G.Morpurgo, Physics Letters 23, 609 (1967)

....

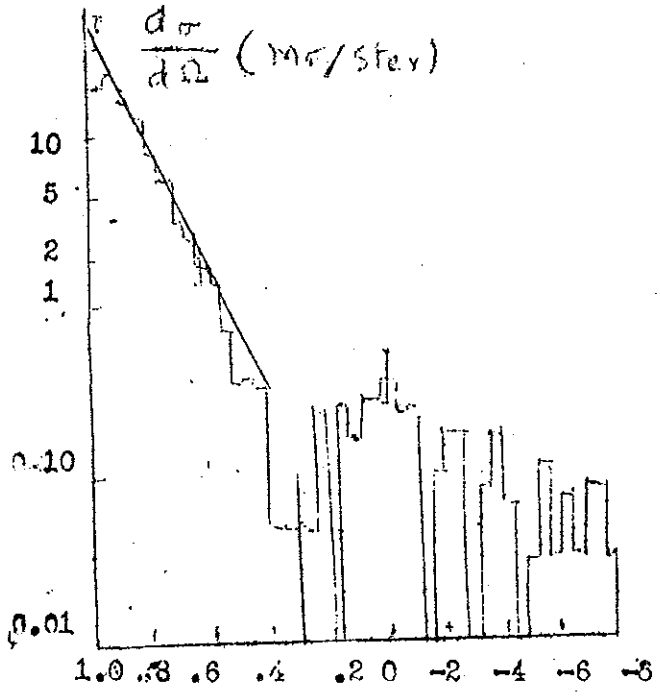

Fig. 1.

MARCH 1967

Introduction

The present report starts with evidence for a new nuclear isobar $N^*_{1/2}(3690)$ of width 0.05 ± 0.03 Bev presented by 8-pions events in π^+-p interactions at 8 Bev/c. The angular correlations of like and unlike pions in this interaction are also presented.

Cross-sections for formation of quasi-two body final states in k^-p interactions at 4.1 and 5.5 Bev/c are given. The predicted equality of the $\Lambda\rho^0$ and $\Lambda\omega$ reaction rates predicted by the quark model is found to be satisfied.

The existence of a $\pi^+\pi^-$ enhancement of mass 1675 Mev and width ~ 100 Mev, reported earlier, is confirmed by a new experiment. The most likely assignment of other quantum numbers is $I^GJ^P = 1^+3^-$.

From measurements in inelastic electron scattering the value of the coupling constant YNN^* is found to be 3.00 ± 0.01.

A new comparison of cross-sections and forward scattering amplitudes with two predictions of SU(3) regarding inequalities for k-p and π-p scattering amplitudes shows good agreement within experimental errors.

Finally cross-sections for elastic and inelastic scattering of electrons from deuterons which are in disagreement with the simple impulse approximation theory are presented.

ELEMENTARY PARTICLES

The heavy nucleon isobar $N^*_{1/2}(3690)$

500 out of 130,000 photographs of π^+-p interactions at 8 Bev/c in the Saclay hydrogen bubble chamber correspond to eight-prong events with a total cross-section $\sigma_8 = (0.30 \pm 0.02)$mb. The individual reactions and the corresponding cross-sections are given in the following table.

Reaction	Number of events	Cross-section (mb)
(1) $\pi^+ + p \rightarrow p + 4\pi^+ + 3\pi^-$	135	0.09 ± 0.02
(2) $\rightarrow p + 4\pi^+ + 3\pi^- + \pi^o$	128	0.09 ± 0.02
(3) $\rightarrow n + 5\pi^+ + 3\pi^-$	51	0.03 ± 0.01

The c.m. momentum distribution of the positive pions show distinct narrow maxima at the same momentum of 0.260 Bev/c in the spectra of positive pions. They do not appear in the π^- spectra. The maxima in the π^+ spectra correspond to the peaks in the $(N\,7\pi)^+$ mass distributions at about 3.7 Bev. For $(N\,7\pi)$ combinations with charge greater than one, no deviation from phase space was observed in the neighbourhood of 3.7 Bev/c which

leads to the assignment T = 1/2 for the isobar. The best Breit-Wigner fit for the mass and width of the resonance.

M = (3.69 ± 0.01) Bev = (0.05 ± 0.03) Bev. The resonance can be thought of as the Regge recurrence of the $N^*(1512)$ succeeding $N^*(3360)$ found recently. The spin theoretically predicted in 2 3/2.

The observed decay modes of the new resonance are given in the following table

Reaction	Decay mode	Number of events
(1)	$p+3\pi^+ + 3\pi^-$	13 ± 10
(2)	$p+3\pi^+ + 3\pi^- + \pi^o$	52 ± 15
(3)	$n+4\pi^+ + 3\pi^-$	33 ± 10

Angular correlations between pions in six- and eight-prong π-p interactions at 8 Bev/c[2)]

The type of angular correlations observed in many-pion $\bar{p}p$ annihilations has been observed in a study of about 750 six-prong and 350 8-prong events of 8 Bev/c π^+ interacting with protons in a hydrogen bubble chamber. The values of the parameter r, defined as the ratio of the number of pion pairs with ϑ c.m.

production opening angle greater than 90^{o} to that with the opening angle smaller than 90^{o} are given for various final states in the following table, γ^{ℓ} correspond to like pions ($\pi^{+}\pi^{+}$ and $\pi^{-}\pi^{-}$) and γ^{n} to unlike pions ($\pi^{+}\pi^{-}$).

Reaction	r^{n}	r^{l}
Six prong interactions		
(1) $\pi^{+}+p \rightarrow p+3\pi^{+}+2\pi^{-}$	1.45 ± 0.09	1.11 ± 0.09
(2) $\rightarrow p+3\pi^{+}+2\pi^{-}+\pi^{o}$	1.29 ± 0.06	1.39 ± 0.07
(3) $\rightarrow n+4\pi^{+}+2\pi^{-}$	1.47 ± 0.09	1.35 ± 0.09
Eight-prong interactions		
(4) $\pi^{+}+p \rightarrow p+4\pi^{+}+3\pi^{-}$	1.46 ± 0.05	1.11 ± 0.04
$\rightarrow p+4\pi^{+}+3\pi^{-}+\pi^{o}$	1.40 ± 0.04	1.09 ± 0.04
$\rightarrow n+5\pi^{+}+3\pi^{-}$	1.25 ± 0.05	1.15 ± 0.05

r^{n} and r^{l} as functions of the momentum difference $|p_i|-|p_n|$ show deviations from the predictions of the statistical model.

Meson-hyperon final states in k^-p interactions at 4.1 and 5.5 Bev/c[3)]

k-p interactions at 4.1 and 5.5 Bev/c were used to study hypercharge exchange processes leading to quasi-two-body final states. The following table gives the various final states observed and the corresponding cross-sections. The predicted equality of the $\Lambda\rho^0$ and $\Lambda\omega$ reaction rates of the quark model is found to be correct by the results for $\bar{\sigma}$, the forward hemisphere cross-section. The backward peak seems to be absent in the $\Lambda\varphi$, ΛX^0 and $\Lambda\eta$ processes.

Final State	k- Momentum (Bev/c)	Number of events corrected	Cross-section (μb)	$\bar{\sigma}$ normalized to $\Lambda\rho^0$ phase space (μb)	Λ polarization (Asymmetry parameter $\alpha = 0.66 \pm 0.05$)
$\Lambda\rho^0$	4.1	38 ± 16	57 ± 26	44 ± 19	- 0.9 ± 0.6
	5.5	35 ± 12	23 ± 8	17 ± 6	- 0.8 ± 0.7
$\Lambda\omega$	4.1	37 ± 10	62 ± 17	43 ± 12	- 1.0 ± 0.5
	5.5	32 ± 10	24 ± 8	19 ± 6	- 0.1 ± 0.6
$\Lambda\varphi$	4.1	15 ± 4	59 ± 16	65 ± 17	+ 0.2 ± 0.8
	5.5	17 ± 5	30 ± 9	32 ± 9	+ 1.0 ± 0.7

Final State	K- Momentum (Bev/c)	Number of events corrected	Cross-section (μb)	$\bar{\sigma}$ normalized to $\Lambda\pi^0$ phase space (μb)	Λ polarization (Asymmetry paramter α=0.06±0.05
$\Lambda\pi^+$	4.1	17 ± 3	42 ± 18	39 ± 17	
	5.5	3 ± 2	8 ± 5	8 ± 5	
ΛK^0	4.1	12 ± 4	51 ± 17	55 ± 18	
	5.5	10 ± 4	19 ± 8	20 ± 8	
$\Sigma^0\rho^0$	4.1	≤ 19 ± 10	≤ 38 ± 20	≤24 ± 13	
	5.5	≤ 7 ± 5	≤ 6 ± 4	≤ 5 ± 4	
$\Sigma^0\varphi$	4.1	≤ 10 ± 4	≤ 53 ± 21	≤ 61 ±24	
	5.5	≤ 11 ± 4	≤ 26 ± 10	≤ 29 ± 11	
$\rho^0 Y_1^*(1385)$	4.1	0 ± 8	0 ± 13	0 ± 16	
	5.5	11 ± 11	8 ± 8	≤ 9 ± 9	

Evidence for an I = 1 di-pion resonance at 1.67 Bev[4)]

The existence of a $\pi^+\pi^-$ enhancement with a mass of 1675 Mev was reported earlier in high energy πN reactions. In the present experiment the existence of the enhancement is confirmed and its parameters are determined. $\pi^\pm$p interactions at 6 Bev/c were studied in the BNL 80" inch liquid hydrogen bubble chamber. 373 events of the $(\pi^+\pi^+n)$, 1308 events of the

($\pi^-\pi^0 p$) and 2661 events of the ($\pi^-\pi^+ n$) final states were observed. The mass distribution plots show no significant structure in the $\pi^+\pi^+$ mass distribution. The $\pi^-\pi^0$ distribution shows the ρ^- and a peak at 1630 Mev with a width of $\sim$ 100 Mev. The $\pi^+\pi^-$ distribution shows the ρ^0, f^0 and a broad $\pi^+\pi^-$ bump from 1560 to 1800 Mev. The results for the quantum numbers of the 1630 Mev enhancement are:

G parity: The strong decay into two pions shows that G is positive.

Isospin:- The $\pi^-\pi^0$ decay mode requires $I \geq 1$. An $I = 2$ assignment would give for the relative intensities for $\pi^+\pi^+\pi^-\pi^0$ and $\pi^+\pi^-$ [illegible] 36, 9 and 2. The data disagree with this assignment are quite compatible with the value $I = 1$.

Spin-Parity:- $I = 1$ implies by Bose statistics, odd parity and odd spin. The moments of the Legendre polynomials of the $\pi^-\pi^0$ scattering angular distribution indicate the assignment, $J^P = 3^-$.

Measurement of the γNN^* form factors[5)]

The magnetic dipole contribution to the inelastic electron scattering process $e^- + p \rightarrow e + N^*(1230)$ gives a measure of the form factor G_M^* which extrapolated to zero momentum transfer yields the value of the magnetic dipole γNN^* form factor. By

measuring the inelastically scattered electrons in coincidence with protons from $N^* \to p+\pi^0$, the value of γ_{NN^*} obtained was 3.00 ± 0.01. SU(6) and its relativistic generalizations predict a value 2.66.

SU(3) predictions and reaction inequalities at high energies[6)]

Two sets of comparisons, one regarding the total inelastic and elastic cross-sections and the other using the forward amplitudes were made between experiment and the SU(3) predicted inequalities

$$M(K^- + p \to \Sigma^+ + \pi^-) \geq |M(\pi^- + p \to \pi^- + p) - M(K^- + p \to K^- + p)| \quad (1)$$

$$M(\pi^+ + p \to \Sigma^+ + K^+) \geq |M(\pi^- + p \to \pi^+ + p) - M(K^+ + p \to K^+ + p)| \quad (2)$$

The comparisons are made as a function of $\mathcal{S}$ the available center of mass energy, $\mathcal{S} = s^{1/2} - m_{out}$ with s the square of the total c.m. energy and m_{out} the total mass of the final state. Contrary to earlier analyses the SU(3) predictions are found to be satisfied within experimental errors. Table 1 below gives the experimental values for the integrated amplitudes and Table 2 the experimental values for the forward amplitudes. The M's are the invariant amplitudes.

Table 1

E_{Lab} Bev	P_{Lab} Bev/c	σ (mb)	M_{Kp} (mb)	$1/2_{Bev}$	P_{Lab} Bev/c	σ mb	$M_{\pi p}$ (mb)	$1/2_{Bev}$	$M_{K_p} - M_{\pi_p}$	P_{Lab} Bev/c	δ Bev	σ (mb)
		$k^- + p \rightarrow k^- + p$				$\pi^- + p \rightarrow \pi^- + p$			Difference	$k^- + p \rightarrow \Sigma^+ + \pi^-$		
0.803	2.0	7.5 ± 0.5	6.12 ± 0.20		1.40	9.6 ± 1.0	5.83 ± 0.30		0.29±0.36	1.95	0.889	0.5 ±0.05
1.183	3.0	4.9 ± 0.3	5.79 ± 0.18		2.26	8.0 ± 1.5	6.40 ± 0.59		0.61±0.61	2.24	1.005	0.29±0.03
1.340	3.46	4.8 ± 0.4	6.07 ± 0.25		2.67	7.5 ± 1.0	6.63 ± 0.44		0.56±0.50	3.0	1.283	0.24±0.02
1.583	4.1	4.3 ± 0.4	6.16 ± 0.25		3.20	6.1 ± 0.7	6.46 ± 0.37		0.30±0.44	3.5	1.460	0.21±0.03
1.948	5.5	4.1 ± 0.4	6.84 ± 0.29		3.92	6.6 ± 0.2	7.77 ± 0.37		0.93±0.32	4.1	1.654	0.10±0.02
2.373	7.2	4.23 ± 0.85	7.82 ± 0.78		5.44	5.57 ± 0.3	8.14 ± 0.52		0.32±0.81	5.5	2.064	0.79±0.01
2.788	9.0	3.95 ± 0.78	8.39 ± 0.76		6.56	5.25 ±0.26	8.16 ± 0.22		0.47±0.79			
		$k^+ + p \rightarrow k^+ + p$				$\pi^+ + p \rightarrow \pi^+ + p$				$\pi^+ + p \rightarrow \Sigma^+ + k^+$		
0.455	1.2	10.6 ± 0.6	6.13 ± 0.17		0.76	13.0 ± 1.0	5.52 ± 0.21		0.61±0.27	1.75	0.364	0.37±0.07
0.802	2.0	5.7 ± 0.5	5.33 ± 0.23		1.40	19.5 ± 2.0	8.30 ± 0.43		2.97±0.49	3.0	0.872	0.12±0.03
1.181	3.0	4.8 ± 0.4	5.72 ± 0.24		2.25	8.5 ± 1.5	6.59 ± 0.58		0.87±0.63	4.0	1.216	0.06±0.006
2.268	6.8	3.48 ±0.43	6.91 ± 0.63		5.04	6.1 ± 1.0	8.26 ± 0.67		1.35±0.79			
2.968	9.8	3.34 ±0.17	8.04 ± 0.20		7.84	5.06 ±0.78	9.10 ± 0.68		1.06±0.71	8.0	2.305	0.025±0.01
3.618	12.8	3.34 ±0.15	9.23 ± 0.20		11.44	4.48 ±0.61	9.94 ± 0.68		0.71±0.71			
3.968	14.8	3.41 ±0.17	9.97 ± 0.25		13.24	4.31 ±0.58	10.5 ± 0.7		0.51±0.7			

Table 2

Q	$\frac{d\sigma}{dt}$ at t = 0 mb/(Bev/c)^2	M_{k_p}	$\frac{d\sigma}{dt}$ at t = 0 mb/(Bev/c)^2	Total (mb)	M_{π_p}	$\lvert M_{k_p} - M_{\pi_p} \rvert$	Q	$\frac{d\sigma}{dt}$ at $\theta^* = 0$ $\frac{mb}{(Bev/c)^2}$	M_t
	$k^- + p \rightarrow k^- + p$		$\pi^- + p \rightarrow \pi^- + p$					$k^- + p \rightarrow \Sigma^+ + \pi^-$	
803	12.9 ± 1.0	8.0 ± 0.3	10.0 ± 1.0		5.9 ± 0.3	2.1 ± 0.4	0.889	0.87±0.16	0.96±0.08
183	41.6 ± 3.7	10.3 ± 0.5		36.0 ± 1.0	9.6 ± 0.3	0.7 ± 0.5	1.005	0.32±0.08	0.67±0.08
340	40.0 ± 2.8	11.6 ± 0.4		33.7 ± 0.3	10.6 ± 0.1	1.0 ± 0.4	1.288	0.80±0.06	1.42±0.06
583	32.3 ± 2.7	12.7 ± 0.5		32.0 ± 0.3	12.6 ± 0.1	0.1 ± 0.5	1.460	0.70±0.02	1.55±0.23
948	32.6 ± 2.7	16.5 ± 0.7		30.6 ± 0.3	16.1 ± 0.2	0.4 ± 0.7	1.650	0.49±0.14	1.52±0.23
373	38.5 ±11.0	23.3 ± 3.3		28.8 ± 0.3	20.2 ± 0.2	3.1 ± 3.3	2.064	0.61±0.14	2.27±0.26
788	37.0 ±11.0	28.6 ± 4.3		27.6 ± 0.3	24.6 ± 0.3	4.0 ± 4.3			
	$k^+ + p \rightarrow k^+ + p$		$\pi^+ + p \rightarrow \pi^+ + p$					$\pi^+ + p \rightarrow \Sigma^+ + k^+$	
802	4.8 ± 0.5	4.9 ± 0.3	12.4 ± 1.5		6.6 ± 0.4	1.7 ± 0.5	0.364	0.71±0.8	0.77±0.1
181	19.5 ± 2.3	7.0 ± 6.4		30.5 ± 0.5	8.2 ± 0.1	1.1 ± 0.4	0.947	1.0 ±0.2	1.69±0.17
268	19.7 ± 4.3	15.7 ± 1.7		26.7 ± 0.9	17.5 ± 0.6	1.8 ± 1.8	1.261	1.05±0.4	2.23±0.45
968	19.7 ± 1.5	22.8 ± 0.9	42.3 ± 2.0		28.7 ± 0.7	5.9 ± 1.1			
618	22.0 ± 1.4	32.2 ± 1.0	38.0 ± 2.0		36.7 ± 1.0	4.5 ± 1.4			
968	22.3 ± 1.6	37.3 ± 1.3	37.5 ± 2.0		42.4 ± 1.1	5.1 ± 1.7			

Electron-Scattering from the deuteron at $\theta = 180^{\circ}$

The differential cross-sections for elastic and inelastic electron scattering (M1 transitions) from the deuteron at a scattering angle of 180° and incident electron energies up to 370 Mev. The results show disagreement with simple impulse approximation theory. The results are given in the following table. $d\sigma_J/dp$ is the differential cross-section at $p = 0.98X$ threshold as predicted by the modified Jankus theory; σ_{el} is the experimental e-D cross-section. σ/σ_J is the ratio of the inelastic cross-section to that predicted by the modified Jankus theory.

E_0 (Mev)	q^2 (F^{-2})	$\frac{\sigma}{\sigma_J}$	$d\sigma_J/dp$ [10^{-36} cm^2 sr^{-1} (Mev/c)$^{-1}$]	σ_{el} (10^{-36} cm^2/sr)
250	5.07	1.08±0.07	50.4	83 ± 9
275	6.01	1.25±0.08	25.9	56 ± 7
360	7.01	1.20±0.35	13.4	
325	8.06	1.38±0.12	6.86	24.5 ± 2.6
350	9.17	1.62±0.18	3.49	13.9 ± 2.4
370	10.09	2.17±0.20	2.01	6.9 ± 1.4

References

(1) J.Bartke et al, Physics Letters 24B, 118 (1967).

(2) J.Bartke et al, Physics Letters 24B, 163 (1967).

(3) J.Mott, Phy. Rev. Letters 18, 365 (1967).

(4) D.J.Crennell et al, Phys. Rev. Letters 18, 323 (1967).

(5) W.W.Ash et al, Physics Letters 24B, 165 (1967).

(6) S.Meshkov and G.B.Yodh, Phys. Rev. Letters 18, 474 (1967)

(7) R.E.Rand et al, Phys. Rev. Letters 18, 469 (1967).

****

INTRODUCTION

The present report starts with a list of resonances (and their parameters) in the $k^- - p \rightarrow \Sigma \pm \pi^{\mp}$ interactions which contains two new ones, one in the D_{03} channel at 1682 Mev and another in the D_{05} channel at 1827 Mev.

Differential cross-sections for backward elastic scattering of $\pi^+ - p$ at π^+ momenta 2.06 - 4.70 Bev/c are given.

A resonance in the $\Lambda\eta^o$ system with isospin T = o and mass about 1680 is reported as also a resonance in the $\pi^o\gamma$ system with a mass of ~ 1300 Mev.

The cross-sections for photoproduction of π^+ in the energy range 1.2 and 3 Bev are given.

A new peak (either $Y_1^*(2065)$ or $Y_o^*(2100)$) seems to be present in the final state of $k^- + p \rightarrow k^- + p + \omega^o$ at 3.8 Bev/c k^- incident momentum.

Cross-sections for various 3 body final states in $k^- p$ interactions at 4.25 Bev/c are given. Evidence for N* resonance with masses 2080 and 2190 Mev are forthcoming in a study of 4 body final states in 3 Bev/c $\pi^- p$ interactions. Clear evidence for two peaks in the mass region 1.7 and 1.84 Bev is present in the 4 pion final states in $p\bar{p}$ annihilation at 2.5 and 3 Bev/c.

The results of phase shift analysis of $k^+ p$ elastic scattering at 780 Mev/c are presented.

Finally the results of an experiment on $k^- p$ scattering which show backward peaking for $k^+ p$ elastic scattering are presented.

Resonances in $k^-p \to \Sigma\pi$ between 780 and 1220 Mev [1]

The reactions $k^-p \to \Sigma^+\pi^-$ and $k^-p \to \Sigma^-\pi^+$ were studied for k^- momenta between 780 and 1220 Mev/c. An energy dependent analysis was made by measuring the partial and differential cross sections and the Σ^+ polarization. A measurement was also made of the $\Sigma\pi$ branching fraction for decay into $Y_0^*(1820)$ and $Y_1^*(1760)$. The existence of a resonance in the D_{03} channel at 1682 Mev was confirmed and another in the D_{05} channel at 1827 Mev found. The masses and widths of the various resonances are given in the following table. $t = (xx')^{1/2}$ is the value of the amplitude at resonance, $x = \frac{\Gamma_{el}}{\Gamma}$ is the elasticity and $x' = \frac{\Gamma_{\Sigma\pi}}{\Gamma}$, the $\Sigma\pi$ branching fraction.

Resonant amplitudes	Mass (Mev)	Width (Mev)	Amplitude at resonance (t)	Elasticity (b)	Branching fraction (x')
D_{03}	1682±2	55 ± 4	0.34 ± 0.02	0.25	0.46 ± 0.06
D_{13}	1685±3	32 ± 4	0.26 ± 0.02	0.10	0.67 ± 0.10
D_{05}	1827±3	75 ± 9	0.15 ± 0.02	0.10	0.23 ± 0.06
D_{15}	1760	120	0.07 ± 0.02	0.44	0.01 ± 0.006
F_{05}	1813±2	87 ± 15	0.27 ± 0.01	0.60	0.12 ± 0.01
F_{15}	1015	65	0.00 ± 0.01	0.66	0.00 ± 0.01
F_{17}	2040	150	-0.12	0.25	0.06
G_{07}	2100	160	-0.12	0.25	0.06

Structure in π^+p elastic backward scattering[2)]

Measurements of the differential cross-sections of π^+p backward elastic scattering were made for π^+ momenta in the range 2.06 - 4.70 Bev/c and at the fixed angle of recoil protons $\theta_p = 1.9^\circ$ in lab. system. The differential cross-sections are given in the following table which shows the maxima corresponding to the baryon resonances $\Delta(2420)$ and $\Delta(2840)$.

p_π (Bev/c)	$\cos\Theta^*$ (c.m.s.)	$d\sigma/d\Omega$ (μb/sterad)
2.06	0.9952	45.2 ± 16.0
2.25	0.9950	93.2 ± 32.2
2.55	0.9946	190.0 ± 27.3
2.79	0.9944	107.0 ± 19.9
2.94	0.9942	83.5 ± 14.3
3.19	0.9940	33.1 ± 7.2
3.46	0.9937	53.5 ± 9.8
3.66	0.9935	51.3 ± 9.7
3.84	0.9932	58.2 ± 9.5
4.03	0.9930	55.0 ± 7.4
4.26	0.9927	29.0 ± 6.5
4.54	0.9924	19.6 ± 4.7
4.70	0.9920	15.9 ± 4.2

The $\Lambda\eta^0$ resonance in π^-p interactions at 4.0 Bev/c[3]

Λ^0 production by 4.0 Bev/c primary pions was studied using the electron-positron pair generated by the conversion of γ rays appearing in the interaction. The effective mass distribution has two characteristic enhancements. One of these in the region $M_{\Lambda\gamma}$ = 1150 - 1200 Mev is due to Σ^0 production while the second in the region $M_{\Lambda\gamma}$ = 1300 - 1400 Mev shows evidence for production of a new resonance $\Lambda\eta^0$ with isospin T = 0 and mass about 1680 Mev.

Study of resonances in the $\pi^0 r$ system[4]

The reaction (involving 3r)

$$\pi^- + p \longrightarrow n + X^0 \quad (X^0 \longrightarrow \pi^0 + \gamma)$$

was studied at 2.8 Bev/c. There was an enhancement for angles greater than 130° which could not be explained as due to the ω-meson (decaying to π^0+r). The enhancement is attributed a $\pi^0 r$ resonance X^0 with mass $\sim$ 1300 Mev.

π^+ photoproduction between 1.2 and 3 Bev at very small angles[5]

The production cross-sections of π^+ by photons of energies between 1.2 and 3 Bev and pion c.m. angles from 2.5 to 15° were measured. The cross-section is strongly peaked in the forward direction and shows resonance structure in the region of the $N^*_{3/2}(1920)$ and $N^*_{1/2}(2190)$. The forward peaking is in contradiction with the simple peripheral models and their Reggeized versions which predict a vanishing cross-section in the forward direction. Interference of s and t channel poles and inclusion of absorptive effects lead to agreement only at small angles and low energies.

The differential cross-sections are given in the following table:

Er (Bev) / $\theta_{\pi}^{c.m.}$	2.5°	5°	7.5°	10°	15°
1.23	6.09 ± 0.41	5.45 ± 0.25	4.04 ± 0.22		3.21 ± 0.20
1.37	4.41 ± 0.44	4.01 ± 0.18		2.71 ± 0.14	
1.52	6.34 ± 0.43	4.81 ± 0.29	4.09 ± 0.21	3.94 ± 0.14	2.71 ± 0.19
1.66	6.40 ± 0.50	5.21 ± 0.27	4.78 ± 0.22	3.41 ± 0.17	
1.80	5.58 ± 0.28	5.58 ± 0.28	4.75 ± 0.19	3.62 ± 0.19	3.34 ± 0.16
1.99	4.94 ± 0.36	4.77 ± 0.19		3.61 ± 0.16	3.30 ± 0.15
2.18	5.70 ± 0.29	4.20 ± 0.20		3.18 ± 0.16	2.60 ± 0.13
2.38	4.39 ± 0.35	3.17 ± 0.16		2.44 ± 0.13	2.28 ± 0.10
2.60	4.38 ± 0.25	2.96 ± 0.10		2.34 ± 0.12	2.24 ± 0.09
2.86		2.96 ± 0.12		2.19 ± 0.09	2.17 ± 0.11

The reaction $k^- + p \rightarrow k^- + p + \omega^0$ at 3.8 Bev/c [6]

events of the type $k^- + p \rightarrow k^- + p + \omega^0$ were observed in k^--p interaction at 3.8 Bev/c in the BNL 80-inch hydrogen bubble chamber. The k^--p distribution shows that $Y_0^*(1520)$ is produced strongly with very little background, $Y_1^*(1660)$ is absent and the $Y_0^*(1815)$ peak is present and does not contain a large admixture of $Y_1^*(1765)$. There appears to be a peak near 2050 Mev which may be $Y_1^*(2065)$ or the $Y_0^*(2100)$. The cross-sections are given in the following table

Channel	Cross section (μb)
$Y_0^*(1520)$	20 ± 3
$Y_1^*(1660)$	< 5
$Y_0^*(1815) \pm Y_1^*(1765)$	23 ± 7
$Y_1^*(2065) + Y_0^*(2100)$	27 ± 8
$k^- p \omega$ nonresonant	6 ± 10

Resonance production in $\Xi\pi$ and $Y\bar{K}K$ final states in K^--p interactions at 4.25 Bev/c[7]

Three body final states were studied in K^- interactions at 4.25 Bev/c. The following table gives the cross-sections. The $k_1^o k_1^o$ system exhibits a resonance, $f^*(1500)$. φ, $\Xi^*(1530)$ and $K^{*+}(890)$ are also present in the appropriate channels.

Final state	Observed No. of events	σ (μb)
$\Xi^- K^+ \pi^o$	23.2	15.6 ± 3.7
$\Xi^- K^o \pi^+$	46.9	19.9 ± 3.2
$\Lambda + \varphi$ ($\varphi \to k_1^o + k_2^o$)	46.0	22.7 ± 3.4
$\Lambda\ k_1^o\ k_1^o$	18.3	9.8 ± 2.4
$\Lambda\ k_1^o\ k_2^o$ (non φ)	16.7	8.0 ± 2.8
$\Sigma^o k_1^o k_1^o$	11.3	6.0 ± 1.9

Evidence for N^* resonances of masses 2080 and 2190 Mev[8)]

Two enhancements in the mass spectrum of ainal state $p\pi^+\pi^-\pi^0$ combinations have been observed in 3 Bev/c π^- - interactions with hydrogen. The mass plot shows deviations from phase space in two regions and are possibly due to N^* resonances of mass 2080 ± 12 Mev and 2190 ± 12 Mev, each with widths of 40 ± 20 Mev. The mass plots for $p\omega$ and $p\eta$ states show no enhancement at these masses. The evidence for the decay of both the enhancements into $N^{*++}(1236)\rho^-$ is strong. Taking account of possible decay into $N^{*+}\rho^0$ and $N^{*0}\rho^+$ the observed yields in these channels are consistent with an assignment of T = 1/2 for the $N^*(2080)$.

Evidence for the existence of mesons decaying into 4 pions[9)]

An analysis was undertaken of the 1988 six-prong events at 3 Bev/c and 2273 six-prong events at 2.5 Bev/c of the annihilation of the proton-antiproton systems into multipions. In the configuration $p\bar{p} \rightarrow 3\pi^+\pi^-$ a structure was observed in the $2\pi^+ 2\pi^-$ mass distribution. Clear evidence is present for two peaks in the mass regions of 1.7 and 1.84 Bev. A Gaussian fit gives the masses and widths:

$$M(1.7) = (1717 \pm 7)\text{Mev}, \quad \Gamma = (40 \pm 12)\text{ Mev}.$$

$$M(1.84) = (1832 \pm 6)\text{ Mev}; \quad \Gamma = (42 \pm 11)\text{ Mev}.$$

The lower peak corresponds to the centre of the R^- group of mesons at 1.691 Bev found earlier by the Maglic group. Assuming strong decay is G parity is +1 and the $\rho^0\rho^0$ decay is forbidden.

Phase shift analysis of k^+p elastic scattering at 780 Mev/c[10)]

45000 pictures of k^+p elastic scattering events at 780 Mev/c were analysed. A phase shift analysis shows that a predominant s-wave scattering with small p and d-waves explains the data. The total elastic scattering cross-section was found to be $\sigma_{el} = (12.6 \pm 0.4)$mb. The differential cross-sections are given in the following table (Table 1) and the phase shifts in Table 2. In the second table A, B and C solutions crorespond respectively to solutions with dominant s-wave, $p_{1/2}$ wave or a mixture of $p_{1/2}$ and $p_{3/2}$ waves. The δ's are phase shifts and the η's are the inelasticity parameters.

Table 1

Cos θ* interval	$d\sigma/d\Omega$ (mb/ster)
-1.00 - -0.90	1.137 ± 0.064
-0.90 - -0.80	1.073 ± 0.061
-0.80 - -0.70	1.055 ± 0.060
-0.70 - -0.60	0.953 ± 0.057
-0.60 - -0.50	0.137 ± 0.064
-0.50 - -0.40	0.984 ± 0.058
-0.40 - -0.30	0.886 ± 0.054
-0.30 - -0.20	0.929 ± 0.056
-0.20 - -0.10	0.929 ± 0.056
-0.10 - -0.00	0.912 ± 0.055
-0.00 - 0.10	0.893 ± 0.055

cos θ* interval	dσ/dΩ (mb/ster)
0.10 - 0.20	0.887 ± 0.055
0.20 - 0.30	0.848 ± 0.053
0.30 - 0.40	0.970 ± 0.058
0.40 - 0.50	0.876 ± 0.055
0.50 - 0.60	1.064 ± 0.062
0.60 - 0.70	1.006 ± 0.060
0.70 - 0.80	1.059 ± 0.063
0.80 - 0.90	1.134 ± 0.065
0.90 - 0.95	1.375 ± 0.095

Table 2

	δ ($s_{1/2}$) / η ($s_{1/2}$)	δ ($p_{1/2}$) / η ($p_{1/2}$)	δ ($p_{3/2}$) / η ($p_{3/2}$)	δ ($d_{3/2}$) / η ($d_{3/2}$)	δ ($d_{5/2}$) / η ($d_{5/2}$)	σ_{tot} (mb)	σ_{inel} (mb)
A^-	-42.68±1.08	-3.96±7.41	2.36±3.98	1.38±3.58	-2.39±1.48	12.667	0.52
spd	.9770±0.0042	0.9923±0.003	0.9953	1.000	1.000		
A^+	41.37±1.84	12.00±3.66	-5.00±1.99	-0.42±1.02	3.54±0.45	13.595	0.518
spd	0.9917±0.0009	0.9777±0.0015	0.9953	1.000	1.000		
p^-	12.01±8.41	-40.47±5.07	-3.21±1.34	-5.17±3.60	0.53±0.79	12.853	0.570
spd	0.9953±0.0007	0.9739±0.0017	0.9953	1.000	1.000	13.467	0.523
p^+	0.370±3.97	44.61±0.75	3.41±0.39	-1.04±2.73	1.24±0.41		
spd	0.9918±0.0092	0.4772±0.0103	0.9954	1.000	1.000	12.586	0.520
n	-3.80±9.06	14.49±2.41	-26.65±0.58	-0.61±0.73	1.91±3.98	13.680	0.521
spd	0.9952±0.0007	0.9739±0.0016	0.9953	1.000	1.000		
$\bar{p}$	-12.64±3.86	-7.56±2.50	36.59±1.20	-1.04±0.97	5.62±1.35		
spd	0.9843±0.0019	0.9849±0.0112	0.9953	1.000	1.000		

Backward elastic scattering in the kp system at 3.55 Bev/c[11)]

kp elastic scattering was studied at angles from 168° to 177° to find out whether there is any backward peak as in pion-nucleon scattering. The differential cross-sections are given in the following table. The K^+p elastic scattering exhibits a backward peak.

Particle	$\cos\theta_{c.m.}$	$-t$ (Bev/c)^2	u (Bev/c)^2	No. of events	$d\sigma/d\Omega$ (μb/sr)	$\frac{(d\sigma/d\Omega)}{(d\sigma/d\Omega)_{\theta=0}} \times 10^3$	$\frac{d\sigma}{dt} = \frac{d\sigma}{d(-t)}$ μb/(Bev/c)^2
K^+	-0.9835	5.607	0.065	7	14.9 ± 5.6	2.13	33.1±12.5
K^+	-0.9940	5.636	0.035	15	21.3 ± 5.5	3.02	47.4±12.2
K^+(average)	-0.9875	5.618	0.016	22	17.3 ± 3.7	2.47	38.6±8.2
K^-	-0.9875	5.618	0.016	0	<6.6	< 0.04	< 1.4
$K^+(u \simeq 0)$	-0.9818	5.602	0.000	-	14.0 ± 6.2	1.99	31.2±13.8
$K^+(180°)$ extrapolated	-1.0000	5.653	0.052	--	26.1 ± 12.0	3.73	58.1±26.7

REFERENCES

1) R. Armenteros et al, Physics Letters 24B, 198 (1967).

2) T. Dobrowski et al, Physics Letters 24B, 203 (1967).

3) E. G. Bubelev et al, Physics Letters 24B, 246 (1967).

4) V. V. Barmin et al, Physics Letters 24B, 249 (1967).

5) G. Buschhorn et al, Phys. Rev. Letters 14, 571 (1967).

6) D. D. Carmony et al, Phys. Rev. Letters 18, 615 (1967).

7) G. S. Abrams et al, Phys. Rev. Letters 18, 620 (1967).

8) T. S. Yoon et al, Physics Letters 24B, 307 (1967).

9) J. A. Danysz et al, Physics Letters 24B, 309 (1967).

10) S. Focardi et al, Physics Letters 24B, 314 (1967).

11) J. Banaigs et al, Physics Letters 24B, 317 (1967).

Total annihilation cross section
Fig 1

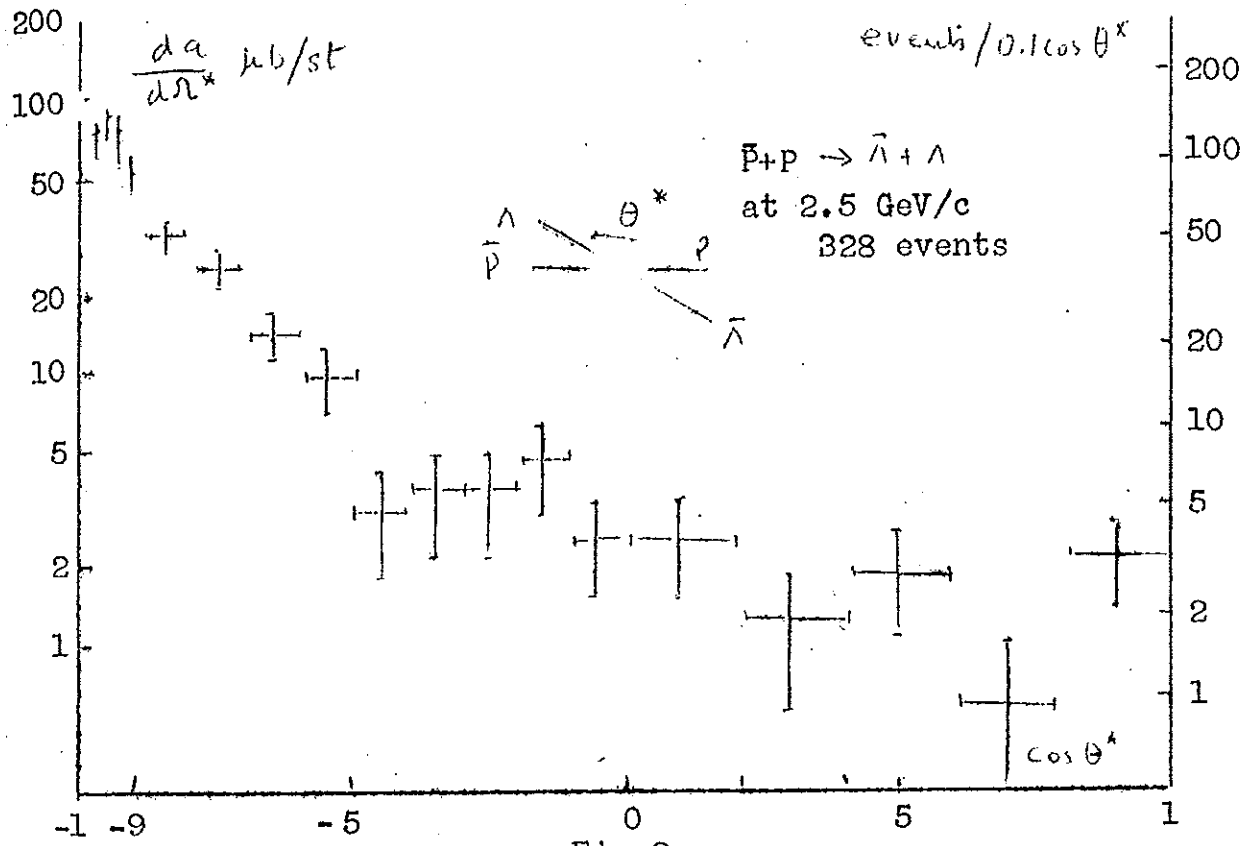
$\frac{d\sigma}{d\Omega^*}$ μb/st
events/0.1 cos θ*
$\bar{p}+p \rightarrow \bar{\Lambda} + \Lambda$
at 2.5 GeV/c
328 events
θ*
cos θ*

Fig 2

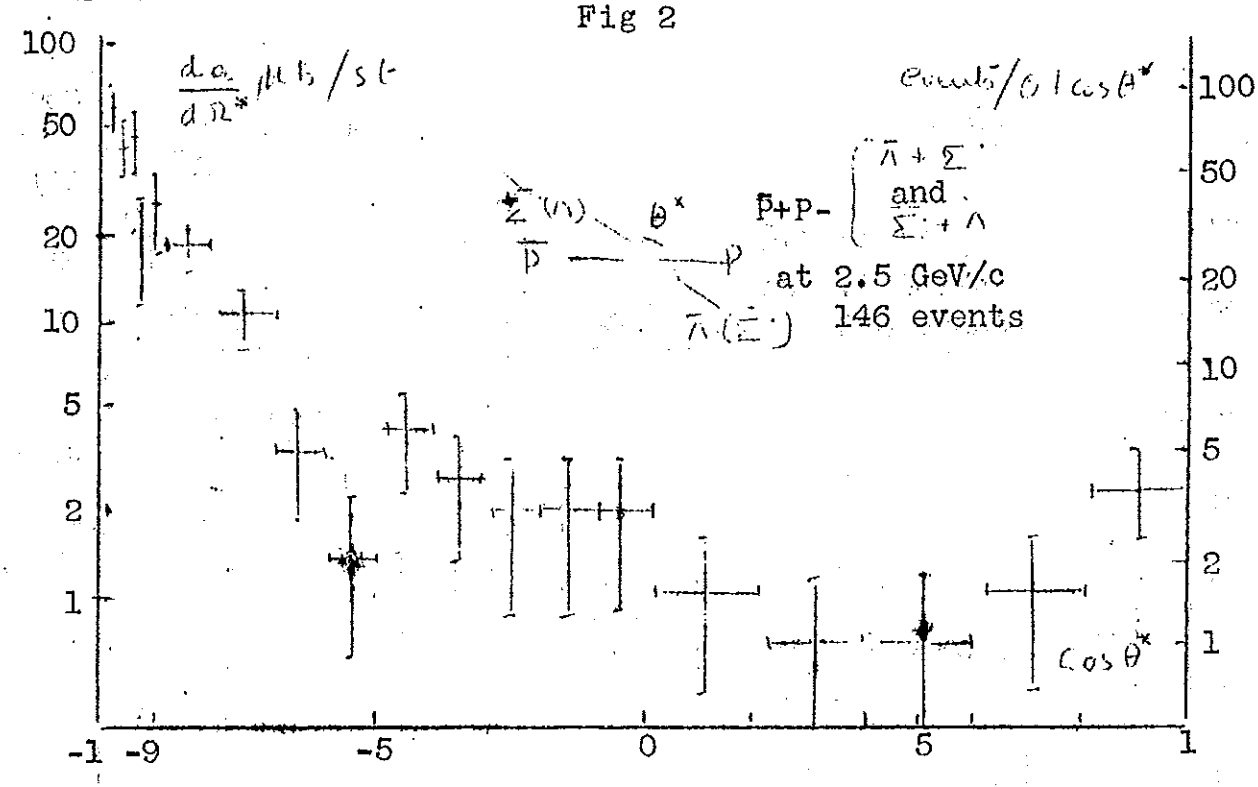
$\frac{d\sigma}{d\Omega^*}$ μb/st
events/0.1 cos θ*
$\bar{p}+p-$ { $\bar{\Lambda} + \Sigma$ and $\bar{\Sigma} + \Lambda$
at 2.5 GeV/c
146 events
θ*
cos θ*

Fig 3

MAY 1967

Introduction

The present report starts with π^o photoproduction cross-sections for incident photon energies in the range 2 to 5 Bev.

The branching ratios for leptonic decays of the vector mesons are given.

The cross-sections. (differential and total) for scattering of photons of energy 970 Mev and 1300 Mev from carbon and Tungsten targets are given.

A determination of the $\eta \longrightarrow \pi^+ + \pi^- + \pi^o + \gamma$ decay rate gives a very small branching ratio for this decay in contradiction with theoretical prediction.

The branching ratios for the decay of η into 2γ, $\pi^o\gamma\gamma$ and $3\pi^o$ are given.

Two experiments to test time reversal invariance, one in β-decay of Ne^{19} and the other in $K^o_{\mu 3}$ decay are given. The results of both experiments are consistent with T-invariance.

ELEMENTARY PARTICLES

π^0 Photoproduction cross sections for incident γ -ray energies of 2.0 to 5.0 Bev[1].

The photoproduction of neutral pions for incident photons in the energy range 2.0-5.0 Bev and of baryon four-momentum transfer squared. 0.5 to 4.0 $(Bev/c)^2$ was studied using the bremsstrahlung beam from the Cambridge Electron Accelerator. The result of the measurements for the differential cross-sections are shown in Fig. 1. Fig. 1a gives $\frac{d\sigma}{dt}$ in units of nano-barns per $(Bev/c)^2$ as a function of -t for several incident photon energies. Fig. 1b gives $d\sigma/dt$ as function of E_γ for several values of $1\ |t|$. The behaviour of the cross-section as a function of $|t|$ is similar to that observed in meson-nucleon scattering and in other photoproductio experiments. In particular the cross-section in the momentum transfer range 0.2 to 0.6 $(Bev/c)^2$ can be expressed in the form $\frac{d\sigma}{dt} \propto e^{Bt}$ with $B \sim 3.0\ (Bev/c)^2$.

Muon-pair decay modes of the vector mesons[2]

4 separate determinations of the $\rho^0 \to 2\mu$ branching ratio based on data taken using carbon and iron targets give the branching ratio

$$\frac{\rho^0 \to \mu^+ + \mu^-}{\rho^0 \to \pi^+ + \pi^-} = (5.1 \pm 1.2) \times 10^{-5}$$

If the SU(3) predictions hold the φ decay into lepton should have a larger branching ratio (with respect to decay into kaons), than the corresponding ρ and ω decays.

Observation of the (e^+e^-)-decay modes of neutral vector mesons[3]

A new method was used to separate the e^+e^- from other modes of decay of the vector mesons produced by 4.0 Bev/c pions in a liquid hydrogen target 50 cm. long in the reaction

$$\pi^- + p \longrightarrow V + n \longrightarrow e^+ + e^- + n$$

To separate lepton decays use was made of a two channel system of spark chamber and cerenkov total absorption gamma-spectrometers. For effective mass calibration of the apparatus the $\eta \to \gamma\gamma$ and $\omega \to \pi^0\gamma$ decays which had been obtained simultaneously with e^+e^- events in the same run were used. Proper account was taken of background sources like simulation of e^+e^- events by $\pi^+\pi^-$ pairs; the e^+e^- production without resonance state formation and conversion of γ-γ events.

The experimental results are given by:

$$\frac{\Gamma(\rho \to e^+e^-)}{\Gamma(\rho)}\,\sigma(\rho) + \frac{\Gamma(\omega \to e^+e^-)}{\Gamma(\omega)}\,\sigma(\omega) = (0.45 \pm 0.12) \times 10^{-4}\ \text{mb} \qquad (1)$$

$$\frac{\Gamma(\varphi \to e^+e^-)}{\Gamma(\varphi)}\,\sigma(\varphi) \leq 1.8 \times 10^{-5}\ mb \qquad (2)$$

Assuming SU(3) symmetry and the data for $\sigma(\rho)$, $\sigma(\omega)$ and $\sigma(\varphi)$ the width of the vector meson octet decay into e^+e^- is given by

$$\Gamma(V_8 \to e^+e^-) = (0.45 \pm 0.14) \times 10^{-2}\ MeV$$

$$\Gamma(V_8 \to e^+e^-) \leq 2.6 \times 10^{-2}\ MeV$$

The evaluation corresponds to the following ratios.

$$\frac{\Gamma(\rho \to e^+e^-)}{\Gamma(\rho)} = (3.9 \pm 1.2) \times 10^{-5}$$

$$\frac{\Gamma(\omega \to e^+e^-)}{\Gamma(\omega)} = (4.8 \pm 1.5) \times 10^{-5}$$

$$\frac{\Gamma(\varphi \to e^+e^-)}{\Gamma(\varphi)} \leq 200 \times 10^{-5}$$

Forward scattering of Bev photons from carbon and Tungsten.[4]

Elastically scattered photons from a $\frac{1}{2}$" carbon target were counted at average bremsstrahlung energies of 1300 Mev and 970. A 0.03" tungston target was used in a measurement at an energy of 1300 Mev.

The measured values of the scattering cross-sections at 3° average angle were normalized to 0° by using a model of difraction scattering from a small slightly absorptive but non-dispersive sphere which gives the scattering amplitude to be proportional to $G(\theta) = J_{3/2}(ka\theta)/(ka\theta)^{3/2}$ where k is the incident photon energy, the radius of the scattering nucleus and θ the scattering angle.

The following table gives the cross-sections, the last column giving the ratio of these to the optical theorem estimate

$$\frac{d\sigma}{d\Omega}(0^\circ) = \left(\frac{kA\sigma_H}{4\pi}\right)^2$$

where A is the number of nucleons and σ_H is the hydrogen cross-section. The total cross-section are:

σ_H (970 Mev) = 182 μ barn

σ_H (1300 Mev) = 146 μ barn

Target	k (Mev)	$\frac{G^2(3^\circ)}{G^2(0^\circ)}$	$\frac{d\sigma}{d\Omega}(3^\circ) \times 10^{28}$ cm^2 (experiment)	$\frac{\text{experiment}}{\text{Optical theorem estimate}}$
Carbon	1300	0.83	0.79 ± 0.11	1.17 ± 0.18
Carbon	970	0.90	0.92 ± 0.30	1.26 ± 0.42
Tungsten	1300	0.33	59.5 ± 12.00	0.95 ± 0.19

Search for $\eta \to \pi^+ + \pi^- + \pi^0 + \gamma$ 6)

This experiment was performed to find out whether the decay mode

$$\eta \longrightarrow \pi^+ + \pi^- + \pi^0 + \gamma$$

had a decay rate comparable to the mode

$$\eta \longrightarrow \pi^0 + \gamma + \gamma$$

or (since $\Gamma(\eta \to \pi^0 + \gamma + \gamma) \approx \Gamma(\eta \to \pi^+ + \pi^- + \pi^0)$) to the mode

$$\eta \longrightarrow \pi^+ + \pi^- + \pi^0$$

Söding's theoretical estimate is that

$$\frac{\Gamma(\eta \to \pi^+ + \pi^- + \pi^0 + \gamma)}{\Gamma(\eta \to \pi^+ + \pi^- + \pi^0)} \approx 1$$

The η was produced in the reaction

$$K^- + p \longrightarrow \Lambda + \eta ,$$

and the decay events corresponding to

$$\Lambda + \eta \longrightarrow (p + \pi^-) + (\pi^+ + \pi^- + \pi^0 + \gamma)$$

From the mass-distribution plots it was concluded that $\gtrsim$ 35% of the $\eta \to \pi^+ + \pi^- + \pi^0 + \gamma$ should have a mass squared greater than 0.04 $(\text{Bev})^2$. Since there was a total of six events above 0.04 $(\text{Bev})^2$ there could not be more than 17 such events in the experiment. This gives

$$\frac{\Gamma(\eta \to \pi^+ + \pi^- + \pi^0 + \gamma)}{\Gamma(\eta \to \pi^+ + \pi^- + \pi^0)} < \frac{17}{246} \approx 0.07$$

Neutral decay modes of the η -meson[6]

As a part of a series of experiments to detect neutral resonances in the reactions $\pi^- + p \to X^0 + n$ the branching ratios of η decaying into 2γ, $\pi^0 + \gamma + \gamma$ and $3\pi^0$ were measured. The ratios are

$$\frac{2\gamma}{\text{all neutrals}} = (57.9 \pm 5.2)$$

$$\frac{\pi^0 + \gamma + \gamma}{\text{all neutrals}} = (24.4 \pm 5.0)$$

$$\frac{3\pi^0}{\text{all neutrals}} = (17.7 \pm 3.5)$$

The last value can be combined with the published values of

$$\frac{\eta \longrightarrow \text{all neutrals}}{\eta \longrightarrow \text{all charged}} = 2.69 \pm 0.5$$

and

$$\frac{\eta \longrightarrow \pi^+ + \pi^- + \pi^0}{\eta \longrightarrow \text{all charged}} = 0.83 \pm 0.07$$

to yield a value

$$R \frac{(\eta \longrightarrow 3\pi^0)}{(\eta \rightarrow \pi^+ + \pi^- + \pi^0)} = 0.57 \pm 0.13$$

in fair agreement with earlier results.

Test for time reversal invariance in the beta decay of Ne^{19} [7)]

The possibility of T violation in β-decays may be tested by studying the presence of a term $D.\hat{I}.\left[\frac{\hat{v}}{c} \times \hat{q}\right]$ (where $\langle I \rangle / I$ is the spin polarization of the initial nucleus $\hat{q}$, a unit vector in the neutrino direction and v, the velocity, the electron) in the differential decay rate; D is proportional to $\sin\varphi$ where $\frac{C_A}{C_V} = \eta e^{i\varphi}$ and T invariance implies that C_A/C_V is real corresponding to $\varphi = 0^\circ$ or 180°. The coulomb correction to D variables to first order in $\frac{Z\alpha}{p}$ for V or A coupling neutron beta decay experiments.

give

$$D(n) = 0.04 \pm 0.05$$

implying $\varphi = 175^{\circ} \pm 6^{\circ}$. In the present experiment $D(Ne^{19})$ was measured by observations of e^{+}-F^{19-} delayed coincidences. The value is

$$D(Ne^{19}) = 0.002 \pm 0.014$$

corresponding to $\varphi = 180.2^{\circ} \pm 1.6^{\circ}$ which is consistent with T invariance.

Test of time reversal invariance in $K^{0}_{\mu 3}$ decay[8]

Various models of CP nonconservation (like that of Sach's) predict a large transverse polarization of the muon in $K^{0}_{\mu 3}$ decay. In the V-A theory all observables except the absolute rates can be expressed in terms of the ratio $\xi(q^2)$ of the two form factors $f^{-}(q^2)$ and $f^{+}(q^2)$. ξ should be real if T invariance holds. For the geometry of the present experiment

$$Im\,\xi = -5.5\, P_T^{lab}$$

where P_T^{lab} is the measured transverse polarization of the muon. The value found was

$$P_T^{lab} = 0.0025 \pm 0.012$$

which gives

$$Im\,\xi = -0.014 \pm 0.066$$

Thus the results of this experiment are consistent with no violation of T invariance.

References

1) G.C. Bolon et al, Phys. Rev. Letters 18, 926 (1967).

2) A. Wehmann et al, Phys. Rev. Letters 18, 829 (1967).

3) M.N. Kachaturyan et al, Physics Letters 24B, 349 (1967).

4) E. Eisenhaudler et al, Physics Letters 24B, 347 (1967).

5) S.M. Flatte, Phys. Rev. Letters 18, 976 (1967).

6) M. Feldman et al, Phys. Rev. Letters 18, 868 (1967).

7) F.P. Calaprice et al, Phys. Rev. Letters 18, 918 (1967).

8) K.K. Young et al, Phys. Rev. Letters 18, 806 (1967).

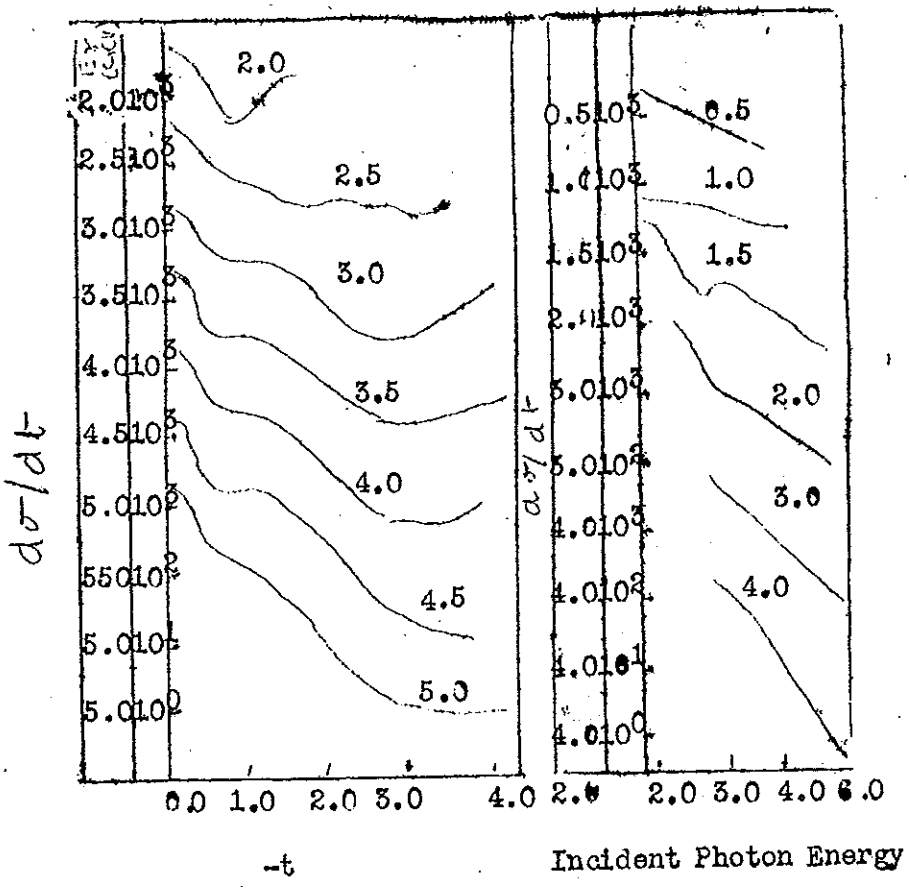
dσ/dt
2.0
2.5
3.0
3.5
4.0
4.5
5.0
0.0 1.0 2.0 3.0 4.0
-t
0.5
1.0
1.5
2.0
3.0
4.0
2.0 3.0 4.0
Incident Photon Energy

Fig 1a

Fig. 1 b.

JUNE 1967

Introduction

The present report starts with an analysis of inelastic K^+p interactions between 860 and 1580 Mev/c which confirms the existence of a peak found earlier by Cool at 1250 Mev/c.

A study of K^+p interactions at 12.7 Bev/c shows a resonance in the $K\pi\pi$ system at 1300 Mev with width 130 ± 15 Mev, isospin 1/2 and spin-parity 1^+. The existence of the peak at 1780 Mev (the L meson) observed in earlier experiments is also confirmed.

A study of the differential cross-sections for production of pions, kaons and antiprotons in proton-proton collisions as a function of the transverse momentum of the produced particle (with the longitudinal momentum fixed) shows a Gaussian shape in contradiction with the exponential dependence first suggested by Cocconi et al.

A new determination of the pion and antipion lifetimes confirms CPT invariance in weak interactions.

A resonance $Y_1^*(1715)$ is present in the $\Lambda\pi$ system with isospin 1 and width 120 Mev.

A new enhancement in the $p\bar{p}\pi^-$ system at 1.32 Bev is found from a study of five-particle final states in $\pi^- d$ interactions at 5 Bev/c.

ELEMENTARY PARTICLES

Inelastic processes near the T=1 K^+p peak at 1250 Mev/c [1)]

An analysis of inelastic K^+p interactions between 860 and 1580 Mev/c with particular reference to a study of the KN (1236) final state was made. Single pion production is the only significant inelastic process in the momentum range under consideration and the process

$$K^+ + p \longrightarrow K^0 + p + \pi^+$$

accounts for the major part of the single-pion production and is richest in the two-body final states $KN^*(1236)$ and $NK^*(891)$.

Fig.1 shows the total partial K^+p cross-sections in the region of a peak found by Cool earlier at 1250 Mev/c (corresponding to a mass of about 1910 Mev) which in a SU(3) could belong to a 27 representation. A study of the angular distribution leads to the conclusions that (i) there must be a strong $P_{3/2}$ state present (ii) the increasing forward-backward asymmetry in the production angular distribution is caused by interference between the dominant P state and higher waves of opposite parity, principally D waves and (iii) the $P_{3/2}$ state is not the only P state present.

The ratio of the $P_{3/2}$ to the $P_{1/2}$ channel cross-section seems to lie closer to unity than to the prediction of the Shodoesky-Sakurai model which gives a ratio $5/1$. The $S_{3/2}$ amplitude leads to a cross-section of less than 100 μb at all momenta and is far too small to account for the Cool peak. The $P_{3/2}$ and $P_{1/2}$ amplitudes are approximately in phase at all

momenta. Thus none of these data suggests or requires that any of the main amplitudes present in KN^* production is dominantly of a Breit-Wigner form.

Production of $K\pi\pi$ resonances at high energy [2]

Preliminary results of an investigation of K^+p interactions at 12.7 Bev/c show the following features. The outstanding part of the $K^+p\pi^+\pi^-$ (395 events) and $K^0p\pi^+\pi^0$ (359 events) final state distributions is the dominance of the wide peak at 1300 Mev in the $K\pi\pi$ system. The peak at 1780 Mev is identified with the L-meson. The 1300 Mev peak has a width 130 ± 15 Mev. The observed ratios for decay into πK^* and $K\rho$ final states are consistent with a T = 1/2 assignment. The angular distribution of the decay products suggests a spin parity assignment 1^+(s wave).

The isospin of the L-meson is also 1/2.

Production of pions, Kaons and antiprotons in high-energy p-p collisions [3]

The differential production cross-section $d^2\sigma/d\Omega dp$ for pions, kaons and antiprotons in p-p collisions were measured at 12.5 Bev/c. Two sets of measurements were made, one in which the longitudinal component of the momentum of the produced particle in the c.m.s p_l, was fixed and the other in which the transverse component, $p_\perp$, was fixed. The experiment was performed on the zero-gradient synchrotron at ANL. The production cross-sections are given in Figs.2 and 3. In

In Fig.2, P_ℓ is fixed and the dependence of $d^2\sigma/d\Omega dp$ on $P_\perp^2$ is studied. The graphs are straight lines on semi log paper which means that the cross-section is a Gaussian in $P_\perp$.

$$\frac{d^2\sigma}{d\Omega dp} = B \exp(-A P_\perp^2)$$

This is in disagreement with the exponential dependence on $P_\perp$ first suggested by Cocconi et al on a phenomenological basis. The slopes of the straight lines are consistent with $A \simeq 35(\text{Bev/c})^{-2}$ except for the K^+ slope which is about $2.7(\text{Bev/c})^{-2}$. $d^2\sigma/d\Omega dp$ continues to drop as a Gaussian all the way out to $P_\perp^2 = 1.5$ $(\text{Bev/c})^2$ in contrast to elastic cross-sections which seem to break sharply around $P_\perp^2 \simeq 0.9(\text{Bev/c})^2$.

Fig.3 gives the cross-sections for $P_\perp^2$ fixed. The cross-section does not have a maximum at zero longitudinal momentum, but peaks at about 0.45 Bev/c and drops rapidly as P_ℓ goes to 0. This indicates that there is no tendency for particles to be produced at rest in the c.m.s. The protons themselves appear to emit all the produced particles.

Pion-antipion lifetime comparison [4]

Pions produced by a proton beam were momentum analysed and the fraction of surviving pions as a function of distance in vacuum was measured by using a liquid-hydrogen differential Cerenkov counter in π^+ and π^- beams which were nearly identical in their momentum space distributions. The π^+/π^- ratio

was thus determined at each point to give a relative lifetime measurement. By a different analysis the absolute lifetimes were also measured. The following table gives a comparison of π^+ lifetime values π^+/π^- lifetime ratios in other experiments and the present one. As is seen there, the agreement with other experiments is good. Also a check on CPT invariance in weak interactions is also upheld.

	τ_+ (ns)	$(\tau_+/\tau_-) - 1$
Other experiments	25.46 ± 0.32	
	26.02 ± 0.04	
	26.40 ± 0.08	
	25.6 ± 0.3	0.0040 ± 0.007
	26.67 ± 0.24	0.0040 ± 0.0018
		0.0023 ± 0.0040
This experiment	26.6 ± 0.2	0.0056 ± 0.0028

Production of a $Y_1^*(1700)$ in K^-p collisions at 6 Bev/c [5]

The channels

$$K^- p \longrightarrow (\Lambda^0 \pi^+)\,\pi^- \qquad (1)$$

$$(Y_1^{*} \pi^+)\,\pi^- \longrightarrow (\Lambda^0 \pi^0 \pi^+)\,\pi^- \qquad (2)$$

$$(\bar{K}^0 p)\,\pi^- \qquad (3)$$

$$(\Sigma^0\pi^+)\pi^- \qquad (4)$$

$$K^-p \longrightarrow (\bar{K}N\pi)\pi^- \qquad (5)$$

$$(\Sigma^\pm\pi^-+\pi^+)\pi^- \qquad (6)$$

were studied in K^-p interaction at 6 Bev/c using data obtained from an exposure of 300,000 pictures in the 1.5 m BNHBC at the CERN P.S. A clear peak of (30 ± 8) events at a $\Lambda\pi^+$ mass of 1715 Mev appears in channel (1). The peak has a width of 120 Mev. There are no statistically significant peaks in the other channels. The isospin of the new resonance is 1, but no conclusion can be drawn regarding its spin. The $\Lambda\pi$ decay distribution is symmetric and nearly isotropic.

<u>A $\rho^-\pi^-$ enhancement at 1.32 Bev observed in 5 Bev/c π^- - d interactions</u> [6]

The reaction

$$\pi^- + d \longrightarrow p + p + \pi^- + \pi^- + \pi^0$$

was studied for a $\rho^-\pi^-$ effect in the A_2 mass region. The experiment was based on the analysis of about 200,000 pictures taken in the 81 cm. Saclay bubble chamber filled with deuterium and exposed at CERN to a 5.04 Bev/c π^- beam. There is a peak in the $\rho^-\pi^-$ mass spectrum centred at (1.32 ± 0.025) Bev and its observed width is approximately 150 Mev. About 34 events contribute to the structure, the corresponding cross-section being $\sigma = (15 \pm 5)$ μbarn.

References

1. R.W.Bland et al, Phys. Rev. Letters 18, 1077 (1967).

2. J.Berlinghieri et al, Phys. Rev. Letters 18, 1087 (1967).

3. L.G.Ratner et al, Phys. Rev. Letters 18, 1218 (1967)

4. D.S.Ayres et al, Physics Letters 24B, 483 (1967)

5. D.C.Colley et al, Physics Letters 24B, 489 (1967)

6. R.Vandertagen et al, Physics Letters 24B, 493 (1967)

...

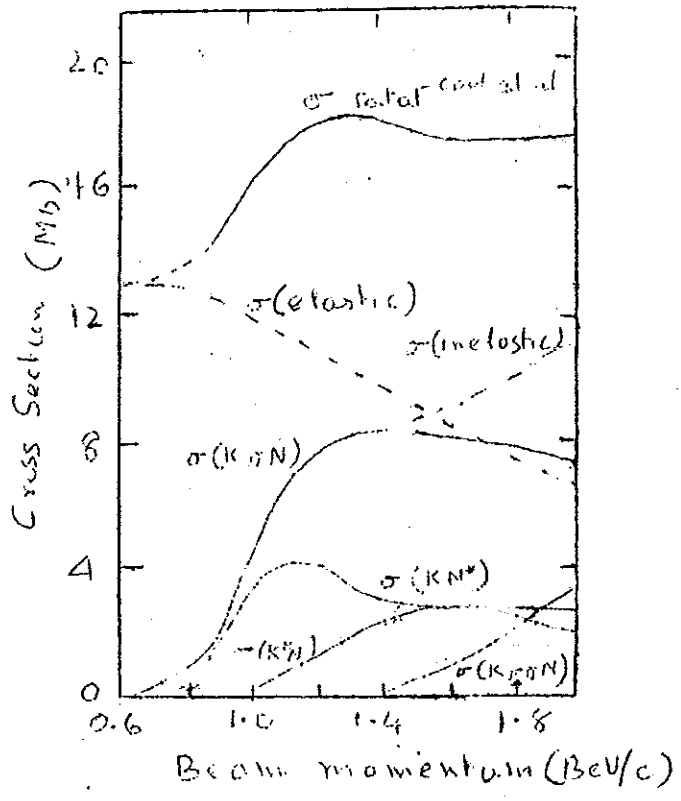
Cross Section (Mb)
20
16
12
8
4
0
0.6
1.0
1.4
1.8
Beam momentum (BeV/c)
σ total (calculated)
σ(elastic)
σ(inelastic)
σ(K⁻n)
σ(K⁻N*)
σ(K*N)
σ(K⁻pπ⁰N)

FIG. 1

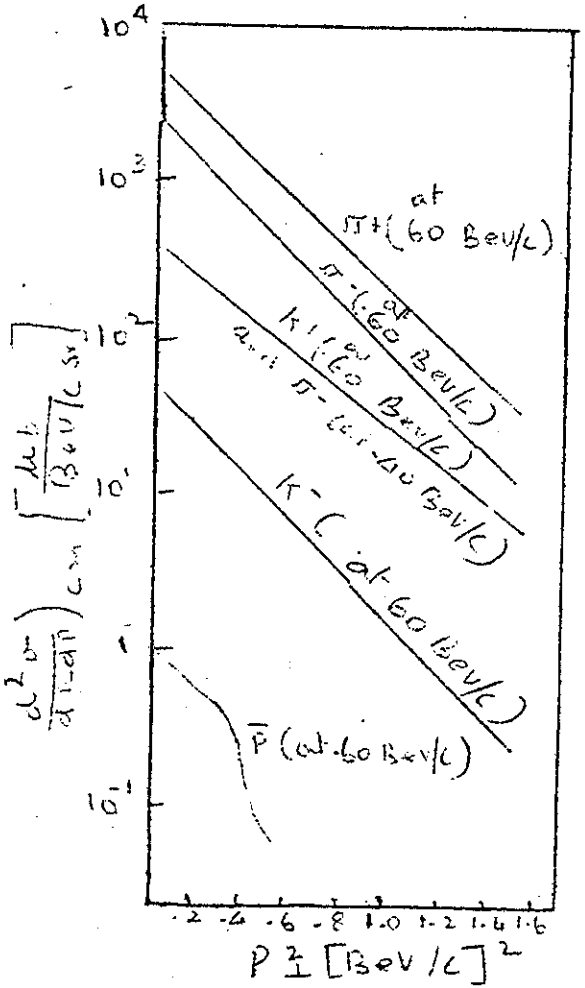
10^4
10^3
10^2
10
1
10^{-1}
$\frac{d^2\sigma}{dP_L dP_T}\Big)_{cm}\left[\frac{\mu b}{(BeV/c)^2}\right]$
at π^+ (60 Bev/c)
π^- at 60 Bev/c)
K^+ (at 60 Bev/c)
K^- (at 60 Bev/c)
$\bar{P}$ (at 60 Bev/c)
.2 .4 .6 .8 1.0 1.2 1.4 1.6
P_T^2 [BeV/c]^2

FIG 2

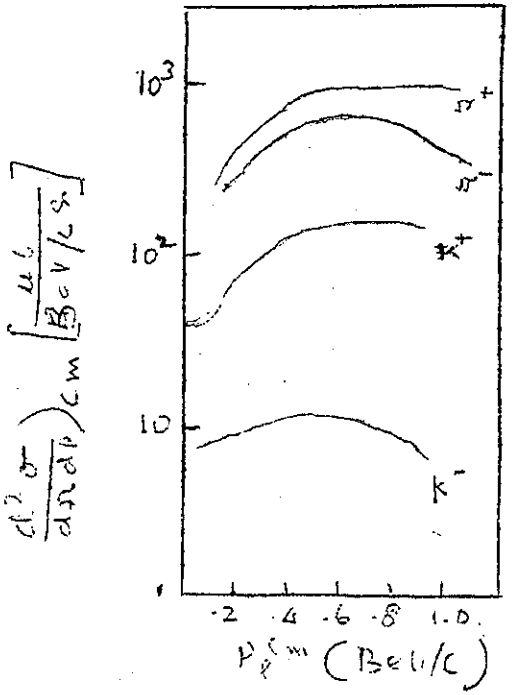
10^3
10^2
10
1
$\frac{d^2\sigma}{dP_L dP_T}\Big)_{cm}\left[\frac{\mu b}{(BeV/c)^2}\right]$
π^+
π^-
K^+
K^-
.2 .4 .6 .8 1.0
P_L^{cm} (BeV/c)

FIG. 3

JULY 1967

Introduction

The present report starts with further evidence for the $K^*(1300)$ with isospin 1/2 observed in π^-p interactions at 6 Bev/c.

A study of the relative partial rates for positive and negative kaons of momentum 3.5 Bev/c decaying into 3 pions yielded a ratio 1.006 ± 0.009 which is consistent with CP conservation in γ -decay.

The branching ratios for the $\Sigma^{\pm} \longrightarrow \Lambda + e^{\pm} + \nu$ decays are given.

Finally differential cross-sections for photo-production of pions from deuterium and hydrogen at photon energies in the range 3.0 to 3.7 Bev are given.

ELEMENTARY PARTICLES

Evidence for the K*(1300) in π^-p interactions at 6 Bev/c[1)]

A $K\pi\pi$ enhancement at 1300 Mev was noticed in earlier experiments in K^+p reactions. It decays strongly into π + K*(890) and possibly into K + ρ (760). Since the K*(1300) mass is not very far from these two-body decay thresholds the possibility exists. of the enhancement being a kinematic effect. In the present experiment the matter was investigated using $\pi^{\pm}p$ interactions at 6 Bev/c in the BNL 80-inch hydrogen bubble chamber. The following channels leading to either neutral or doubly charged $K\pi\pi$ states were studied:

$\pi^- + p \longrightarrow \Lambda + K^0 + \pi^+ + \pi^-$ 647 events (1a)

$\longrightarrow \Lambda + K^+ + \pi^0 + \pi^-$ 401 events (1b)

$\pi^+ + p \longrightarrow \Lambda + K^0 + \pi^+ + \pi^+$ 127 events (2a)

$\longrightarrow \Lambda + K^+ + \pi^+ + \pi^0$ 163 events (2b)

The $(K\pi\pi)^0$ mass spectrum shows two enhancements at 1300 and 1440 Mev while the $(K\pi\pi)^+$ distribution shows little structure. Both the decay modes $K + \rho$ and $\pi + k^*(890)^+$ were strongly favoured. The width of K*(1300) is $\sim$ 60 Mev, much narrower than expected for a kinemetic effect. Diagrams leading to kinemetic effects

would not lead to states of definite isospin but such states were not observed. The absence of a $(K\pi\pi)^{++}$ is also indicative that we have a dynamical effect in the present resonance.

The reaction $\pi^- + p \to \Lambda + K^*(1300)$ limits the isospin of the resonance to 1/2 and 3/2. If T = 3/2, only the T = 3/2 $\pi^{\pm}p$ state can contribute giving.

$$\frac{\sigma(\pi^- + p \to \Lambda + K^*(1300)^{++})}{\sigma(\pi^- + p \to \Lambda + K^*(1300)^0)} = 3$$

which is not borne out. So T = 1/2 is favoured. The study of decay angular distribution excludes $J^P = 0^-$.

The relative partial decay rates for $K^{\pm} \to \pi^{\pm} + \pi^+ + \pi^-$ [2)]

To investigate the possibility of a violation of CP invariance in the charged $K \to 3\pi$ channel which is parity-conserving and strangeness changing, an experiment was performed using a kaon beam from an external proton beam of the Argonne ZGS. The relative partial rates for positive and negative kaons of momentum 3.5 Bev/c decaying into 3 pions, $\Gamma(--+)/\Gamma(++-)$ was measured. If this ratio is different from unity there is CP violation (possibly due to $\Delta I = \frac{5}{2}$ transitions). The value obtained in the experiment was

$$\frac{\Gamma(--+)}{\Gamma(++-)} = \frac{\gamma^-/K^-}{\gamma^+/K^+} = 1.005 \pm 0.009$$

where $\tau^{\pm}$ is the number of τ -decays observed and $K^{\pm}$ is the number of kaons from which they occurred. Thus the experiment indicates that there is no CP violation.

On the decay $\Sigma^{\pm} \rightarrow \Lambda^{0} + e^{\pm} + \nu$ 3)

The Σ's were produced in the reaction $K^{-} + p \rightarrow \Sigma^{\pm} + \pi^{\mp}$ in the 30-inch BNL hydrogen bubble chamber. 51 Σ^{-} and 12 Σ^{+} fit the sequence:

$$K^{-} + p \longrightarrow \Sigma^{\pm} + \pi^{\mp}$$
$$\lfloor \Lambda^{0} + e^{\pm} + \nu$$
$$\lfloor \pi^{-} + p$$

The branching ratios found were:

$$\frac{\Sigma^{-} \rightarrow \Lambda + e^{-} + \nu}{\text{all } \Sigma^{-} \text{ decays}} = (0.64 \pm 0.12) \times 10^{-4}$$

$$\frac{\Sigma^{+} \rightarrow \Lambda + e^{+} + \nu}{\text{all } \Sigma^{+} \text{ decays}} = (0.20 \pm 0.08) \times 10^{-4}$$

In the Cabibbo theory of hyperon decay

$$\frac{\Sigma^- \to \Lambda + e^- + \nu}{\text{all } \Sigma \text{ decays}} = 0.60 \times 10^{-4} \cos^2\theta \left(\frac{3}{2}\right) 3 D^2$$

which yields value $D = 0.76 \pm 0.7$ and $\alpha = \frac{D}{D+F} = 0.64 \pm 0.0$ which are in agreement with several previous determinations.

Photoproduction of single charged pions $\pm$ 0 cm in deuterium and hydrogen[4)]

Photons of energy $E_\gamma = 3.41$ Bev from a bremstrahlung beam from the Cambridge electron accelerator were allowed to interact with deuterium and hydrogen and the differential cross-sections for the following processes were measured for pion centre-of-mass angles $\theta_{c.m}$ between 30° and 90°

$$\gamma + d \to \pi^- + p + p \qquad (1)$$

$$\gamma + d \to \pi^+ + n + n \qquad (2)$$

$$\gamma + p \to \pi^+ + n \qquad (3)$$

The differential cross-sections were also measured for E_γ between 3.0 and 3.7 Bev for $\theta_{c.m} = 45^\circ$, this energy range being chosen to search for the presence of the $N^*_{1/2}(2645)$.

The differential cross-sections $\frac{d\sigma}{dt}$ and $\frac{d\sigma}{d\Omega_{c.m}}$ for π^+ production from protons and π^- production from neutrons are given in Fig.1(c) and 1(d). There is an exponential decrease;

$$\frac{d\sigma}{dt} \propto e^{Bt}$$

with $B = 3.3$ (Bev/c)$^{-2}$ up to $|t| \simeq 1.0$ Bev/c^2 for both π^- and the π^+. The cross-section ratio, $\frac{\pi^-}{\pi^+}$ are given in Fig.(1a) and (1b). The ratio is smaller than unity at $E_\gamma = 3.41$ Bev and increases with angle. It is appreciably less than 1 at $\theta_{c.m} = 45^\circ$ and increases above $E_\gamma = 3.4$ Bev.

The ratio of cross-section $\frac{d\sigma}{d\sigma}$ (π^+ from hydrogen) to $d\sigma$ (π^+ from deuterium) is also shown in the figure, and is consistent with unity. Thus the impulse approximation seems to be good for this case.

References

1) D.J.Crennell et al, Physical Review Letters, 19, 44 (1967).

2) C.R.Fletcher et al, Physical Review Letters, 19, 98 (1967).

3) N.Barash et al, Physical Review Letters, 19, 181 (1967).

4) Z.Bar-Yam et al, Physical Review Letters, 19, 40 (1967).

--

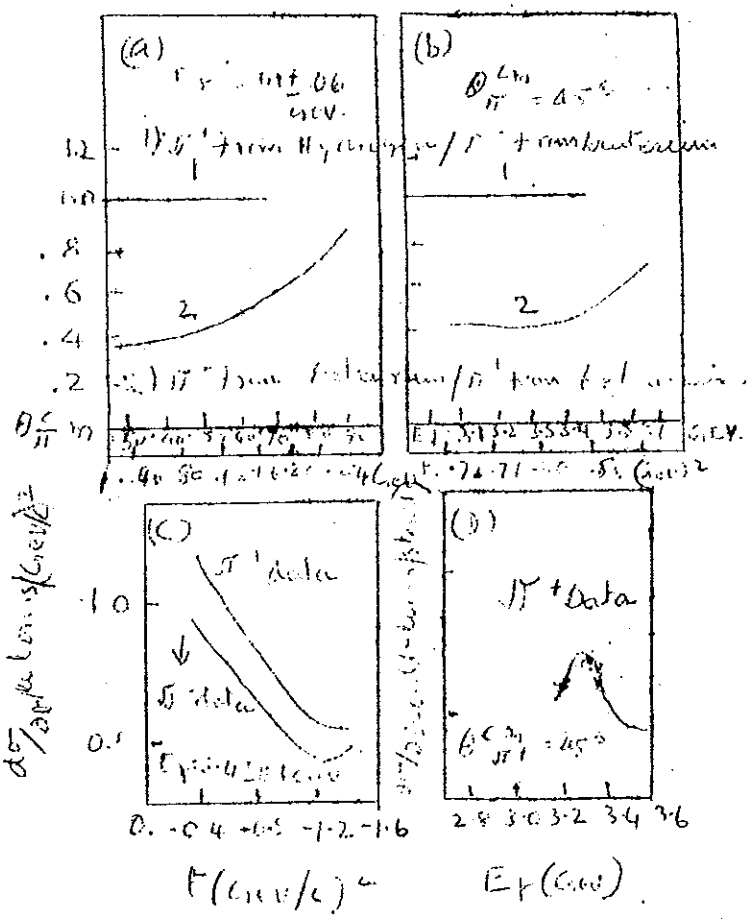
(a)
(b)
(c)
(d)
1.2
1.0
.8
.6
.4
.2
1
2
1.0
0.1
π^+ Data
π^- Data
π^+ Data
$\theta^{Lab}_{\pi^+} = 45°$
0.4 0.5 0.6 0.7 0.8 0.9 1.0 1.1 1.2 1.3 1.4 1.5 1.6
2.8 3.0 3.2 3.4 3.6
GeV.
E_T (GeV)

FIG. 1

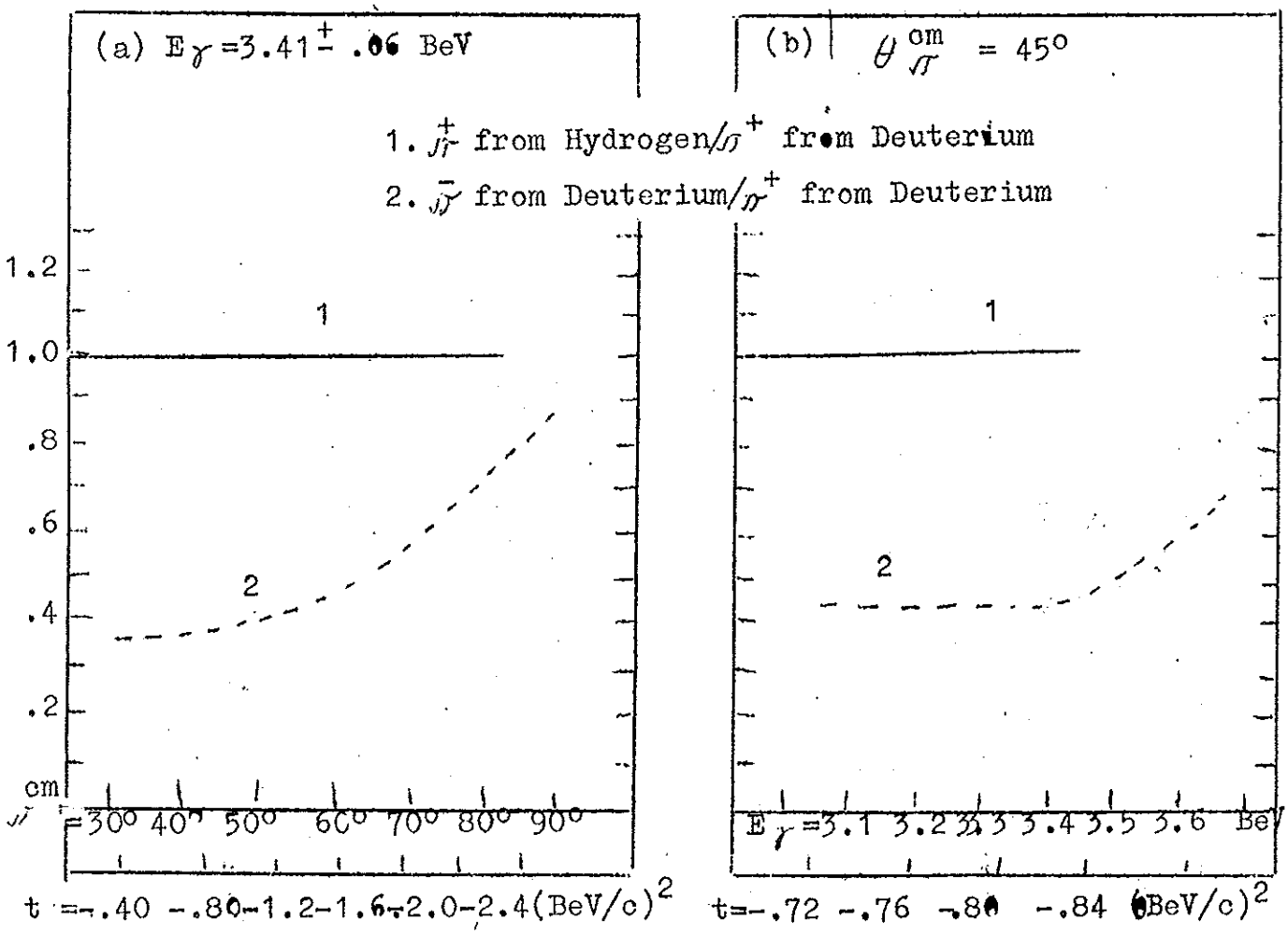
(a) $E_\gamma = 3.41 \pm .06$ BeV
(b) $\theta^{cm}_{\pi} = 45^\circ$
1. π^+ from Hydrogen/π^+ from Deuterium
2. π^- from Deuterium/π^+ from Deuterium
1.2
1.0
.8
.6
.4
.2
1
2
cm
30° 40° 50° 60° 70° 80° 90°
E_γ = 3.1 3.2 3.3 3.4 3.5 3.6 BeV
t = -.40 -.80 -1.2 -1.6 -2.0 -2.4 (BeV/c)^2
t = -.72 -.76 -.80 -.84 (BeV/c)^2

Fig. 1 (a & b)

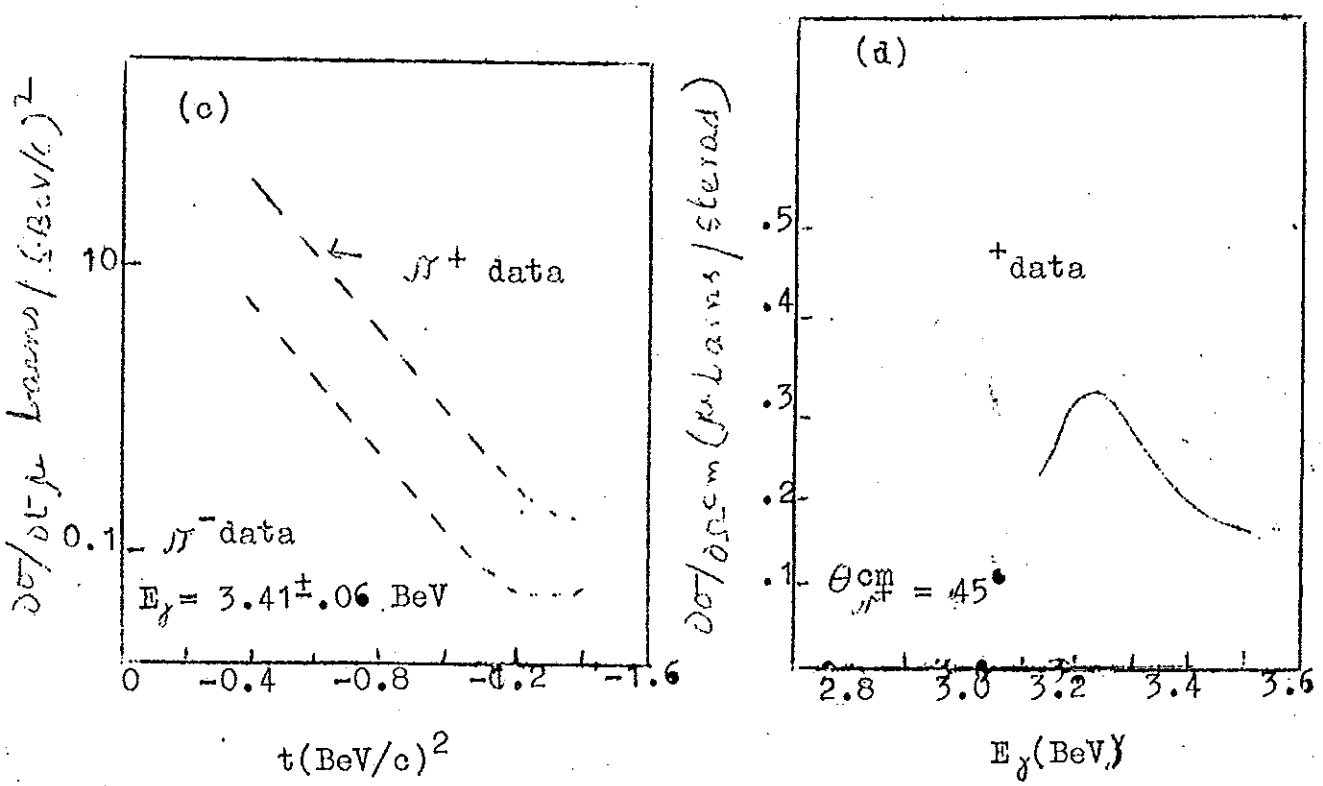
(c)
π^+ data
π^- data
E_γ = 3.41±.06 BeV
10
0.1
0
-0.4
-0.8
-1.2
-1.6
t(BeV/c)^2
(d)
$^+$data
$\theta^{cm}_{\pi^+}$ = 45°
.5
.4
.3
.2
.1
2.8
3.0
3.2
3.4
3.6
E_γ(BeV)

Fig.1 (c&d)

AUGUST 1967

Introduction

The present report starts with a high-precision determination of the $\pi^{\pm} p$ total cross-sections in the momentum range 8 to 29 Bev/c.

An experiment investigating the nature of the backward peaks in elastic pion-proton scattering from 6 to 17 Bev/c is given.

The meagre data on π^{+} photoproduction in the energy range 450 to 600 Mev is supplemented by a recent experiment the results of which are given.

The branching ratios for $K^{*}(1410)$ decaying into $K^{*}\pi$, $K\rho$, $K\omega$ and $K\eta$ which are in agreement with the SU(3) predictions are given. The branching ratio for the leptonic decay of the ρ-meson which is in qualitative agreement with the vector meson dominance prediction is also given.

The differential cross-sections for elastic scattering of 2.7 Bev/c antiprotons by protons is given.

Finally in the section on Low Temperature Physics, kindly prepared by Dr.R.Vasudevan and Mr.R.Sridhar[+], details of an important experiment of Hess and Fairbank who have demonstrated for the first time a rotational Meissner effect for liquid helium are given.

+) We wish to thank Dr.R.Vasudevan and Mr.R.Sridhar for making this material available for inclusion in the present report.

ELEMENTARY PARTICLES

High-Precision $\pi^{\pm} p$ total cross sections from 8 to 29 Bev/c [1]

Total cross sections for $\pi^- p$ interactions in the region 8 to 29 Bev/c and for $\pi^+ p$ in the range 8 to 22 Bev/c were obtained using a counter-hodoscope system with an accuracy of 0.3% bettering previous measurements where the accuracy was about 1%. Corrections were made for coulomb-nuclear interference, multiple scattering and muon contamination. The results for the cross-sections at various momenta are given in the following tables.

Momentum (Bev/c)	$\sigma(\pi^- p)$ (mb)	Momentum (Bev/c)	$\sigma(\pi^+ p)$ (mb)
7.38	27.755 ± 0.089	7.73	25.564 ± 0.084
7.60	27.671 ± 0.088	9.84	24.921 ± 0.079
9.78	26.871 ± 0.084	11.90	24.517 ± 0.078
12.01	26.273 ± 0.083	14.07	24.187 ± 0.081
14.13	25.915 ± 0.081	15.96	24.025 ± 0.076
15.21	25.799 ± 0.082	18.02	23.805 ± 0.081
16.31	25.642 ± 0.081	20.29	23.731 ± 0.079
17.32	25.509 ± 0.081	22.10	23.422 ± 0.098
18.36	25.327 ± 0.084		
18.68	25.344 ± 0.081		
19.22	25.308 ± 0.081		
20.17	25.150 ± 0.082		
22.09	25.064 ± 0.079		
24.27	24.955 ± 0.082		
26.19	24.822 ± 0.079		
28.68	24.774 ± 0.083		

Momentum (Bev/c)	$\sigma_{\pi^-} - \sigma_{\pi^+}$	Momentum (Bev/c)	$\sigma_{\pi^-} + \sigma_{\pi^+}$
8	2.04 ± 0.09	8	52.98 ± 0.12
10	1.93 ± 0.09	10	51.71 ± 0.12
12	1.78 ± 0.09	12	50.79 ± 0.12
14	1.74 ± 0.09	14	50.14 ± 0.12
16	1.66 ± 0.09	16	49.71 ± 0.12
18	1.56 ± 0.09	18	49.18 ± 0.12
20	1.92 ± 0.09	20	48.92 ± 0.12
22	1.64 ± 0.10	22	48.50 ± 0.13

Backward peaks in elastic pion-proton scattering from 6 to 17 Bev/c[2)]

The elastic differential cross-sections for pion-proton scattering were obtained at 5.9, 9.9, 13.7 and 16.3 Bev/c for negative pions and 5.9, 9.9, 13.7 and 17.1 Bev/c for positive pions. A study of the backward distribution shows, as found previously that the cross-sections do rise in the region of small u and this effect continues at least up to 17 Bev/c. The $\pi^+ - p$ backward peaks are narrower than the forward $\pi^- - p$ diffraction peaks and become steeper in the region $0.06 < -t < 0.15$ $(\text{Bev/c})^2$. Expressed in the form $\frac{d\sigma}{du} \propto e^{Au}$ the backward $\pi^+ - p$ peaks have $A = 13.1 \pm 0.6 (\text{Bev/c})^{-2}$ for $u \geq 0.66 (\text{Bev/c})^2$

and for 5.9 Bev/c pions. $A = 18.2 \pm 1.9$ for 9.9 Bev/c, 21.9 ± 27 for 13.7 Bev/c and 27 ± 10 for 17.1 Bev/c. This indicates that the width of the $\pi^+ p$ backward peak is decreasing with increasing energy.

At 180° the $\pi^- p$ cross-sections are about $\frac{1}{4}$ of the corresponding π^+ cross-sections, but the backward peaks are several times wider. The maxima seem to occur at $-u \approx 0.05$ (Bev/c)^2. The energy dependence of the cross-sections $\left(\frac{d\sigma}{d\omega}\right)_{180}$ at 180° are $(P_{lab})^{-1.40 \pm 0.10}$ and $(P_{lab})^{-1.10 \pm 0.12}$ for π^+ and π^- respectively.

The differential cross-sections are given in the following table.

p_o (Gev/c)	cos θ c.m.	u (GeV/c)^2	Δu (GeV/c)^2	$-t$ (GeV/c)^2	$d\sigma/du$ $\mu b/$(GeV/c)^2
			$\pi^+ p \rightarrow p\pi^+$		
5.9	-0.9987	0.055	0.01	11.145	41.52
	-0.9967	0.045	0.01	11.135	35.40
	-0.9948	0.035	0.01	11.125	29.38
	-0.9929	0.025	0.01	11.115	32.25
	-0.9899	0.01	0.02	11.100	20.81
	-0.9865	-0.0075	0.015	11.083	17.11
	-0.9836	-0.0225	0.015	11.068	16.23
	-0.9802	-0.04	0.02	11.050	12.89
	-0.9763	-0.06	0.03	11.030	8.48
	-0.9695	-0.095	0.05	10.995	4.45
	-0.9588	-0.15	0.06	10.940	1.55
9.9	-0.9988	0.0275	0.015	18.508	10.07
	-0.9971	0.0125	0.015	18.493	7.57
	-0.9957	0	0.01	18.480	6.66
	-0.9945	-0.01	0.01	18.470	5.65
	-0.9934	-0.02	0.01	18.460	4.98
	-0.9920	-0.0325	0.015	18.448	2.90
	-0.9903	-0.0475	0.015	18.433	2.48
	-0.9886	-0.0625	0.015	18.418	1.84
	-0.9866	-0.08	0.02	18.400	1.38
	-0.9832	-0.11	0.04	18.370	0.41
	-0.9758	-0.175	0.09	18.305	0.31

p_0 (GeV/c)	$\cos\theta$ c.m.	u $(GeV/c)^2$	Δu $(GeV/c)^2$	$-t$ $(GeV/c)^2$	$d\sigma/du$ $\mu b/(GeV/c)^2$
			$\pi^+ p \to p\pi^+$		
13.7	-0.9969	0.0125	0.015	25.773	4.89
	-0.9934	-0.005	0.02	25.755	2.95
	-0.9889	-0.0275	0.025	25.733	1.34
	-0.9824	-0.06	0.04	25.700	0.93
	-0.9754	-0.095	0.03	25.665	0.62
	-0.9674	-0.135	0.05	25.625	0.30
	-0.9544	-0.20	0.08	25.560	0.25
17.1	-0.9979	-0.01	0.02	32.020	2.75
	-0.9969	-0.025	0.02	32.005	1.49
	-0.9952	-0.0525	0.035	31.978	0.66
	-0.9920	-0.1025	0.065	31.928	0.46
	-0.9862	-0.1925	0.115	31.838	0.37
			$\pi^- p \to p\pi^-$		
5.9	-0.9987	0.055	0.01	11.145	6.45
	-0.9967	0.045	0.01	11.135	6.60
	-0.9933	0.0275	0.025	11.118	6.14
	-0.9885	0.0025	0.025	11.093	7.51
	-0.9841	-0.02	0.02	11.070	7.23
	-0.9802	-0.04	0.02	11.050	7.93
	-0.9753	-0.065	0.03	11.025	5.84
	-0.9685	-0.100	0.04	10.99	6.26
	-0.9588	-0.150	0.06	10.94	3.80
9.9	-0.9994	-0.0325	0.015	18.513	2.23
	-0.9976	-0.0175	0.015	18.498	1.93
	-0.9957	0	0.02	18.480	1.81
	-0.9931	-0.0225	0.025	18.458	2.15
	-0.9903	-0.0475	0.025	18.433	2.56
	-0.9877	-0.070	0.02	18.410	2.41
	-0.9846	-0.0975	0.035	18.383	1.85
	-0.9807	-0.1325	0.035	18.348	1.87
	-0.9753	-0.18	0.06	18.300	1.45
13.7	-0.9986	0.0015	0.02	25.775	1.13
	-0.9951	-0.015	0.04	25.745	1.31
	-0.9903	-0.0575	0.045	25.703	1.03
	-0.9838	-0.115	0.07	25.645	0.89
	-0.9747	-0.195	0.09	25.565	0.70
16.3	-0.9967	-0.005	0.04	30.485	0.53
	-0.9894	-0.070	0.09	30.420	0.80
	-0.9761	-0.187	0.145	30.303	0.80

Photoproduction of positive pions from hydrogen between 300 and 750 Mev[3)]

The data on π^+ photoproduction between 450 and 600 Mev are meagre. The present experiment was performed to complete this gap and resolve certain discrepancies of the results below 450 Mev and above 600 Mev. By keeping the maximum bremstrahlung energy sufficiently close to the useful photon energy background from multipion production was avoided. The following table gives the differential cross-sections in $\mu b/sr$ in the c.m.s.

Differential and total cross-sections (μ barn)

E_γ \ $\theta_{c.m.}$	30°	40°	50°	60°	70°	80°	90°	100°	110°	120°	130°	σ_{tot}
305			14.21 0.41	16.66 0.49	19.50 0.58	21.55 0.64	21.59 0.66	21.15 0.64	20.58 0.65	20.53 0.67		225
325			15.93 0.46	17.23 0.50	18.33 0.53	19.56 0.57	19.62 0.58	19.36 0.58	18.88 0.58	18.08 0.56		212
350			15.07 0.43	16.17 0.46	16.20 0.46	16.81 0.48	16.62 0.48	14.84 0.44	14.48 0.43	13.61 0.41	13.37 0.41	180
375			12.46 0.34	13.77 0.38	13.16 0.37	12.82 0.37	12.01 0.35	11.44 0.33	10.70 0.31	10.03 0.30	10.18 0.31	141
400			11.41 0.31	11.33 0.31	11.11 0.31	10.37 0.29	9.42 0.27	8.62 0.25	8.00 0.23	7.12 0.21	6.80 0.23	117
425				9.75 0.26	9.04 0.24	8.85 0.24	7.95 0.22	6.84 0.19	6.43 0.18	5.35 0.16	5.55 0.16	97
450	10.34 0.27	9.42 0.25	9.72 0.25	9.14 0.24	8.78 0.23	7.91 0.21	7.07 0.19	6.25 0.18	5.57 0.16	4.55 0.13	4.40 0.13	88
475	10.42 0.27	9.64 0.25	9.03 0.23	8.77 0.23	8.10 0.21	7.54 0.20	6.60 0.18	5.79 0.16	4.96 0.14	4.17 0.12	3.95 0.11	85
500	10.02 0.31	9.57 0.25	9.14 0.24	8.15 0.21	7.91 0.20	7.23 0.19	6.47 0.17	5.38 0.15	4.65 0.13	4.04 0.12	3.62 0.10	81

Differential and total cross-sections (μ barn) (ctd.)

$\theta_{c.m}$ / E	30°	40°	50°	60°	70°	80°	90°	100°	110°	120°	130°	σ_{tot}
525	10.62 0.33	9.63 0.30	9.26 0.28	8.38 0.22	7.96 0.20	7.28 0.19	6.50 0.17	5.52 0.15	4.58 0.13	3.93 0.11	3.46 0.10	81.5
550	10.35 0.32	9.80 0.30	9.35 0.28	8.63 0.26	7.81 0.20	7.16 0.18	6.10 0.16	5.27 0.14	4.23 0.11	3.54 0.10	3.32 0.09	80
575	10.84 0.34	10.75 0.33	10.19 0.31	9.21 0.28	7.93 0.24	7.15 0.18	6.45 0.16	5.20 0.14	4.46 0.12	3.77 0.10	3.45 0.10	835
600	10.13 0.31	10.29 0.32	10.28 0.30	9.82 0.29	8.23 0.24	7.09 0.18	6.21 0.16	5.12 0.13	4.41 0.12	3.67 0.10	3.26 0.09	83
625	10.59 0.33	10.78 0.33	10.42 0.31	10.41 0.31	9.01 0.26	7.58 0.22	6.22 0.16	5.26 0.13	4.64 0.12	3.75 0.10	3.40 0.09	86
650		11.43 0.35	11.15 0.33	10.74 0.32	9.78 0.29	8.44 0.25	6.76 0.17	5.82 0.15	4.66 0.12	4.00 0.11	3.61 0.10	91
675				11.39 0.32	9.97 0.28	9.11 0.26	7.66 0.22	6.25 0.16	5.29 0.13	4.53 0.12	3.92 0.11	
700				11.96 0.34	10.65 0.30	9.89 0.28	8.35 0.24	6.71 0.17	6.02 0.15	5.26 0.14	4.66 0.12	
725					9.57 0.27	9.04 0.26	8.39 0.24	6.81 0.20	6.27 0.16	5.49 0.14	4.78 0.13	
750					8.35 0.24	7.79 0.22	7.59 0.22	6.30 0.18	5.60 0.14	4.65 0.12	4.48 0.12	

K^-p elastic scattering at 2.24 Bev/c [4]

Elastic total scattering cross-sections for K^-p collisions at 2.24 Bev/c incident momentum were measured.

The total cross-sections for various incident momenta from other experiments and from the present experiment are shown in the following table.

P_{K^-lab} (Bev/c)	σ (mb)	P_{K^-lab} (Bev/c)	σ (mb)
0.300	44.5 ± 6.4	2.0	7.18 ± 0.30
0.400	38.9 ± 4.7	2.24	6.2 ± 0.7
0.820	18.7 ± 0.7	3.0	4.95 ± 0.22
1.040	23.3 ± 1.0	3.46	4.94 ± 0.39
1.150	17.3 ± 1.1	7.2	4.23 ± 0.85
1.260	15.2 ± 0.7	9.0	3.95 ± 0.78

Experimental $K^*(1410)$ branching ratios[5]

The reactions

$$K^- + p \rightarrow K^- + p + \pi^+ + \pi^- \quad (1)$$

$$K^- + p \rightarrow K^- + p + \pi^+ + \pi^- + \pi^0 \quad (2)$$

were studied using 3.8 Bev/c K^--mesons in the 80" BNL hydrogen bubble chamber. An analysis of the intermediate state

$$K^- + p \rightarrow K^*(1410) + p \quad (3)$$

for the $K^*(1410)$ branching ratios $K^*\pi : K\rho : K\omega : K\eta$ gives the value 1:(<0.4):0.10 ± 0.04: 0.07 ± 0.04. These are consistent with the ratios from SU_3 symmetry, 1:0.29:0.11:0.04.

Elastic scattering of 2.7 Bev/c antiprotons on protons[6]

The interaction 2.7 Bev/c antiprotons with protons was

studied in the 20" BNL bubble chamber. The differential cross-sections are given in the following table.

$\cos\theta$	$\cos\theta$ (average)	Number of events	$\frac{d\sigma}{d\Omega}$ $\left(\frac{mb}{steradian}\right)$
1.00 - 0.99	0.9930	568	
0.99 - 0.98	0.9851	1047	64.3 ± 2.4
0.98 - 0.97	0.9753	849	52.0 ± 2.1
0.97 - 0.96	0.9650	625	38.2 ± 1.17
0.96 - 0.95	0.9552	540	33.0 ± 1.6
0.95 - 0.94	0.9452	420	25.7 ± 1.4
0.94 - 0.93	0.9352	292	17.9 ± 1.1
0.93 - 0.92	0.9251	264	16.2 ± 1.1
0.92 - 0.91	0.9151	222	13.6 ± 1.0
0.91 - 0.90	0.9056	162	9.91 ± 0.80
0.90 - 0.88	0.891	221	6.36 ± 0.47
0.88 - 0.86	0.871	120	3.67 ± 0.34
0.86 - 0.84	0.850	68	2.08 ± 0.26
0.84 - 0.82	0.832	40	1.22 ± 0.19
0.82 - 0.80	0.809	20	0.61 ± 0.14
0.80 - 0.75	0.780	25	0.31 ± 0.06
0.75 - 0.70	0.721	14	0.17 ± 0.05
0.70 - 0.65	0.670	22	0.27 ± 0.06
0.65 - 0.60	0.621	31	0.38 ± 0.07
0.60 - 0.55	0.575	36	0.32 ± 0.05

(table continued from previous page)

$\cos\theta$	$\langle\cos\theta\rangle$ (average)	Number of events	$\frac{d\sigma}{d\Omega}$ ($\frac{mb}{steradian}$)
0.55 - 0.50	0.528	38	0.34 ± 0.06
0.50 - 0.45	0.477	40	0.35 ± 0.06
0.45 - 0.40	0.429	19	0.17 ± 0.04
0.40 - 0.20	0.321	51	0.113 ± 0.016
0.20 - 0.00	0.122	31	0.069 ± 0.013
0.00 to - 0.20	-0.102	13	0.029 ± 0.009
0.20 to - 0.40	-0.318	11	0.024 ± 0.008
0.40 to - 0.60	-0.485	10	0.022 ± 0.007
0.60 to - 0.80	-0.748	3	0.009 ± 0.005
0.80 to - 1.00	-0.985	1	0.003 ± 0.003

Leptonic decay branching ratio of the ρ-meson[7]

By observing the reactions

$$\pi^- + LiH \rightarrow \mu^+ + \mu^- + \cdots$$

$$\pi^- + LiH \rightarrow \pi^+ + \pi^- + \cdots$$

the branching ratio for the leptonic mode was found to be

$$\frac{\rho \rightarrow \mu + \mu}{\rho \rightarrow \pi + \pi} = 9.7^{+2}_{-2.3} \times 10^{-5}$$

This result is in qualitative agreement with the vector meson dominance prediction.

11

LOW TEMPERATURE PHYSICS

Measurement of angular momentum in superfluid Helium[8)]

Recently Professor G.B. Hess and Professor W.M.Fairbank at Stanford have for the first time demonstrated a rotational Meissner effect for liquid helium. This effect analogous to the magnetic Meissner effect in superconductors has been demontrated for liquid helium when the container with the liquid is cooled through the lambda temperature at sufficiently low angular helicities. The superfluid is observed to have a state of zero total angular momentum.

An irrotational superfluid velocity field for Helium II was first proposed by Landau as early as 1941 and later an experiment was suggested by London in 1946 to test whether the superfluid state is irrorational. The experiment suggested by London was to cool a cyclindrical container containing liquid helium through the lambda temperature when the container has angular velocity less than the critical angular velocity which is of the order of $\hbar/mR^2$ where m is the mass of the helium atom and R is the inside radius of the container.

Following London's suggestion a host of experiments were performed previously to detect the irrotational nature of liquid Helium below the λ-temperature. In all these experiments when the superfluid was supposed to be in equilibrium with the container it was found to have the same angular velocity as the container.

If no case a stationary superfluid state was reported. The reason for this is that in all these experiments the achieved angular velocity of the container was not sufficiently low. Hess and Fairbank have achieved sufficiently low angular velocities by supporting a container of small radius with a Beams-type magnetic bearing. The angular velocity thus achieved is of the order of L_0 in which the superfluid state would have one Vortex singularity along the cyclinder axis (as per the Onsager-Feynman quantised Vortex model). To give a little description of the experimental set up, a ferrite slug is attached to the end of a 0.089 c.m. i.d. tube containing 7 mg of helium and the rotor is then suspended in free space inside a vacuum chamber at $1^{\circ}K$. Just above this chamber is an electromagnet at $4^{\circ}K$ controlled by feed back from a height sensor which attracts the ferrite slug. The rotor may rotate with very small dissipative torque and is cooled by temporarily admitting exchange gas to the vacuum chamber. It is then heated above the lambda temperature in about 10 sec. by shining light through a window. A set of small induction coils are used to set the rotor in rotation and the period of rotation is monitored with an autocollimator which observes a small mirror attached to the rotor.

Angular momentum of the superfluid is estimated by noting the small change ΔW in the angular velocity W of the container as the container is heated above the λ temperature and helium I acquires rigid rotation. The angular momentum L

of the superfluid in the initial state is given by

$$\frac{L}{L_0} = \frac{1}{2}\frac{W}{W_0}\left\{1 + \frac{I_R}{I_{sc}}\frac{\Delta W}{W}\right\}$$

with $W_0 = \hbar/MR^2$

I_R = Moment of inertia of the rotor

$I_{sc} = \frac{1}{2}(N m l_s/\rho)R^2$

Note that if the superfluid behaved classically $\Delta W/W = 0$. In fig.1 the superfluid angular momentum in units of $L_0 = 9.4\times10^{-7}$ dyn cm sec. (at 1.6°K) is plotted against the angular velocity of the rotor in units of $W_0 = 0.0808$ rad/sec. The temperature of the rotor just before heating ranged from 1.6 to 1.73 K. The horizontal heavy segments in the figure represent the equilibrium angular momentum predicted by the Vortex model. It increases in steps as the number of vortices increases. The equilibrium angular momentum of a classical fluid is represented by the diagonal broken line.

The principal systematic uncertainity is in the determination of I_R/I_{sc}. This is chiefly due to the uncertainity about the amount of helium in the rotor.

Fig.2. gives the fractional change in the angular velocity of the rotor of heating, versus the temperature just before heating. The same heat input was used at each temperature.

It is clear that the angular momentum transfer is proportional to ρ_s / ρ (of course within experimental error).

In some additional trials the superfluid was initially formed at rest and then accelerated into rotation. There is some evidence that the superfluid may acquire some angular momentum by mechanical generation of vortices (Further experimental information on these lines are expected).

It is concluded that the superfluid, for sufficiently low angular velocities, does not partake in the rotation of its container when cooled through the lambda temperature. This is evidently an equilibrium phenomenon. At larger angular velocities the superfluid is found to have more or less the same angular velocity as predicted by the vortex model.

References

1) K.J.Foley et al, Physical Review Letters, 19, 330 (1967)

2) A.Ashmore et al, Physical Review Letters, 19, 460 (1967)

3) C.Betourne et al, Physics Letters 24B, 590 (1967)

4) M.Dickinson et al, Physics Letters 24B, 596 (1967)

5) J.Field et al, Physics Letters 24B, 638 (1967)

6) V.Domingo et al, Physics Letters 24B, 642 (1967)

7) B.D.Hayms et al, Physics Letters 24B, 634 (1967)

8) G.B.Hess and W.M.Fairbank, Physical Review Letters, 19, 216 (1967).

--

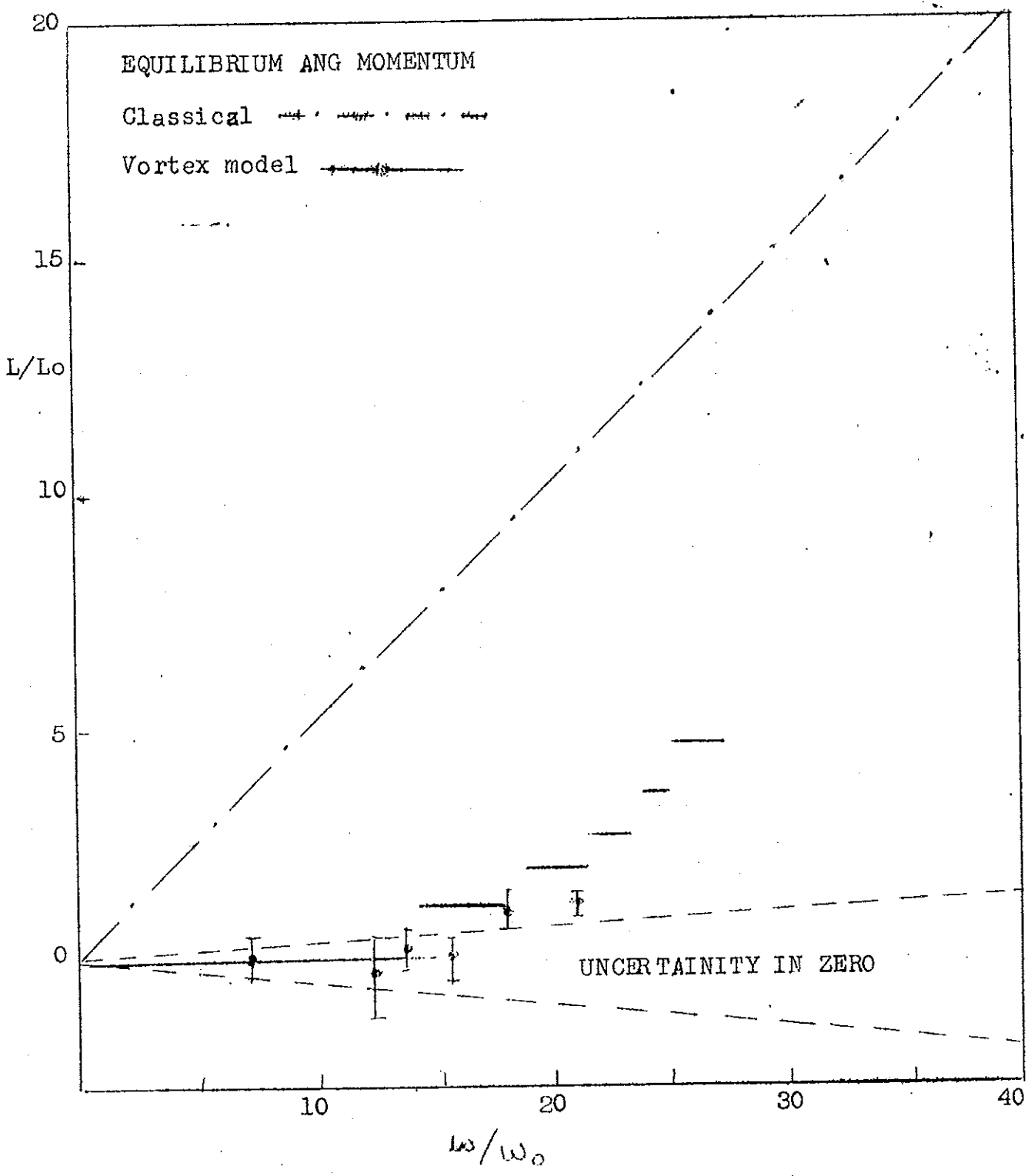
EQUILIBRIUM ANG MOMENTUM
Classical
Vortex model
20
15
10
5
0
L/Lo
UNCERTAINITY IN ZERO
10
20
30
40
ω/ω₀

Fig.1

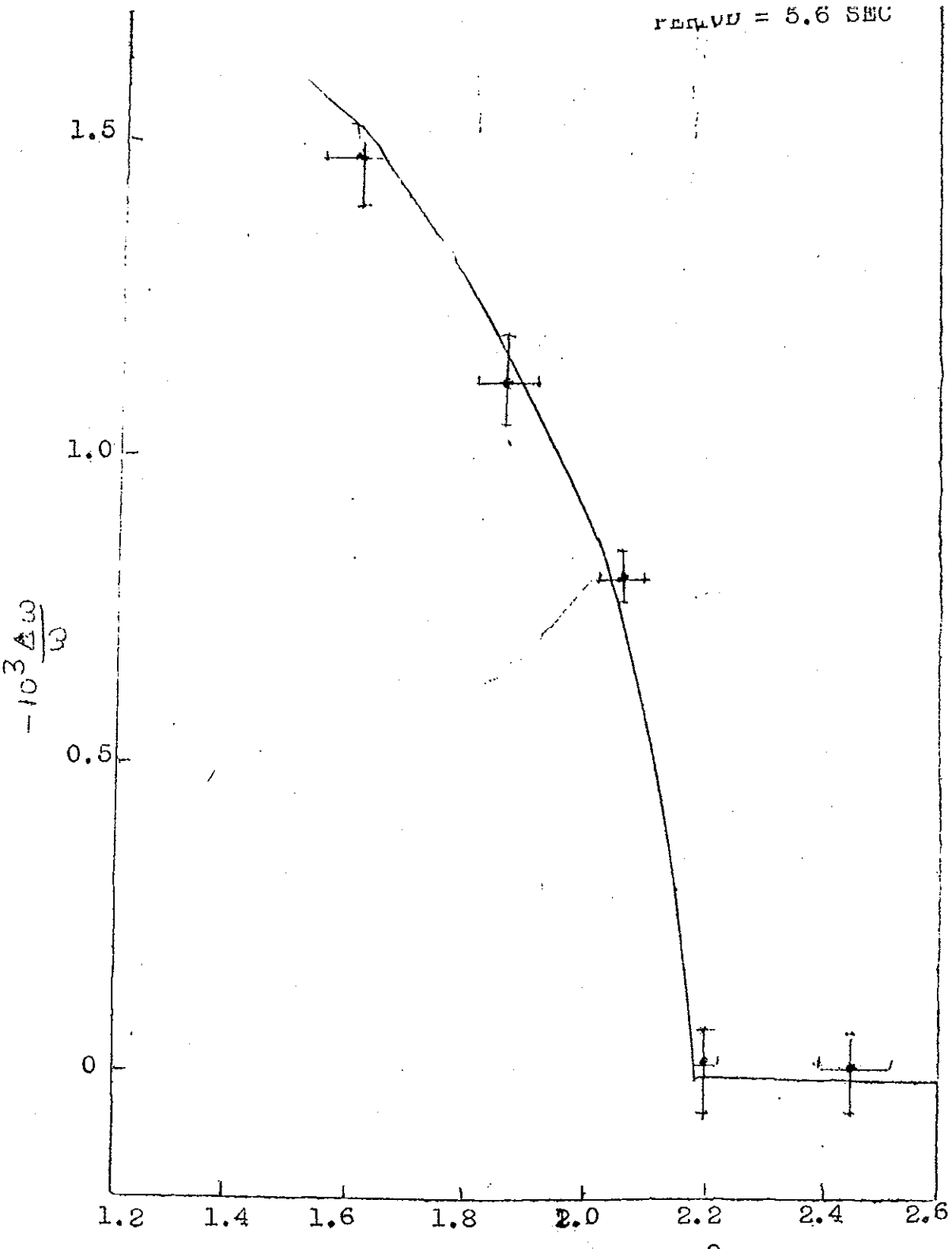
PERIOD = 5.6 SEC
1.5
1.0
0.5
0
$-10^3\frac{\Delta\omega}{\omega}$
1.2
1.4
1.6
1.8
2.0
2.2
2.4
2.6
INITIAL TEMPERATURE T_1(°K)

Fig.2

SEPTEMBER 1967

Introduction

The report starts with measurements of k^--p and k^--d cross-sections in the momentum interval 2.45 to 3.70 Bev/c which indicate presence of two enhancements of mass 2455 ± 10 and 2595 ± 10 Mev and width 140 Mev in the I = 1 state.

Cross-sections for multiple pion production in π^+n and π^-p interactions at 1.7 Bev/c are given.

Polarization parameters for elastic scattering of negative pions from a polarized proton target are given for the momentum range 600 to 3300 Mev/c.

In the section in Low Temperature Physics, prepared by Dr. R. Vasudevan and R. Sridhar, details of two interesting experiments on the condensation of liquid helium II due to rotation have been given. An interesting observation is that a jump in the density of rotating helium II occurs while going into the superfluid state from the non-superfluid state. It has been suggested that the phenomenon of He II going into the vortex state may be a 1st order transition. In the other experiment it has been shown that compressibility does not depend very much on the rotation velocity.

ELEMENTARY PARTICLES

New structures in the k^-p and k^-d total cross sections between 2.4 and 3.3 Bev/c[1]:

The k^--p and k^--d total cross-sections were measured in the momentum interval 2.45 to 3.30 Bev/c using a partially separated k- beam at the Brookhaven AGS. The cross-sections for various values of laboratory momenta are given in Figs. 1a and 1b. Fig. 1a referes to k^-p and Fig. 1b to k^-d reaction.

In addition to the structure at 2.3 Bev/c previously reported, there appear to be two significant changes in the slope of the k^--p data, one at about 2.6 Bev/c and the other near 3.0 Bev/c. The k^--d data also suggest similar but less pronounced structures. An isotopic spin analysis favours the I = 1 state. If the new structures are interpreted as Y_1^*'s, a Breit-Wigner fit yields masses of 2455 ± 10 and 2595 ± 10 Mev, widths of approximately 140 Mev and peak cross-sections of 1.3 and 1.1 mb respectively. The Y_1^*(2455) could be a Regge recurrence of the Y_1^*(1385) and have a spin-parity assignment of 11/2 +. The Y_1^*(2595) could be a recurrence of the Y_1^*(1770) and have a spin parity of 13/2.

Single and multiple pion production in π^+n and π^-p interactions at 1.7 Bev/c[2]

The following reactions were studied in pion-nucleon collision at 1.7 Bev/c.

$$\pi^- + p \longrightarrow \pi^+ + \pi^- + n \qquad (1)$$

$$\pi^+ + d \longrightarrow \pi^+ + \pi^- + p + p_s \qquad (2)$$

$$\pi^+ + d \longrightarrow \pi^+ + \pi^- + \pi^0 + p + p_s \qquad (3)$$

$$\pi^+ + d \longrightarrow \pi^+ + \pi^- + \pi^+ + p + n \qquad (4)$$

$$\pi^+ + d \longrightarrow \pi^+ + \pi^- + \pi^+ + d \qquad (5)$$

$$\pi^+ + d \longrightarrow \pi^+ + \pi^- + \pi^+ + \pi^- + p + p_s \qquad (6)$$

$$\pi^+ + d \longrightarrow \pi^+ + \pi^- + \pi^+ + \pi^- + \pi^0 + p + p_s \qquad (7)$$

Reactions (1) and (2) are dominated by ρ^0 and (3) by ω production. Reactions (4) and (6) go essentially through production of N*(1238), p_s in the above represents the spectator proton.

The following tables give the cross-sections for the various processes. Table I gives the cross-sections in mb for $\pi^- p$ interactions at 1.08, 1.23, 1.38 and 1.71 Bev/c incident pion momenta. Table II gives the cross-sections for $\pi^+ n$ reactions obtained from $\pi^+ d$ reactions at 1.68 Bev/c while Table III gives the cross-section for $\pi^+ d$ reactions at 1.68 Bev/c. In Table IV the resonance production cross-sections in mb are given for interactions at 1.08, 1.38 and 1.71 Bev/c.

Table I

Reaction	[illegible] (1.08)	[illegible] (1.23)	[illegible] (1.38)	[illegible] (1.71)
$\pi^- p \to \pi^- p$	25.1 ± 3.0	14.6±0.8	15.0 ± 0.2	10.4 ± 0.6
$\pi^- p \to \pi^- p \pi^0$	6.5 ± 0.5	4.3±0.3	4.3 ± 0.2	5.8 ± 0.4
$\pi^- p \to \pi^+ n \pi^-$	10.6 ± 0.6	7.3±0.6	7.4 ± 0.2	7.4 ± 0.5
$\pi^- p \to \pi^- p +$ more than one neutral	0.2 ± 0.1	0.8±0.1	1.0 ± 0.1	1.3 ± 0.2
$\pi^- p \to \pi^- \pi^+ n +$ more than one neutral	0.8 ± 0.2	3.1±0.5	3.7 ± 0.2	4.6 ± 0.4

Table II

Reaction	σ(1.68)
$\pi^+ n \to \pi^- \pi^+ p$	6.6 ± 0.3
$\pi^+ n \to \pi^- \pi^+ \pi^0 p$	5.0 ± 0.3
$\pi^+ n \to \pi^- \pi^+ p +$ more than one neutral	0.7 ± 0.1
$\pi^+ n \to \pi^- \pi^+ \pi^- \pi^+ p$	0.23 ± 0.04
$\pi^+ n \to \pi^- \pi^+ \pi^- \pi^+ \pi^0 p$	0.04 ± 0.02

Table III

Reaction	σ (1.68)
$\pi^+ d \to \pi^- \pi^+ \pi^+ n p$	3.27 ± 0.14
$\pi^+ d \to \pi^- \pi^+ \pi^+ d$	0.67 ± 0.02

Table IV

Final State	σ (1.08)	σ (1.38)	σ (1.71)
$N \rho^0$	Negligible	4.4 ± 0.3	4.7 ± 0.2
$N^*_{3/2}\ \pi$	3.6 ± 0.6	1.4 ± 0.2	1.0 ± 0.3
$p\ \omega_{+-0}$			1.8 ± 0.2
$p\ \eta_{+-0}$			0.15 ± 0.04
$p\ \eta^*(960)_{+-0}$			< 0.025

Measurement of the polarization parameter in the π^-p elastic scattering from 600 to 3300 Mev/c[3].

A beam of negative pions of selected momentum was focussed on a polarized proton target and the final state particles were detected with a pair of counter hodoscopes, one above and one below the unscattered beam.

The differential cross section for scattering of pions from a proton target of polarization $\vec{P}_T$ is given by

$$I(\theta) = I_0(\theta)\left[1 + P(\theta)\hat{n}\cdot\vec{P}_T\right]$$

where $I_0(\theta)$ is the differential cross-section from unpolarized protons, $n = \vec{k_i} \times \vec{k_f}$ is the normal to the scattering plane and $P(\theta)$ is the polarization parameter.

The polarization for various incident π^- momenta are given in Figs. 2-12. Fig.2 corresponds to .596 Bev/c incident momentum; Fig.3 to 0.671 Bev/c, Fig.4 to 0.745 Bev/c, Fig.5 to 0.820 Bev/c, Fig.6 to 0.895 Bev/c, Fig.7 to 1.165 Bev/c, Fig.8 to 1.352 Bev/c Fig.9 to 1.988 Bev/c, Fig.10 to 2.535 Bev/c, Fig. 11 to 2.912 Bev/c and Fig. 12 to 3.260 Bev/c.

CONDENSATION OF ROTATING HELIUM II[4,6)]

Two interesting experiments have been reported on the condensation of liquid helium II due to rotation. The first of these experiments by Andronikashvili et al demonstrates the velocity dependence of the density of helium II and the jump that occurs in the density of rotating helium while going into the superfluid state from the non-superfluid state. A remarkable suggestion has been made that Helium II going into the vortex state may be a 1st order transition. The second one by Bablidze et al, by measuring the velocity of first sound in rotating helium II, have shown that compressibility does not depend very much on the rotation velocity.

The experimental set up of Andronikashvili et al can be briefly described as follows. Sensitive pycnometers, inserted into a vessel of organic glass and immersed into a bath of liquid helium, were set to rotate. To the upper end of the capillary in the pycnometer was attached a valve which regulated the amount of helium into the pycnometer. During the experiment the valve was tightly closed. The experiment was performed both for stationary and rotating helium.

To determine the temperature dependence of the density of stationary helium II the following procedure was used. The level of helium in the pycnometer was fixed at a certain temperature T_1. Then the change in the level of helium was measured as it was heated from temperature T_1 and T_2. If $\Delta_1 h$ is the

change and ρ_1 is the density of helium II at temperature T_1, the following formula gives the density ρ_2 at temperature T_2

$$\rho_2 = \rho_1 + \rho_1 \frac{\pi r^2}{V_0} (\Delta_1 h + \Delta_2 h)$$

r being the radius of the capillary and V_0, the volume of the pycnometer. $\Delta_2 h$ takes care of evaporation and the change in the density of the liquid and the vapour.

For the case of rotating helium the following formula was used.

$$\Delta\rho = \rho\omega_0 - \rho = \pi r^2 V_0^{-1} \rho \Delta_3 h$$

ω_0 being the velocity of rotation and $\Delta_3 h$ being the level difference due to rotation.

Results for the case of rotating helium are given in Fig.13 for various temperatures. The remarkable features are the following; As the liquid is rotated more and more, it becomes denser and denser and this effect is increasing as the temperature is lowered.

For the case of stationary liquid the results are given in Fig.14. The solid curve gives the dependence of the density of stationary helium on temperature whereas the dashed curve drawn through circles, shows the change in the density when helium has an angular velocity of 30 sec^{-1}. Above the λ -point the data for stationary and rotating helium coincide.

In order to draw the conclusion, that a jump in the density of rotating helium occurs while crossing the λ -point, in an unambiguous manner the experiment was performed in the temperature interval 2.14 to 2.18°K with a fixed amount of liquid in the pycnometer. The results of this special investigation shown in Fig.15, demonstrates the abrupt change in the density of liquid helium in the temperature interval 2.171-2.176°K.

As a result of condensation the liquid helium II level in the capillary drops. The decrease in the hydrostatic pressure due to this was unexpectedly large.

Coming back to the case of rotating helium the velocity dependence of the relative condensation $\Delta\rho/\rho$ is closely described by

$$\Delta\rho/\rho = C(T)\,\omega^{3/2}$$

where $C(T)$ is a monotonically decreasing function of T. It abruptly becomes zero at the transition point.

Unsuccessful attempts were made to explain this phenomenon by the action of centrifugal pressure. If centrifugal pressure is the cause then

$$\Delta\rho/\rho = 0.25\,\chi_T\,\rho\,\omega^2 R^2$$

R being the distance to the axis of rotation. χ_T is the coefficient of isothermal compressibility. Though centrifugal pressure is the most important factor that could cause compression

the above formula alone does not explain the situation fully. To reconcile the change in the density expressed by the above equation one has to take for χ a valve which is 200 times larger and this change in χ_T will bring in a change in the velocity of sound which is 14 times larger. Thus the possibility of χ_T becoming different due to rotation of Helium II can be checked and eliminated if the change in the density is to be ascribed to a new phenomenon.

Such an experimental verification can be had if the velocity of first sound in liquid helium given by

$$C = \left(1/\chi_S \rho\right)^{1/2} = \left(\gamma/\chi_T \rho\right)^{1/2}$$

is not changed very much. Here $\gamma = C_P/C_V = \chi_T/\chi_S$ and C_P & C_V being the specific heat of the liquid at constant pressure and constant volume. χ_S is the co-efficient of adiabatic compressibility.

Bablidze et al made such measurements of the velocity of first sound using a pulse procedure. Short sound pulses were transmitted through the liquid and the travel time of these pulses along a segment of definite length was measured.

A schematic diagram of the apparatus used has been given in Fig.16. The rotation is about the vertical shaft 2. The sound pulses radiated by plate 1 were reflected by plate 4 and sent back to be received by plate 1. In course of the travel from platell to 4 and then from 4 to 1 the sound pulses crossed

Onsager-Feynman Vortex lines at a right angle. There is another such pair of plates (plates 3 and 5) deal with sound pulses travelling along the vortex lines. Thus this set up makes it possible to study the propagation of sound pulses both along the vortex lines and transverse to them. When sound pulses propagate perpendicular to the axis of rotation, the number of vortices that are crossed by the sound pulses and subtended by one wave length obviously depend on the speed of sound, its frequency and the angular velocity of rotation of the helium II as a whole.

Bablidze et al measured the speed of sound both with stationary and rotating helium II. The angular velocities were varied in the range 0-70 sec^{-1} while the temperature was varied in the interval 1.40-2.10^{o}K. Comparison of the results of measurements on stationary and rotating helium II show that the angular velocity of rotation has no influence on the velocity of propagation of sound waves in it. Also the notion that there exists some anomalous compressibility was not confirmed.

It is evident from this observation that some other mechanism has to be found out to explain the condensation effect of rotating heliums II.

References

1) R.J.Abrams et al, Physical Review Letters 19, 678 (1967)

2) T.C.Jacon et al, Physical Review 157, 1263 (1967)

3) M.Hansroul, Preprint (UCRL-17263).

4) E.L.Andronikashvili and Dz.S.Tsakadze, Soviet Phys.(JETP) 24, 907 (1967).

5) R.A.Babl idze and N.S.Gavrilidi, Soviet Phys.(JETP), 24, 905 (1967).

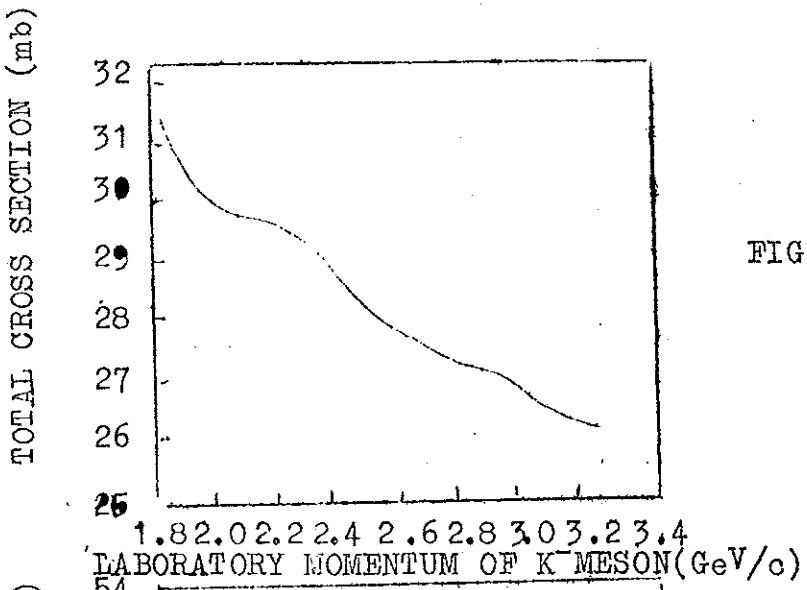
TOTAL CROSS SECTION (mb)
32
31
30
29
28
27
26
25
1.8 2.0 2.2 2.4 2.6 2.8 3.0 3.2 3.4
LABORATORY MOMENTUM OF K⁻ MESON(GeV/c)

FIG. IA

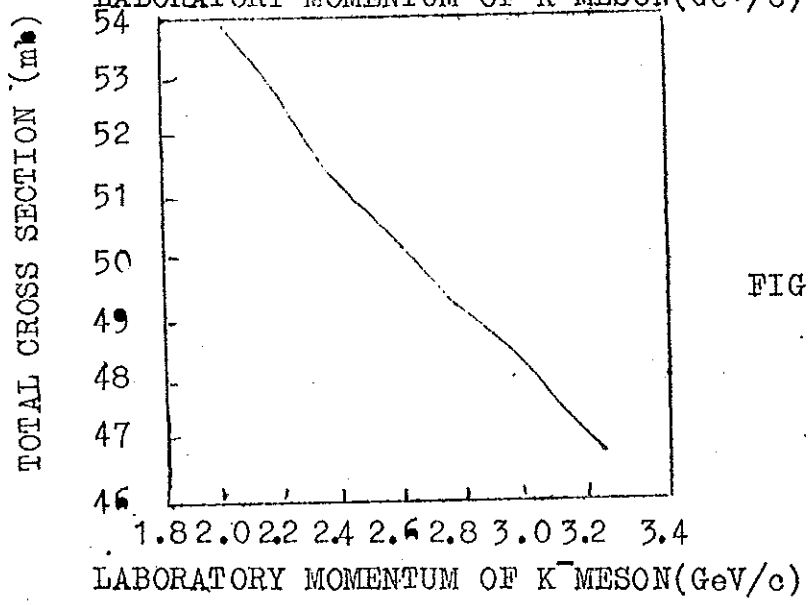
TOTAL CROSS SECTION (mb)
54
53
52
51
50
49
48
47
46
1.8 2.0 2.2 2.4 2.6 2.8 3.0 3.2 3.4
LABORATORY MOMENTUM OF K⁻ MESON(GeV/c)

FIG. IB

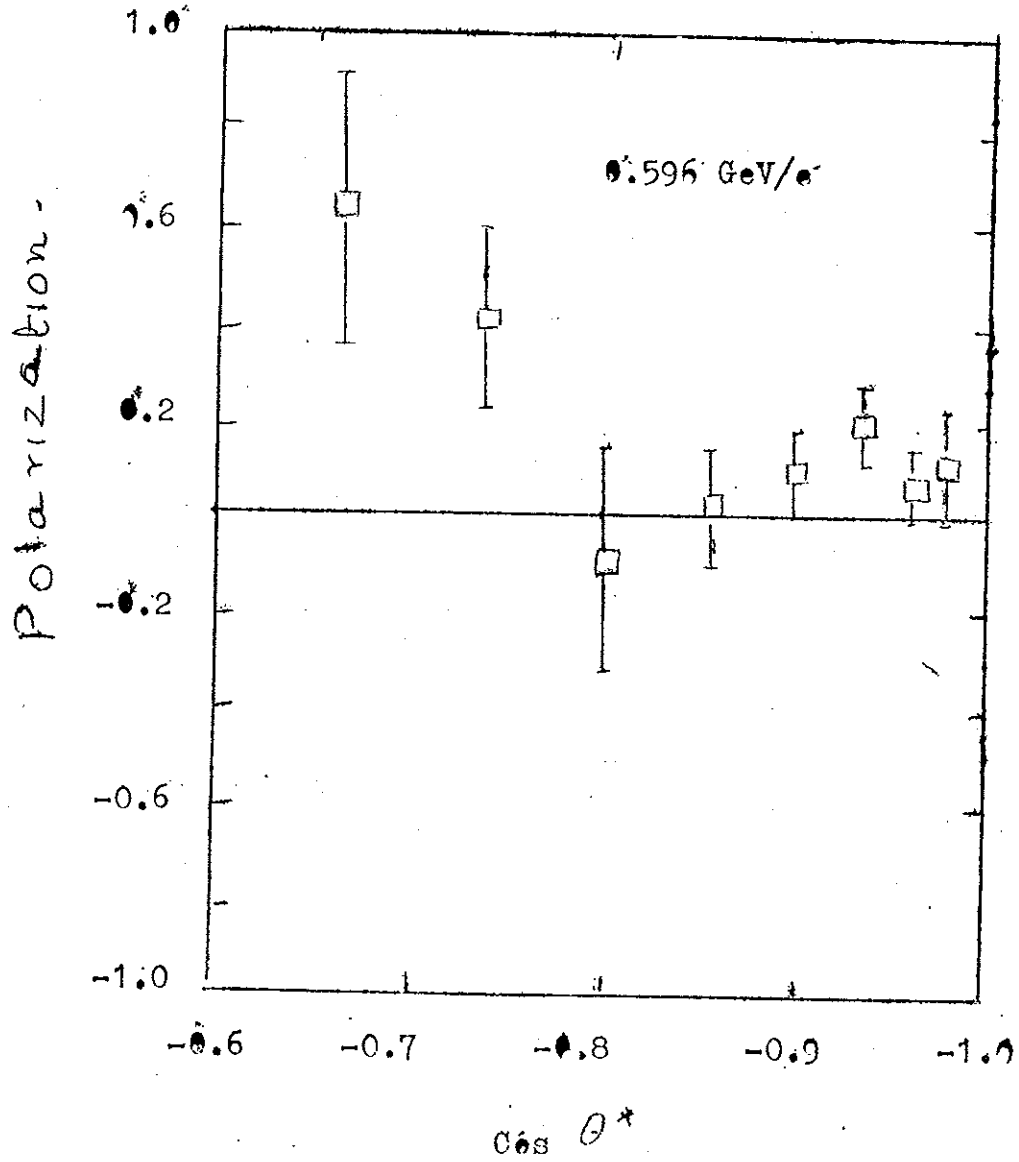

FIG. 2.

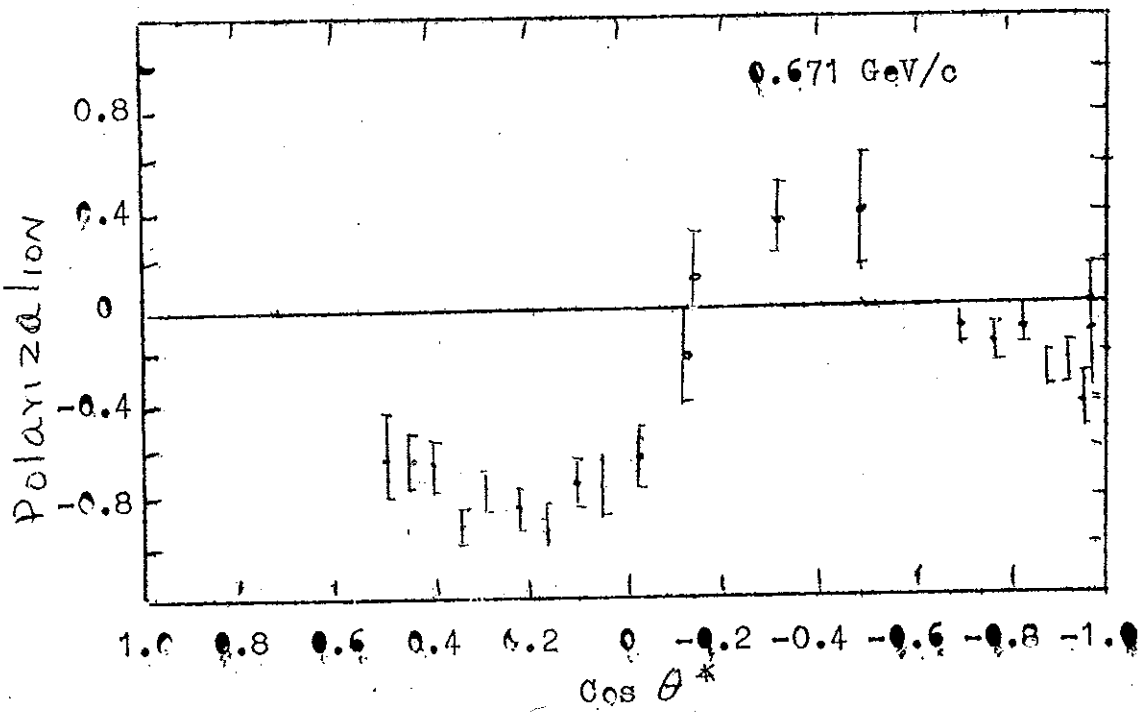
0.671 GeV/c
Polarization
0.8
0.4
0
-0.4
-0.8
1.0 0.8 0.6 0.4 0.2 0 -0.2 -0.4 -0.6 -0.8 -1.0
Cos θ*

Fig. 3

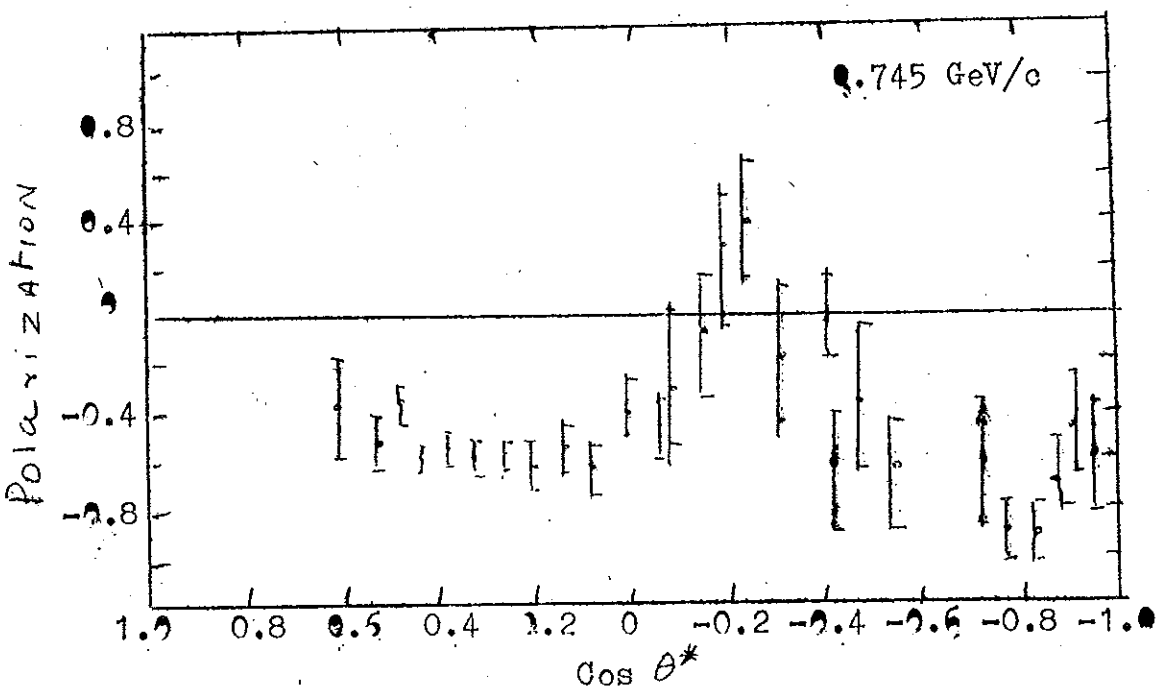
0.745 GeV/c
Polarization
0.8
0.4
0
-0.4
-0.8
1.0 0.8 0.6 0.4 0.2 0 -0.2 -0.4 -0.6 -0.8 -1.0
Cos θ*

Fig. 4

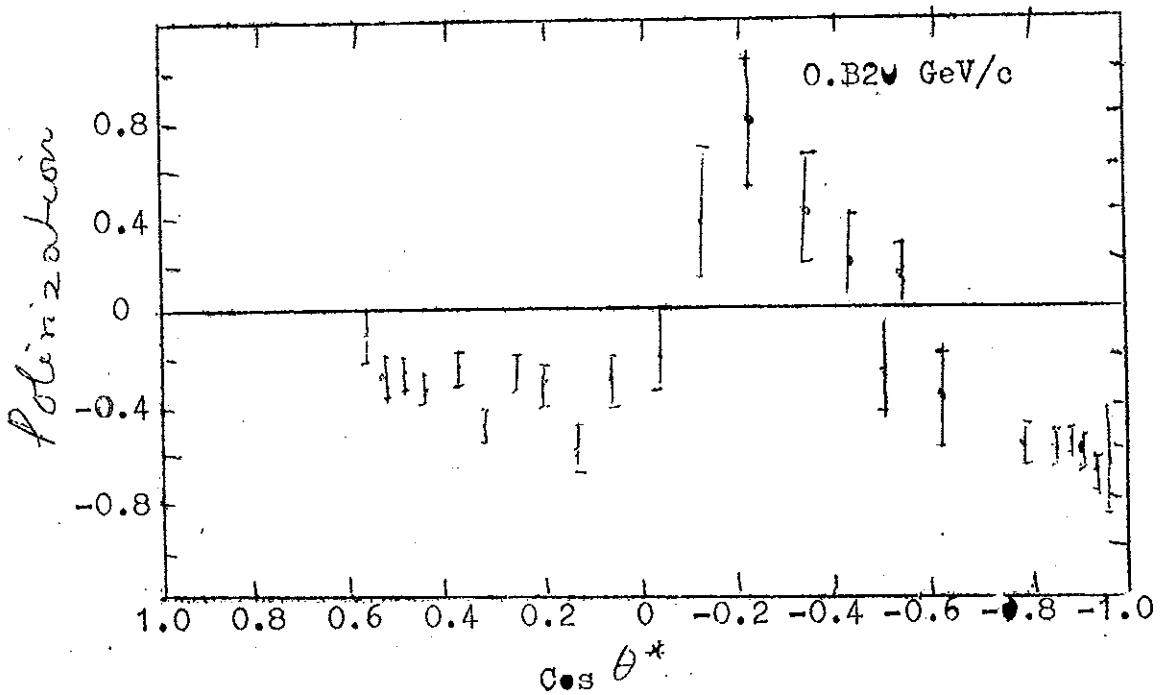
0.B2 GeV/c
Polarization
0.8
0.4
0
-0.4
-0.8
1.0 0.8 0.6 0.4 0.2 0 -0.2 -0.4 -0.6 -0.8 -1.0
Cos θ*

FIG. 5

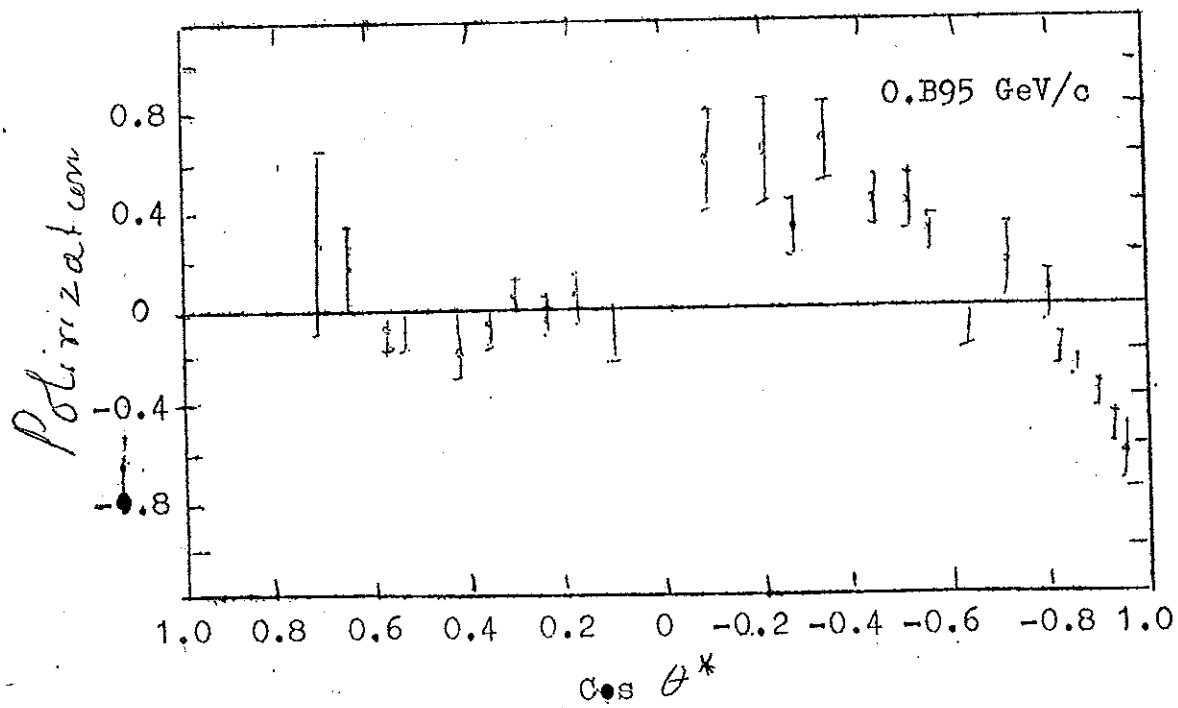
0.B95 GeV/c
Polarization
0.8
0.4
0
-0.4
-0.8
1.0 0.8 0.6 0.4 0.2 0 -0.2 -0.4 -0.6 -0.8 1.0
Cos θ*

FIG. 6

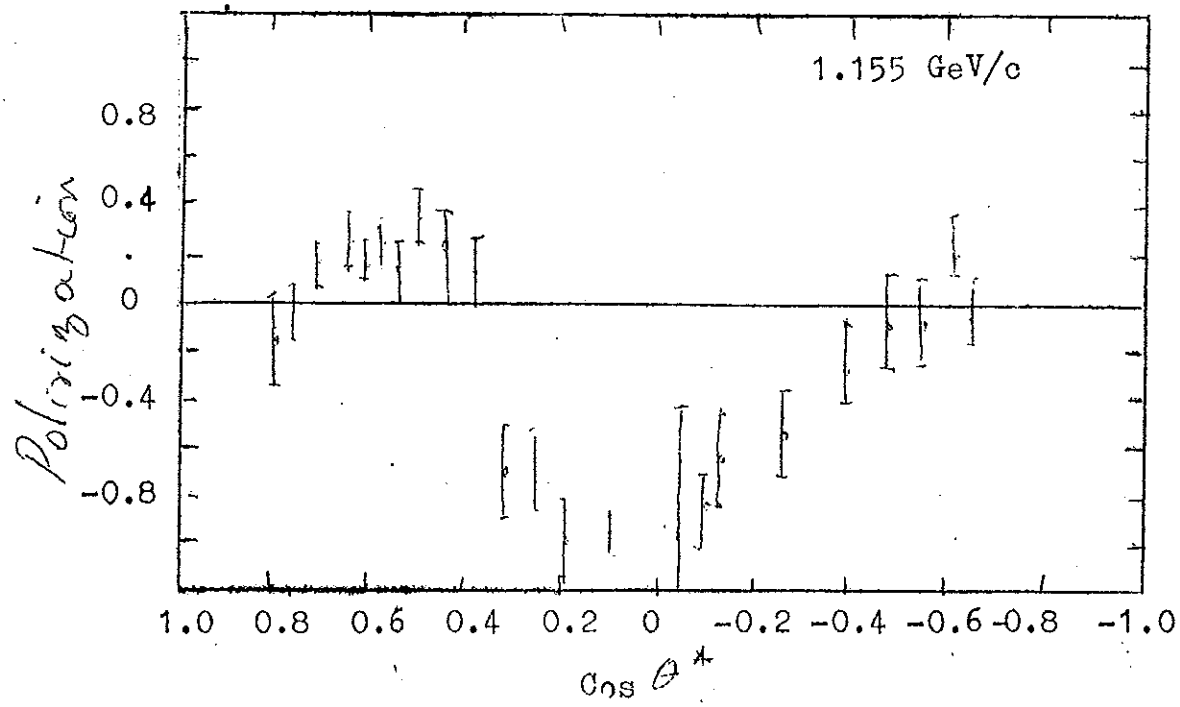
1.155 GeV/c
Polarization
0.8
0.4
0
-0.4
-0.8
1.0 0.8 0.6 0.4 0.2 0 -0.2 -0.4 -0.6 -0.8 -1.0
Cos θ*

FIG.7

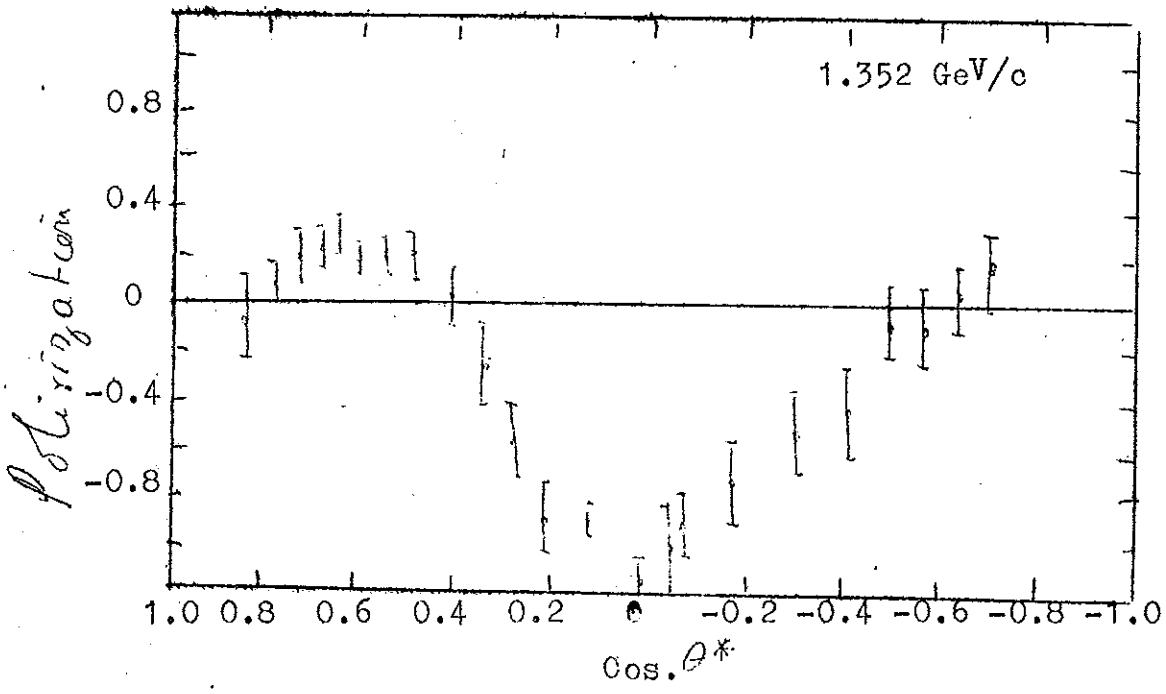
1.352 GeV/c
Polarization
0.8
0.4
0
-0.4
-0.8
1.0 0.8 0.6 0.4 0.2 0 -0.2 -0.4 -0.6 -0.8 -1.0
Cos. θ*

FIG.8

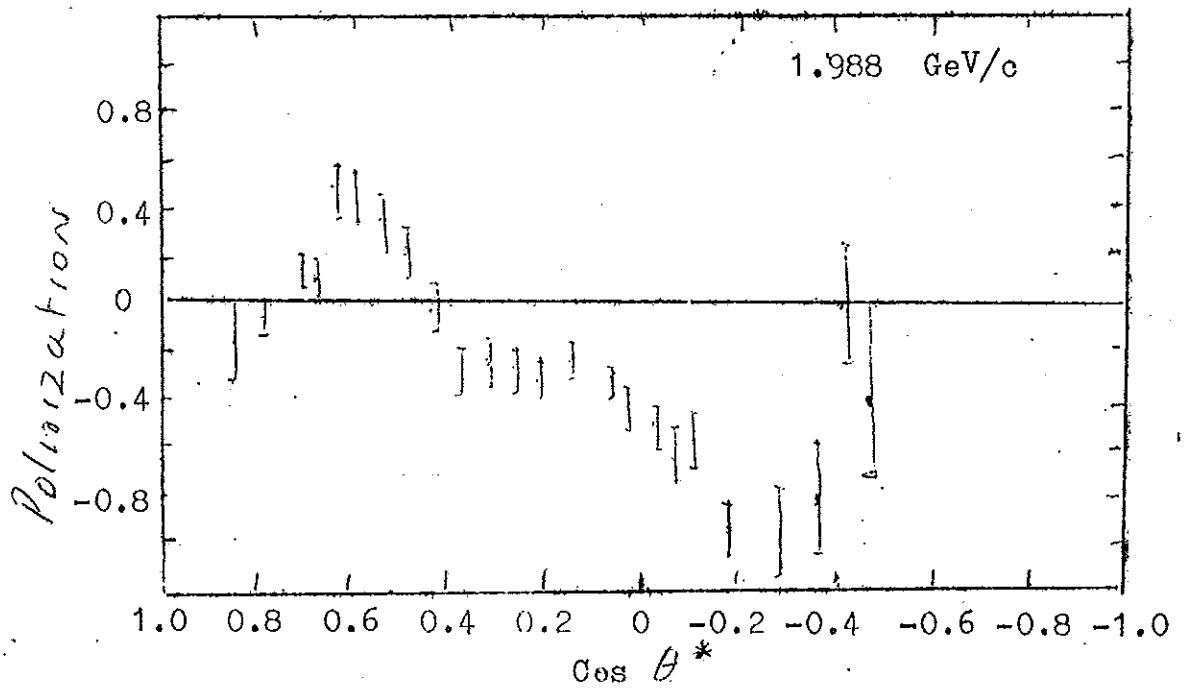
1.988 GeV/c
Polarizations
0.8
0.4
0
-0.4
-0.8
1.0 0.8 0.6 0.4 0.2 0 -0.2 -0.4 -0.6 -0.8 -1.0
Cos θ*

FIG. 9

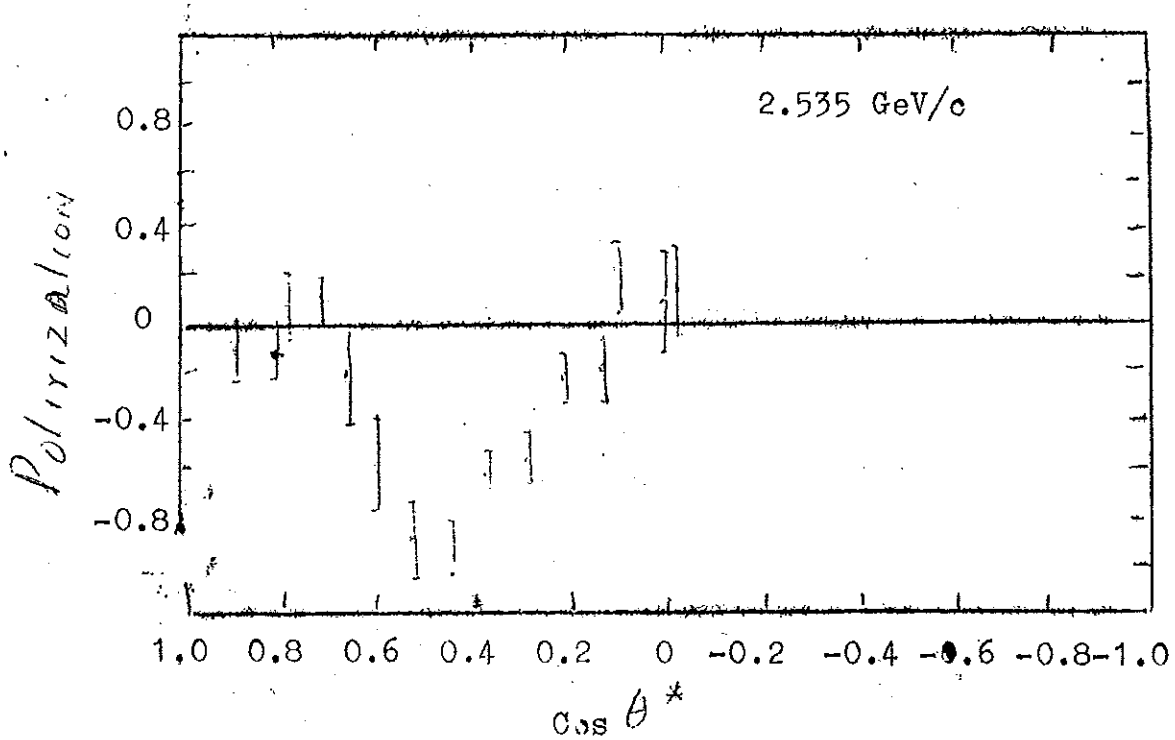
2.535 GeV/c
Polarization
0.8
0.4
0
-0.4
-0.8
1.0 0.8 0.6 0.4 0.2 0 -0.2 -0.4 -0.6 -0.8 -1.0
Cos θ*

FIG.10

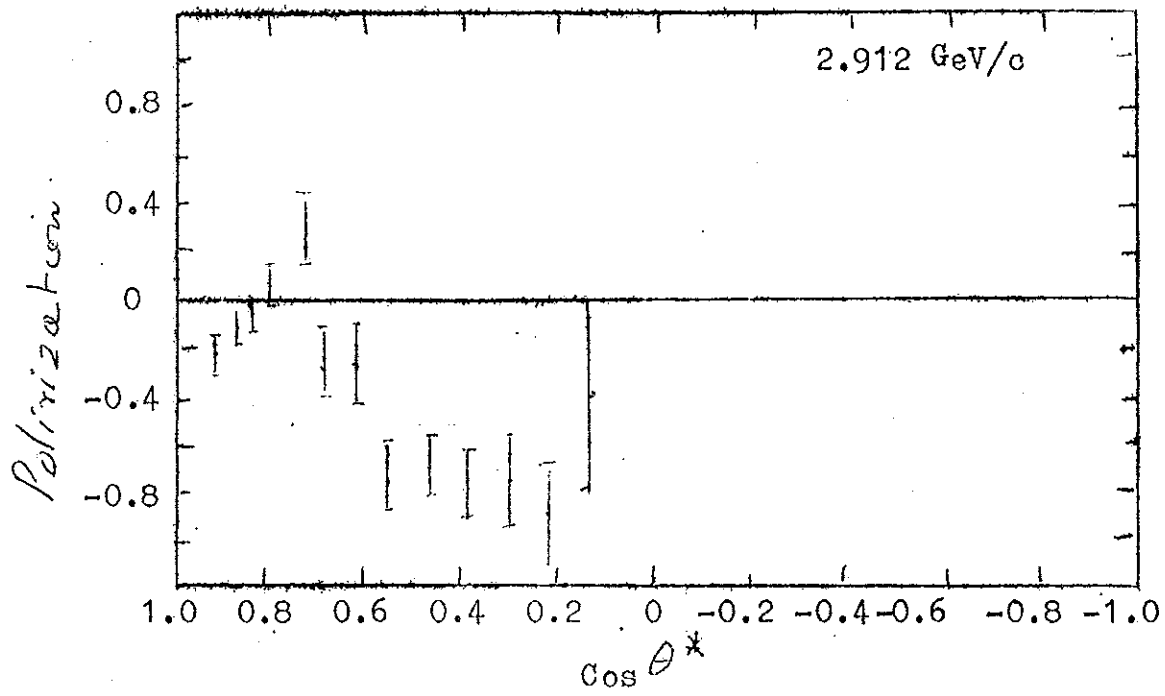
2.912 GeV/c
0.8
0.4
0
-0.4
-0.8
1.0 0.8 0.6 0.4 0.2 0 -0.2 -0.4 -0.6 -0.8 -1.0
Cos θ*

FIG.11

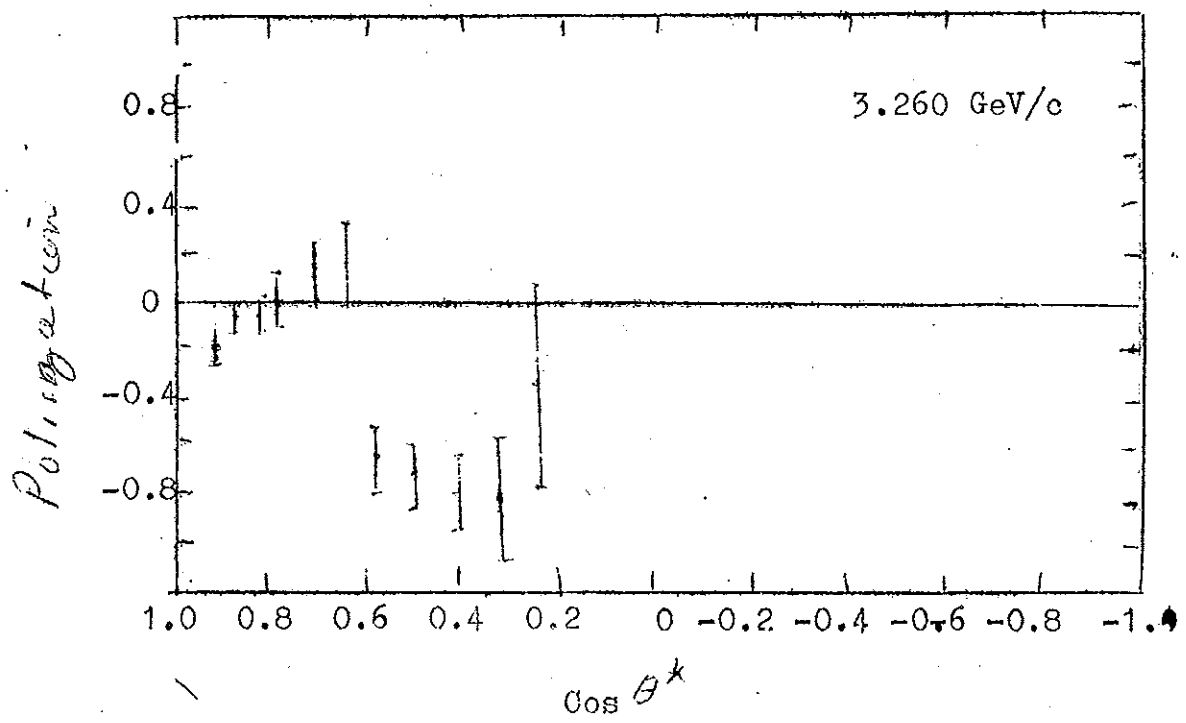
3.260 GeV/c
0.8
0.4
0
-0.4
-0.8
1.0 0.8 0.6 0.4 0.2 0 -0.2 -0.4 -0.6 -0.8 -1.0
Cos θ*

FIG.12

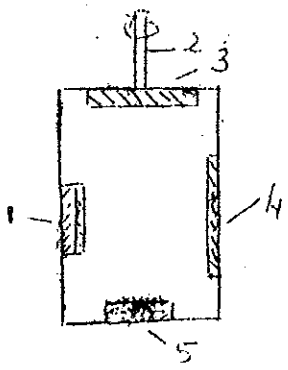

Fig.16

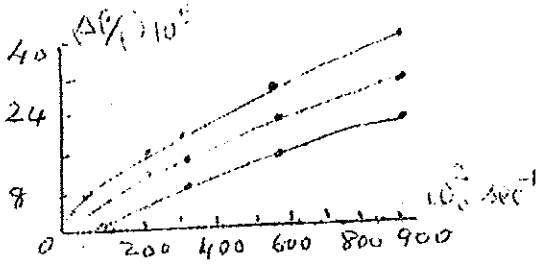

Fig.13

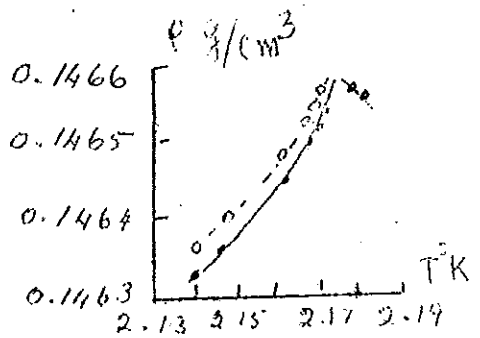

Fig.14

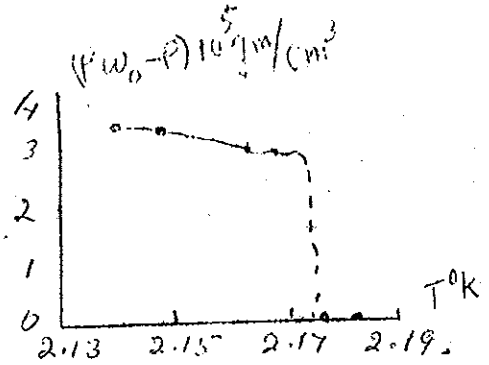

Fig.15

OCTOBER 1967.

Introduction

The first three experiments of the present report have to do with high energy p-p and $\bar{p}$-p scattering and production cross-sections both at small and large angles. The first experiment gives the total cross-sections for p-p scattering in the range 8 to 26 Bev/c and α, the ratio of the real to the imaginary part of the nuclear amplitude. The corresponding value of α for $\bar{p}$-p scattering at 12 Bev/c is given. The second experiment gives the differential and total cross-sections for the production of $\bar{\Lambda}\Lambda$, $\bar{\Sigma}^0\Lambda$ and $\bar{\Lambda}\Sigma^0$ in $p\bar{p}$ collision at 2.5 Bev/c. The third experiment on large angle proton-proton elastic scattering at energies in the range 8 - 21 Bev/c shows up a discontinuous behaviour in the shape of the angular distribution between 8 and 11 Bev/c.

Two experiments on k^-p interactions at 4.6 and 5.0 Bev/c are reported. The first gives the branching ratios for the decay modes of the $f^*(1500)$ meson and establishes its C-parity to be even. The second gives the branching ratios for $k^*(1420)$ decays and also a comparison with SU(3) prediction for the partial widths of the decays of the various members of the 2^+ nonet.

2

ELEMENTARY PARTICLES

High-Energy, small angle p-p and $\bar{p}$-p scattering p-p total Cross-sections[1)]

The small angle p-p differential elastic scattering cross-sections were measured from 8 to 26 Bev/c and $\bar{p}$-p cross-sections were measured at 12 Bev/c. The real part of the nuclear amplitude was deduced from Coulomb-nuclear interference under the assumption of spin independence. This latter is necessary since unlike in pion-nucleon scattering the p-p interaction at $t = 0$ is complicated by the existence of a singlet and two triplet amplitudes. The assumption of spin independence allows an analysis in terms of a single scattering amplitude. Using the optical theorem, the imaginary part of the amplitude was deduced from the total cross-sections.

The p-p total cross-sections are given in Table I below and the results for α, the ratio of the real to the imaginary part of the nuclear amplitude in Table II . For $\bar{p}$-p at 11.9 Bev/c, $\alpha = -0.006 \pm 0.034$ which is in agreement with the dispersion-relation prediction of -0.06.

Table I

Momentum (Bev/c)	σ_{p-p} (mb)
7.82	40.34 ± 0.12
9.80	39.84 ± 0.12
11.90	39.62 ± 0.12
14.01	39.42 ± 0.12
16.03	39.23 ± 0.12
17.91	39.18 ± 0.12
20.22	39.05 ± 0.12
20.46	39.09 ± 0.12
22.06	38.88 ± 0.12
24.0	38.89 ± 0.12
26.0	38.90 ± 0.12

Table II

Momentum (Bev/c)	α
7.81	-0.331 ± 0.014
9.86	-0.345 ± 0.018
9.86	-0.343 ± 0.009
11.94	-0.290 ± 0.013
14.03	-0.272 ± 0.013
20.24	-0.205 ± 0.013
24.12	-0.157 ± 0.018
26.12	-0.154 ± 0.025

Reactions $\bar{p}p \rightarrow \bar{\Lambda}\Lambda$ at 2.5 Bev/c[2)], J.

2.434 ± 0.030 Bev/c antiprotons were used in an experiment to measure the differential and total cross-sections for $\bar{\Lambda}\Lambda$, $\bar{\Lambda}\Sigma^0$ and $\bar{\Sigma}^0\Lambda$ production. The masses (m) and lifetimes (γ) of the Λ and $\bar{\Lambda}$ were estimated:

$$m(\bar{\Lambda}) - m(\Lambda) = 0.29 \pm 0.15 \text{ MeV/c}^2$$

$$\frac{1}{2}[m(\bar{\Lambda}) + m(\Lambda)] = 1116.0 \pm 0.2 \text{ MeV/c}^2$$

$$\gamma_{\Lambda}(\bar{\Lambda}) = (2.44 \pm 0.15) \times 10^{-10} \text{ sec.}$$

$$\gamma_{\Lambda}(\Lambda) = (2.55 \pm 0.15) \times 10^{-10} \text{ sec.}$$

The cross-sections for the various processes in μb are

$\bar{\Lambda}\Lambda = 127 \pm 9$; $\bar{\Sigma}^0\Lambda = 33 \pm 5$; $\bar{\Lambda}\Sigma^0 = 31 \pm 5$

$\bar{\Sigma}^0\Lambda + \bar{\Lambda}\Sigma^0 = 64 \pm 5$, $\bar{\Sigma}^0\Sigma^0 = 11 \pm 5$, $\bar{\Lambda}\Lambda\pi^0 = 19 \pm 5$

Fig.1 shows the variation of cross-sections with total energy which shows a decrease like s^{-2}. The differential cross-sections are given in Figs.2 and 3. They show the exponential peak for small momentum transfer.

Large angle proton-proton elastic scattering at high energies[3].

The elastic differential cross-sections for p-p scattering were measured at 8, 9, 10, 11, 14, 19 and 21 Bev/c and in the angular range 65° to 90° c.m.s. The results are given in Table I below. The values of the parameter b in

$$\left(\frac{d\sigma}{d\Omega}\right)_{c.m.} \propto \exp(-p \sin\theta / b)$$

are given in Table II. The rapid change of b between 8 and 11 Bev/ corresponding to a flattering of the angular distribution is striking.

Table I

Incident Momentum (Bev/c)	θ c.m. degrees	$(d\sigma/d\Omega)_{c.m.}$ $(cm^2\,sr^{-1}) \times 10^{33}$
8.1	68.8	543 ± 16
	72.2	455 ± 20
	76.2	323 ± 10
	82.2	214 ± 7
9.1	68.1	188 ± 5
	74.2	118 ± 3
	82.2	94 ± 3
10.0	67.0	106.2 ± 1.7
	70.0	79.1 ± 1.7
	75.0	58.9 ± 1.5
	83.0	49.4 ± 1.1

Incident Momentum (Bev/c)	$\theta_{c.m.}$ degrees	$(d\sigma/d\Omega)_{c.m.}$ $(cm^2\ sr^{-1} \times 10^{33})$
11.0	73.0	36.0 ± 0.9
	78.0	29.6 ± 0.7
	86.0	26.9 ± 0.9
14.25	67.0	7.58 ± 0.23
	71.0	5.86 ± 0.19
	77.0	4.36 ± 0.14
	90.0	3.31 ± 0.09
16.9	67.0	2.01 ± 0.04
	70.0	1.58 ± 0,06
	72.0	1.43 ± 0.05
	75.0	1.21 ± 0.04
	77.0	1.03 ± 0.03
	80.0	0.92 ± 0.04
	82.0	0.86 ± 0.03
	85.0	0.81 ± 0.04
	90.0	0.75 ± 0.05
19.3	64.0	0.682 ± 0.029
	69.0	0.419 ± 0.026
	75.0	0.270 ± 0.020
	90.0	0.188 ± 0.017
21.3	66.0	0.220 ± 0.018
	70.0	0.135 ± 0.011
	75.0	0.101 ± 0.008
	87.0	0.061 ± 0.009

Table II

Incident Momentum	b (Mev/c)
3.0	251 ± 12
3.0	177 ± 4
4.0	120 ± 6
5.0	147 ± 3
5.0	158 ± 6
6.0	152 ± 6
7.1	154 ± 6
7.1	132 ± 12
8.1	118 ± 13
9.1	172 ± 27
10.0	191 ± 21
11.0	294 ± 50
14.25	240 ± 2
16.9	225 ± 5
19.3	224 ± 9
21.3	209 ± 17

Properties of the f* meson[4)]

k^--p interactions at 4.6 and 5.0 Bev/c incident k^--momentum using the BNL 80-inch bubble chamber were analysed for the following final states relevant to the study of f^0:

$(\Lambda^0, \Sigma^0) K^0 \bar{K}^0$, $(\Lambda^0, \Sigma^0) K^+ K^-$, $(\Lambda^0, \Sigma^0) \pi^+ \pi^-$, $(\Lambda^0, \Sigma^0) K \bar{K}$

$(\Lambda^0, \Sigma^0) \pi^+ \pi^- MM$, $\Lambda \pi^+ \pi^+ \pi^- \pi^- \pi^0$, $(\Lambda^0, \Sigma^0) MM$

The absence of the $K_1 K_2$ mode establishes that the f* must be even under C and restricts the possible J^P assignments to the values 0^+, 2^+, 4^+ etc. Studies of the $k\bar{k}$ decay angular distributions to rule out the possibility, 0^+.

The following table gives the branching ratios for the various decay modes of the f*(1500) meson.

Final state	Total number of events	Events in f* region	Decay mode	Branching ratios	
				Without k*k signal	With k*k signal
$(\Lambda, \Sigma) K\bar{K}$	502	200 ± 32	$k\bar{k}$	0.80±0.13	0.72±0.12
$(\Lambda, \Sigma)\pi^+\pi^-$	1150	< 36		< 0.14	< 0.13
$(\Lambda, \Sigma) KK\pi$	330	< 28		<00.11	0.13±0.10
$(\Lambda, \Sigma)\pi^+\pi^- MM$ + $(\Lambda, \Sigma)\pi^+\pi^-\pi^+\pi^-\pi^0$	120°	or 28±21 50±25		0.20±1.10	0.18±0.10
(Λ, Σ) MM	900	15 ± 50		< 0.4	< 0.36

Decay rates of k*(1470) and the 2^+ nonet[5])

The data relevant for the determination of the branching ratios for the various k*(1420) decay mode comes from a study of the k^-p interactions at 4.6 and 5.0 Bev/c for the following final states:

$K^0\pi^+\pi^- n$, $\bar{K^0}\pi^- p$, $\bar{K^0}\pi^-\pi^0 p$

The branching ratios are given in Table I below. In Table II, the experimental values for partial widths for the various decay modes of the members of the $J^P = 2^+$ nonet together with the SU(3) predictions are given.

Table I

Final state	Decay mode	Raw No. of events	Derived branching ratios
$K^0\pi^+\pi^-n$	$(K^*\pi)^0$	18 ± 4	$\frac{K\rho}{K\pi + K\pi\pi} = 0.14 \pm 0.10$
	$K\rho^0$	4 ± 4	
$K^0\pi^-p$	$(K\pi)^-$	39 ± 8	$\frac{K\pi}{K\pi + K\pi\pi} = 0.39 \pm 0.11$
$K^0\pi^-p\pi^0$	$(K^*\pi)^-$	32 ± 9	$\frac{K^*\pi}{K\pi + K\pi\pi} = 0.47 \pm 0.10$

Table II

Decay Mode	$\Gamma_{expt.}$ (Mev)	SU(3) Rates Γ (Mev)
Type A decah: $2^+ \rightarrow 1^- + 0$		
$A_2(1320) \rightarrow \rho\pi$	56 ± 19	67
$K^*(1420) \rightarrow K^*\pi$	34 ± 12	22
$K^*(1420) \rightarrow \rho K$	10 ± 9	6
$K^*(1420) \rightarrow \omega^0 K$	4 ± 3	2
$f^*(1500) \rightarrow K^*K$	9 ± 9	10

Type B decays: $2^+ \to 0^- + 0^-$

$A_2 \to K\bar{K}$	2.5 ± 2	4
$A_2 \to \eta^0 \pi$	6.5 ± 6	7
$K^*(1420) \to K\pi$	29 ± 13	29
$K^*(1420) \to K\eta^0$	3 ± 3	1
$f^0 \to \pi\pi$	117 ± 21	121
$f^0 \to K\bar{K}$	0 ± 12	7
$f^0 \to \eta^0\eta^0$	0 ± 12	1
$f^* \to \pi\pi$	0 ± 6	1
$f^* \to K\bar{K}$	62 ± 15	33
$f^* \to \eta^0\eta^0$	0 ± 16	8

References

1) K.J. Foley et al, P.R.L. 19, 857 (1967).

2) J. Badier et al, Physics Letters 25B, 152 (1967).

3) J.V. Allaby et al, Physics Letters 25B, 156 (1967).

4) V.E. Barnes et al, P.R.L. 19, 964 (1967).

5) D. Bassano et al, P.R.L. 19, 968 (1967).

Introduction

The present report starts with data on πp elastic scattering in the backward direction at 2.85 and 3.30 Bev/c.

Precise values for the masses of Σ hyperon and the muon neutrino obstained from range measurements on tracks in nuclear emulsions are given.

The lifetime of η-meson determined using the Primakoff effect (production of a meson by interaction of a photon with the virtual photon associated with the Coulomb field of the target nucleus) which can be considered the inverse of the meson decay into two photons is given.

Data from two experiments on photoproduction of π^+ mesons on nucleons are given, the first for low energies at 0° and forward angles and the second at energies of 3.4 and 5.0 Bev. The former data agree with calculations based on the GLN amplitudes. The latter cannot be fitted well with a simple reggeized pion model.

Evidence for an enhancement in the ΛK^+ system at 1.7 Bev is forthcoming from the reaction $\pi^- p \rightarrow \Lambda K^+ \pi^-$. Evidence for the existence of the hypernucleus Λ^{Li^6} is obtained from a systematic study of mesonic decays of hypernuclei with four charged-particle final states. The large mass difference between the mirror hypernuclei Λ^{Li^6} and Λ^{He^6} may indicate breakdown of charge symmetry in ΛN interactions.

Finally the branching ratio for η decay into two photons is given.

ELEMENTARY PARTICLES

Backward πp elastic scattering at 2.85 and 5.30 Bev/c [1)]

$\pi^+ p$ elastic scattering was measured at two incident momenta, 2.85 ± 0.05 and 3.30 ± 0.05 Bev/c at c.m.s. angles 164° to 176° $\pi^- p$ elastic scattering was measured at 3.30 ± 0.05 Bev/c at c.m.s. angles 163° to 176°. A total of 100,000 spark chamber photographs were taken of which 975 events turned out to be elastic. The differential cross-sections are given in table I below. The value of B from the exponential fit $\frac{d\sigma}{du} = A e^{Bu}$ where u is the four-momentum transfer squared between the incident and outgoing proton is given in Table II. There is no significant change in slope with energy. The π^+ data show steeply rising backward peaks.

The $\pi^+ p$ data agrees with calculations based assuming only the resonances in the direct channel. All but one of the known resonances in this channel have odd ℓ and hence add constructively at 180°. In the $\pi^- p$ system both odd and even ℓ amplitudes are present and give rise to a smaller cross-section. Baryon exchange may also influence the $\pi^- p$ backward scattering. $\pi^+ p$ scattering is not affected by such a mechanism at 180°, but away from the backward direction with onset of a dip at 2.84 Bev, There is a decrease in the differential cross-section which may necessitate destructive interference, possibly with baryon exchange graphs.

Table I

Particle Momentum	$\cos\theta_{c.m.}$	u $(Bev/c)^2$	$d\sigma/d\Omega$ $(\mu b/sr)$	$d\sigma/du$ $(\mu b/(Bev/c)^2)$
$\pi^+ p$	-0.995	0.107	163 ± 14	448 ± 37
2.85 Bev/c	-0.991	0.098	150 ± 13	412 ± 35
p.c.m. = 1.07 Bev/c	-0.987	0.089	142 ± 13	384 ± 36
$s = 6.25(Bev)^2$	-0.983	0.080	129 ± 14	354 ± 38
	-0.979	0.070	119 ± 15	327 ± 41
	-0.975	0.061	113 ± 17	310 ± 46
	-0.971	0.052	109 ± 19	300 ± 51
	-0.967	0.043	68 ± 17	187 ± 47
	-0.963	0.034	37 ± 14	101 ± 38
	-1.000	0.118	177 ± 15	487 ± 41
$\pi^+ p$	-0.994	0.088	57 ± 7	132 ± 16
3.30 Bev/c	-0.988	0.072	45 ± 7	104 ± 15
pc.m.=1.16 Bev/c	-0.982	0.056	35 ± 7	82 ± 15
$s = 7.10(Bev)^2$	-0.976	0.040	27 ± 7	63 ± 16
	-0.970	0.023	24 ± 8	56 ± 18
	-0.964	0.007	20 ± 8	46 ± 17
	-1.000	0.104	70 ±10	163 ± 24
	-0.961	0.000	17 ± 4	39 ± 9
$\pi^- p$	-0.992	0.083	10.4±1.4	24.1 ± 3.7
3.30 Bev/c	-0.982	0.056	7.5±1.5	17.5 ± 3.4
	-0.972	0.029	7.9±2.0	18.4 ± 4.8
	-0.962	0.002	5.8±2.2	13.5 ± 5.1
	-1.000	0.104	11.6±2.2	27.0 ± 5.1
	-0.961	0.060	5.8±1.5	13.6 ± 3.6

Table II

Incident momentum (Bev/c)	B (BeV/c)^2 π^+	π^-
2.85	7.9 ± 2.4	-
3.30	13.7 ± 3.4	6.6 ± 3.9
3.55	11.9 ± 1.7	2.4 ± 2.0

Mass measurements using the range-energy relation[2)]

Precise values of particle masses are obtained by making range measurements on tracks in nuclear emulsions. In the present experiment using a stopping K^--beam in a helium bubble chamber, the range data on the following reactions were obtained.

$$\pi^- + {}^4He \longrightarrow {}^3H + n \qquad (1)$$

$$K^- + {}^4He \longrightarrow {}^4_\Lambda H + \pi^0 \qquad (2)$$

$$\Sigma^+ \longrightarrow p + \pi^0 \qquad (3)$$

$$\pi^+ \longrightarrow \mu^+ + \nu_\mu \qquad (4)$$

$$\pi^- \longrightarrow \mu^- + \nu_\mu \qquad (5)$$

The masses of Σ^+ and ν_μ were determined. The mass of the ν_μ gets involved in an interesting way with possible violation of T-invariance, in the expression for the muon decay rate.[3] Thus a precise knowledge of its mass is important. The values obtained were

$$m_{\Sigma^+} = 1189.39 \pm 0.14$$

$$m_{\nu_\mu} \leq 2.2 \text{ Mev/c}^2.$$

Determination of η lifetime.[4]

Mesons decaying into two gammas (like $\eta \to \gamma\gamma$) can be produced by the interaction of an incident photon with a virtual photon (which for small momentum transfer can be considered very nearly real) associated with the Coulomb field of the target nucleus. This process (Primakoff effect) can be considered the inverse of the meson decay into two photons and the resulting cross-section is directly proportional to the $\Gamma_{\gamma\gamma}$ decay width

$$\frac{d\sigma_p}{d\Omega} = 8\alpha\,\Gamma_{\gamma\gamma} Z^2 \frac{\beta^3 E^4}{\mu^3} \frac{|F_{pn}(\theta)|^2}{8\pi} \sin^2\theta$$

where α is the fine structure constant, z the charge number of the target nucleus, M, β and θ, the meson mass, velocity and angle respectively; E is the energy of the incident photon, Using this technique; the decay width of $\eta \to \gamma\gamma$ was found to be

$$\Gamma_{\gamma\gamma} = (1.21 \pm 0.26) \text{ kev}$$

Photoproduction of π^+ at 0° and forward angles[5)]

The difficulty in detecting π^+ at 0° is the background of e^+ from e^+e^--pairs produced by the photon when traversing the target material. The electron was eliminated by using lead absorbers associated in the magnetic analysis and by discrimination at detection. The following table gives the differential cross-sections for various photon energies and c.m.s. angles of the emitted pion. The best fit to the data seems to be calculations based on the CGLN theory of photoproduction.

E_γ	$\theta_{c.m.}$	$\frac{d\sigma}{d\Omega}$ ($\mu b/sr$)	Error %
598	0	20.6	4
594	2.3	21	4.3
597	5	19.1	3.2
597	7.6	17.5	3.2
598	10.6	15.8	3.3
601	15.1	14.2	3.7
608	21.5	11.2	3.4
574	0	19.3	4.3
574	5.3	18.0	3.2
575	7.5	15.8	3.3
576	10	15.5	3.3
579	15	13.6	3.4
582	20	11.3	3.6

E_γ	$\theta_{c.m.}$	$d\sigma/d\Omega$ ($\mu b/sr$)	Error %
544	0	18.9	3
544	2.25	18.7	3
545	5	18.0	3.2
547	7.5	16.7	3
546	10.6	15.0	3
547	15	12.9	3
555	21.2	10.7	3
562	30	10.2	3
576	35	10.2	3.6
576	38	10.0	3.3
526	0	19.8	4.2
545	30	10.7	4.1
496	0	18.3	4.5
496	2.2	17.3	3.4
496	5	17.2	4
497	7.3	15.8	3.7
497	10	14.1	3.7
500	15	12.3	3.5
503	20	10.7	3.7
476	0	18.8	4
448	0	19.4	4
448	2.9	18.4	4.4
448	4.3	17.9	3.7

E_γ	$\theta_{c.m.}$	$d\sigma/d\Omega$ ($\mu b/sr$)	Error %
449	7.2	16.8	3.8
450	10.75	15.3	3.9
451	13.45	14.2	3
455	21.5	11.1	4.3
462	30	10.8	4
426	0	20.6	3.5
411	0	19.1	4.5
398	0	18.7	4.7
398	2.5	19.5	3.2
398	4.6	18.5	3.5
399	7	18.6	3.5
399	10	16.4	4.9
400	14.5	15.5	3.6
404	21	13.4	3.8
410	30	11.6	5
389	21	21.0	4.3
389	4.2	20.8	4.3
389	7	19.7	4.5
390	10.5	18.5	4.5
391	13.9	17.7	4.6
401	32	12.9	4.2

E_r	$\theta_{c.m.}$	$d\sigma/d\Omega$ ($\mu b/sr$)	Error %
379	0	20.0	3.6
381	2.1	18.8	4
381	4.2	18.5	3.8
359	0	18.8	5.9
359	2.1	19.8	5.3
359	4.8	16.4	5.6
360	6.9	18.5	5.4
350	0	18.4	4
350	2	17.8	5
350	2.7	18.4	4.1
350	5	18.7	7
350	7.5	16.7	7.3
350	10	17.5	7.2
352	15	14.9	6.9
339	0	17.1	6.1
339	4.1	16.4	4.8
339	6.8	14.4	5
326	0	14.2	5
326	2.7	14.9	5
319	0	14.0	8.8
301	0	8.1	17
300	2.7	8.2	10
298	4	8.4	5.4
298	6.7	8.3	5.5
299	10	8.3	5.5
300	13.3	8.3	5.5

Photoproduction of π^+ mesons at 3.4 and 5.0 Bev[6].

The photoproduction of π^+ mesons were studied at 3.4 and 5.0 Bev in the Cambridge Electron Accelerator. Other competing processes were suitably eliminated. The differential cross-sections are given in the following table.

k_0 (Bev)	θ (deg.)	$-t$ $(Bev)^2$	$d\sigma/dt$ ($\mu b/(Bev/c)^2$)
3.4	5.1	0.09	3.82 ± 0.46
	9,9	0.33	1.94 ± 0.16
5.0	5.1	0.19	1.30 ± 0.12
	7.1	0.37	0.89 ± 0.09
	9.9	0.69	0.43 ± 0.05
	15.1	1.45	0.060 ± 0.014

The results of the experiment can be fitted with

$$\frac{d\sigma}{dt} = A \exp(Bt)\ \mu b/Bev^2$$

where $A = 5.53 \pm 1.00$, $B = 2.93 \pm 0.64$ Bev^{-2} for $k_0 = 3.4$ Bev; $A = 2.32 \pm 0.21$, $B = 2.41 \pm 0.15$ Bev^{-2} for $k_0 = 5.0$ Bev.

A simple Reggeized pion exchange does not describe the data correctly. Gauge-invariant amplitudes may yield a better result.

ΛK enhancement at 1.7 Bev[7].

A study of 230,000 $\pi^- p$ and 80,000 events of $\pi^- p$ and $\pi^+ p$ interactions at 6 Bev/c in the BNL 80-inch liquid-hydrogen bubble chamber indicates a ΛK^+ enhancement centred at 1.7 Bev in the reaction $\pi^- p \rightarrow \Lambda K^+ \pi^-$. There are no similar enhancements in the processes: $\pi^{\pm} p \rightarrow \Lambda K^{+,0} \pi^{+,0}$

The cross-sections for the various processes are shown in the following table.

Reaction	Number of events	Visible cross-section (μb)
$\pi^- p \rightarrow \Lambda K^+ \pi^-$	346	17 ± 1
$\pi^- p \rightarrow \Lambda K_1^0 \pi^0$	99	4 ± 0.5
$\pi^+ p \rightarrow \Lambda K^+ \pi^+$	95	19 ± 2

Evidence for the existence of the hypernucleus $_{\Lambda}Li^6$[8].

A systematic investigation of the mesonic decays of hypernuclei with four charged-particle final states shows evidence of an event described by

$$_{\Lambda}Li^6 \rightarrow \pi^- + p + p + He^4$$

The observed stability of the hypernucleus $_{\Lambda}Be^7$ imposes an upper limit of 3.72 ± 0.15 Mev on the total binding energy of $_{\Lambda}Li^6$.

The present experiment yields a value 3.92 ± 0.37 relative to the free-particle system $\Lambda + p + He^4$.

Charge symmetry of the Λ -nuclear interaction demands equal binding energy in mirror hypernuclei. Actually in the case of the mirror hypernuclei $_{\Lambda}H^4 - _{\Lambda}He^4$, it was found that

$$B_{\Lambda}(_{\Lambda}He^4) - B_{\Lambda}(_{\Lambda}H^4) = 0.27 \pm 0.06 \text{ Mev}$$

The difference was explained as breaking of charge symmetry in the Λ -nucleon interaction. With $B_{\Lambda}(_{\Lambda}He^6) = 4.19 \pm 0.17$ Mev and with a binding energy of $_{\Lambda}Li^6$ relative to the ground state of Li^5, $B_{\Lambda}(_{\Lambda}Li^6) = 5.89 \pm 0.37$ Mev, the binding energy difference for $_{\Lambda}Li^6 - _{\Lambda}He^6$ is

$$B_{\Lambda}(_{\Lambda}Li^6) - B_{\Lambda}(_{\Lambda}He^6) = 1.7 \pm 0.4 \text{ Mev}$$

which is much larger than in the previous case.

Branching ratio $\Gamma(\eta \to 3\pi^0)/\Gamma(\eta \to 2\gamma)$ [9]

In view of the various discrepant values for

$$R = \Gamma(\eta \to 3\pi^0)/\Gamma(\eta \to 2\gamma)$$

a fresh experiment based on 4 π spark chamber observation of five (5s) and six-shower (6s) events produced in $\pi^- p \to \eta n$ and other $\pi^- p \to$ neutrals was done. The value of R is

$$R = \frac{\Gamma(\eta \to 3\pi^0)}{\Gamma(\eta \to 2\gamma)} = 1.1 \pm 0.2$$

References

1) W.F.Baker et al, Physics Letters 25B, 361 (1967)

2) L.G.Hyman et al, Physics Letters 25B, 376 (1967)

3) Alladi Ramakrishnan et al, Nuovo Cimento 37, 1046 (1965)

4) C.Bemporad et al, Physics Letters 25B, 380 (1967)

5) F.C.Bizot et al, Physics Letters 25B, 489 (1967).

6) P.M.Joseph et al, Physical Review Letters 19, 1206 (1967)

7) D.J.Crennell et al, Physical Review Letters 19, 1212 (1967)

8) D.M.Harmsen, Physical Review Letters 19, 1186 (1967).

9) R.J.Cence et al, Physical Review Letters 19, 1393 (1967).

--

INDEX